Infiltration, hydrogeology, and heterogeneity

- Management of pressure and flow: A case study for the Varberg tunnel project

Lisa Risby

Degree of Master of Science (120 credits)
with a major in atmospheric science,
climate and ecosystems
60 hec

Department of Earth Sciences
University of Gothenburg
2020 B1107

Faculty of Science

UNIVERSITY OF GOTHENBURG

UNIVERSITY OF GOTHENBURG
Department of Earth Sciences
Geovetarcentrum/Earth Science Centre

Infiltration, hydrogeology, and heterogeneity

- Management of pressure and flow:

A case study for the Varberg tunnel project

Lisa Risby

ISSN 1400-3821

B1107
Master of Science (120 credits) thesis
Göteborg 2020

Mailing address
Geovetarcentrum
S 405 30 Göteborg

Address
Geovetarcentrum
Guldhedsgatan 5A

Telephone
031-786 19 56

Geovetarcentrum
Göteborg University
S-405 30 Göteborg
SWEDEN

UNIVERSITY OF GOTHENBURG

DEPARTMENT OF EARTH SCIENCES

Abstract

This thesis aims to describe a conceptual model of the sedimentology for Swedish (or nordic) conditions of heterogeneous aquifers but focus is on a case study in Varberg. This to facilitate the identification of main water-bearing units (e.g. upper and lower aquifers, two-dimensional and one-dimensional flow) by short duration hydraulic tests evaluated by the Hvorslev method. The purpose was to provide guidance in relation to location and design of mitigation measure for the mitigation of pressure and flow focusing on infiltration and pumping. The analysis assumes that the geometric mean (median) of the saturated hydraulic conductivity in a lognormal isotropic two-dimensional medium (aquifer) is the exact upscaled hydraulic conductivity (effective hydraulic conductivity) (Gupta, Rudra, Parkin, & Parkin, 2006; Renard, Le Loc'h, Ledoux, De Marsily, & Mackay, 2000). Based on this assumption the median hydraulic conductivity from short duration hydraulic tests was compared to the effective hydraulic conductivity obtained from transient (time-dependent) pumping test to explain aquifer heterogeneity and spatial variability in hydraulic conductivity. The conceptual model, in combination with short duration hydraulic tests, was found to be a valuable tool for describing the spatial distribution of measured hydraulic conductivities. Deviation of median values of short duration hydraulic tests from hydraulic conductivity obtained from pumping test could be described by the spatial variability (aquifer heterogeneity) of hydraulic conductivity. The flow pattern in the aquifers in Varberg generally seem to be disturbed by channel flows in structures or geological materials with high hydraulic conductivity (glaciofluvial) that create deviation from a two-dimensional isotropic aquifer. The location and design of infiltration is suggested to depend on the spatial variability of hydraulic conductivity and these one-dimensional channel flows.

Keywords: Short duration hydraulic tests, hydraulic conductivity, radius of influence, infiltration, heterogeneity, confined and unconfined aquifer

Table of content

1. Introduction

Groundwater movement and aquifer characterisation are two important aspects in infrastructure projects. If the hydrogeology is not described in a relevant way for an infrastructure project it may lead to damages such as spreading of contamination in groundwater (Kitanidis, 1994), settling and unwanted dewatering (Wada et al., 2010). Therefore, infrastructure projects commonly apply for a permit for groundwater withdrawal. An application is submitted to the Swedish Land and Environment Court in case there is a risk that public or private interests can be damaged. If there is a risk for damage to sensitive objects or environment, infiltration might be needed to maintain the groundwater levels. Where pumping in an aquifer occurs due to an excavation or similar, the groundwater surface level is lowered locally around the well (excavation). The groundwater moves along the pressure gradient (hydraulic gradient) toward the well and a radius of influence (or cone of depression) develops (Fetter, 2001). The radius of influence depends upon aquifer characteristics such as hydraulic conductivity (describes a fluids ability to flow in a porous media), aquifer heterogeneity (the contrast and distribution of hydraulic conductivity), and the type of aquifer (unconfined or confined) (Kruseman & De Ridder, 1994).

Hydraulic conductivity (K) variability tends to exhibit a log normal distribution (Gupta et al., 2006; Nielsen & Biggar, 1973; Tuli, Kosugi, & Hopmans, 2001; Wen, 1994; Zarlenga, Janković, Fiori, & Dagan, 2018). In a two-dimensional isotropic (the hydraulic properties is the same in all directions) homogenous medium the variability of K is assumed to be log normal and the central tendency can be described as the geometric mean (Gupta et al., 2006). Further, for a log normal distribution, the geometric mean equals the median of the population (Renard et al., 2000).

The focus of this thesis was to evaluate aquifer anisotropy and behaviour with the purpose to select better locations for artificial infiltration (in principle, not object-specific) in a case study for the Varberg tunnel project. Infiltration might be needed where sensitive objects are situated within the radius of influence from a pumped well or excavation (if no settlement occurs, only a drawdown may not be sufficient to damage an object). A conceptual sedimentological model was connected to aquifer heterogeneity and the spatial variability of hydraulic conductivity. Short duration hydraulic test was used to measure the spatial variability of hydraulic conductivity.

The hydraulic conductivity obtained from pumping tests is assumed to be equal to the median (bulk or effective) hydraulic conductivity (Zech, Müller, Mai, Heße, & Attinger, 2016). For a two-dimensional isotropic system with a lognormal distribution of K, the median K should describe the effective hydraulic conductivity obtained from pumping test (Gupta et al., 2006; Renard et al., 2000). Therefore, the central tendency (median) of hydraulic conductivity was evaluated for a qualitative comparison to the effective hydraulic conductivities which would, for a homogenous isotropic aquifer, be equal (Gupta et al., 2006)

1.1 Aim and hypothesis

The aim of the thesis was to conceptualize a sedimentological model and use it as a basis for description and analysis of spatial relationships in relation to measured hydraulic conductivity. The purpose was to evaluate the usefulness of the conceptual model as a first step for an aquifer conceptualisation and characterisation. This was then used to evaluate aquifer behaviour (connectivity and anisotropy) and to select possible locations for infiltration and pumping. Further, the median hydraulic conductivity obtained from short duration hydraulic tests was compared to the effective hydraulic conductivity.

1. Is the conceptual model of sedimentology in Varberg in agreement with results from short duration hydraulic tests?
2. Can horizontal aquifer heterogeneity be described by short duration hydraulic tests?
3. Under the assumption of two-dimensional isotropic aquifers, can the effective hydraulic conductivity from transient pumping tests be described by the median value resulting from short duration hydraulic tests?

Slug test data (and basic time lag) can provide key input for evaluation of aquifer behaviour and infiltration design. The focus was on hydraulic conductivity, K (or transmissivity, T), variability (how spread out or closely clustered a set of data is) and median (50% larger, 50% smaller) for a better selection of infiltration well location(s) (Renard et al., 2000).

In this work it was assumed that a transient (time dependent) pumping test 1) describes the effective (median) hydraulic conductivity (transmissivity) of a two-dimensional isotropic aquifer and that 2) observations in adjacent wells reflects the connectivity of the aquifer. The intention was to investigate if there is an agreement between the median value obtained from local slug testing and results from transient tests. A high median K (T) and a low variability is thought to result in a need for few(er) infiltration points. A low median K (T) and a high variability is expected to result in a larger number of points.

1.2 Delimitations

This work focuses on the unconsolidated sediments expected in Sweden and more specifically Varberg and do not consider the bedrock. The effect of pumping (and infiltration) and the development of a radius of influence will be considered in relation to aquifer characteristics. The thesis focuses on artificial recharge systems as a measure to maintain groundwater levels in infrastructure projects. Specific and sensitive objects (e.g. specific buildings and their foundation, specific energy wells or energy wells) that could be sensitive to a decline in the groundwater surface will not be discussed in this thesis. Further, parameters related to technical specifications such as pumping rates and capacity of artificial recharge facilities will not be discussed. The focus will be on the lower aquifers.

2. Background

2.1 Infiltration and hydraulic testing

Infiltration and/or pumping deals with restoring the mass balance and the hydrologic equation in an aquifer system. The hydrologic equation is based on the law of mass conservation. The hydrologic equation can be expressed according to Fetter (2001) as inflow equals outflow plus or minus the change of storage in the system. For a given hydrogeological system the inflow (recharge) and the outflow (discharge) are defined within a groundwater basin. The groundwater basin is the subsurface area which is delineated by boundaries (or groundwater divides) where no groundwater flow contributes to the system budget outside the boundaries.

The movement of water in a porous media (in this case groundwater in sediments) is defined by Darcy's law. Darcy's law states that the discharge (Q) is proportional to the difference in height or pressure of the water (h, hydraulic head) between two locations and inversely proportional to the flow length (L). Further, the flow is proportional to the cross-sectional area (A) of the porous medium. In combination with the proportional constant (hydraulic conductivity, K), which is related to the character of the porous media, the one-dimensional discharge for the system can be calculated by equation 1 (Fetter, 2001).

$$Q = -KA\left(\frac{dh}{dl}\right) \quad (1)$$

Where dh is the hydraulic gradient between two points and dl is the distance between these points. This means that groundwater moves from high hydraulic head to low hydraulic head, indicated by the negative sign in equation 1. Lines between points with the same hydraulic head (or potentiometric head) are called equipotential lines (or groundwater contours). The groundwater flow is perpendicular to this line, from high hydraulic head to low (Fetter, 2001).

When pumping water from a well connected to an aquifer the hydraulic head is lowered in and around the well (drawdown) and groundwater is moving towards the well according to equation 1. Under the assumption that an aquifer is homogenous and isotropic this will produce a radial flow towards the pumped well. As groundwater level decline a cone of depression or radius of influence will develop. The growth of the radius of influence depends on duration of the pump test, discharge rate, aquifer transmissivity (amount transferred water per time unit through the cross-section of the aquifer) or hydraulic conductivity, aquifer heterogeneity, type of aquifer (confined or unconfined) and boundary conditions (Kruseman & De Ridder, 1994). The radius of influence will grow with time until steady state is reached. This is a state of equilibrium where no further drawdown with time occur which simply state that the water pumped from the well is equal to the water transmitted by the aquifer.

Where the pumped aquifer does not reach equilibrium (steady state) the radius of influence will continue to grow until it reaches a boundary, or the hydrologic equation is balanced by recharge from a supplying facility (artificial recharge) (Fetter, 2001). The radius of influence in a homogenous and isotropic unconfined aquifer can be calculated by a simple equation suggested by Kirieleis-Sichardt (1930), equation 2.

$$R = 3000 \times s_w \times \sqrt{K} \quad (2)$$

Where R is the radius of influence and s_w is the drawdown at the pumped well.

In a confined aquifer pumped groundwater is released from elastic or specific storage (S). A confined aquifer does not get direct recharge from precipitation (due to the confining layer) and the radius of influence will grow until a boundary is reached. Boundaries are divided into recharge and barrier boundaries. A recharge boundary is where the system (aquifer) is replenished. Barrier boundaries are where the aquifer terminates by either meet an impermeable boundary or thinning (Fetter, 2001). If no recharge occur the radius of influence will grow continuously as pumping continues (nonequilibrium or transient flow) (Fetter, 2001). Transient flow means that the inflow parameter in the hydrological equation is not in balance with the outflow and the change in the storage of the aquifer. The growth of the radius of influence is hence time-dependent for transient flows. Therefore, the development of the radius of influence for a two-dimensional homogenous and isotropic compressible confined aquifer, which is horizontal and infinite in extent with no source of recharge pumped at constant rate can be calculated by equation 3 (Cooper & Jacob, 1946).

$$R = \sqrt{\frac{2.25Tt}{S}} \quad (3)$$

Where r is the radius of influence, T is the transmissivity, S is the specific storage and t is the time since the pumping began.

For radial flow and a symmetrical radius of influence to develop the aquifer must be homogeneous and isotropic. In most natural aquifers these conditions are seldom the case (Fetter, 2001). A nonhomogeneous (heterogenous) and anisotropic aquifer will create an unsymmetrical radius of influence due to the change in the porous media (sediment). Where there is high hydraulic conductivity in the system (aquifer) the radius of influence tends to be wide and flat. As the hydraulic conductivity decrease the radius of influence gets steep and narrow (Kruseman & De Ridder, 1994).

These aquifer parameters are important when determining the radius of influence for pumping or infiltration and to determent if a radius of influence will reach sensitive objects (environmental or cultural) that need to be protected. Therefor, determination of artificial infiltration location depends upon these parameters. Artificial infiltration can be used to limit the development of the radius of influence by creating an artificial recharge boundary (Fetter, 2001).

2.1.1 Artificial groundwater recharge

Artificial groundwater recharge (infiltration) system are systems that aim to restore or enhance the mass balance in the aquifer. Artificial recharge can be used for community water supply, enhance groundwater quality and remediation, prevent saltwater intrusion (Bouwer, 2002) and prevent dewatering of surface water and subsidence (settling) (Wada et al., 2010). Infiltration can be done both in unconsolidated sediments and in the bedrock. There are several types of

infiltration facilities dependent on local conditions. Surface infiltration in basins, vadose zone (the unsaturated zone between ground surface and the groundwater table) by infiltration in wells or trenches and direct injection in wells are common methods for artificial recharge (Bouwer, 2002).

In this thesis the focus is on artificial recharge systems as a method to prevent the radius of influence of growing in the unconsolidated sediments. In an aquifer system the drawdown from the pumping decreases the pore pressure and the effective stress with the consequence of compression and consolidation of the sediments. This situation is more pronounced in confined aquifers (e.g. a confining unit with low hydraulic conductivity covering more permeable sediments). If the pore pressure increases, as in the case of too high-water pressure (too high water column), in the infiltration facility the effective stress will increase and consequently the sediments will expand (Zhang, Wang, Chen, & Li, 2017). Therefore, recharge is limited by the infiltration capacity of the sediments. The infiltration capacity is defined by the capacity of soil to allow water to percolate under the influence of gravity. The infiltration capacity varies dependent on sediment heterogeneity (Pedretti, Barahona-Palomo, Bolster, Sanchez-Vila, & Fernàndez-Garcia, 2012). This leads to that there are limits to which capacity and pressure an artificial recharge facility can have dependent on the sediment type and heterogeneity.

2.1.1.1 Surface infiltration

Surface infiltration uses infiltration basins where water is gathered and can infiltrate the sediments and percolate to the groundwater. This method requires that the vadose zone have high enough permeability, or that the confining layer is thin enough to be remove, and enough land areas. Where there are semi-confined to confined aquifers with thicker confining bed or high vertical heterogeneity, this method is not recommended since perched water-tables can form and restrict the downward flow and recharge to the aquifer. Also, this type of infiltration method requires adequate maintenance since clogging occurs due to accumulation of suspended solids, formation of biofilms or gases. This reduces the hydraulic conductivity and hence groundwater recharge decreases (Bouwer, 2002).

2.1.1.2 Vadose zone infiltration

Where the unsaturated zone has lower hydraulic conductivity or where there is lack of land area for infiltration basins, vertical infiltration methods can be used. Water can be infiltrated in trenches or wells in the vadose zone. Trenches are generally dug to a depth of 5 meter with a surface area of approximately 1 meter in cross section. The trench is filled with coarse sand or gravel. Water is usually applied in the trench through a perforated pipeline. Wells are also filled with gravel or sand, is approximately 1 meter in diameter and water is applied through a perforated pipeline in the centre of the well. The well is typically deeper than the trenches (up to 60 meters) and is hence more suitable for areas with a thick vadose zone. Vadose zone infiltration is a rather inexpensive infiltration method. A disadvantage is that the system eventually clogs up since backwashing (reverse pumping of water to wash out the clogged layer) is impossible. Both Vadose zone and surface infiltration has the advantage of geopurification, as the water percolate through the unsaturated zone (Bouwer, 2002).

2.1.1.3 Well injection

Where land surfaces are insufficient, the vadose zone has low permeability, aquifer is deep, or the aquifer is confined, direct injection of water through groundwater wells are often used. This method of infiltration sets high demand on the water quality of the water infiltrated since no geopurification occur. If the groundwater is used as drinking water the infiltrated water needs to be of drinking water quality. The advantage of this method is that clogging can be prevented by backwashing and hence the construction has a longer lifespan (Bouwer, 2002).

2.1.2 Risks and opportunities with infiltration

The need for infiltration is dependent on whether there are objects within the radius of influence sensitive to a change in the groundwater levels. Therefore, risks and opportunities for the usage of infiltration facilities must be evaluated to the risks that follows if no measures are taken.

2.1.2.1 Remediation and spreading of contaminants

Where infiltration is needed there is a possibility to remediate contaminated aquifers. Pumping gives the option to remove polluted groundwater by the method “pump and treat”, clean the water, then infiltrate it back into the aquifer (Chen et al., 2019). If surface infiltration is possible (basins) pumped groundwater can by geopurification be remediated where the unsaturated zone is of acceptable thickness and permeability. If geopurification is not possible (for example in confined aquifer) the groundwater needs to be treated before injection in the aquifer (Bouwer, 2002). Though, there is a risk with these systems that contamination plumes spread or dilute in the aquifer rather than get remediated. In the long-term there is a risk of increasing dilution of contamination plumes in heterogenous aquifer systems because of spatial variability in flow velocities (Kitanidis, 1994).

2.1.2.2 Aquifer depletion

If aquifer depletion occurs in the vicinity of the ocean, the risk of saltwater intrusion must be considered. If the groundwater levels are lowered, the hydraulic gradient could cause saltwater to intrude into the groundwater system. In the long-term sea-level rise as a consequence of global warming could lead to saltwater intrusion, if sea-levels rise above the groundwater levels (Werner et al., 2013). Another risk associated with aquifer depletion is the risk of subsidence and settling (Wada et al., 2010). In confined aquifers these effects are generally irreversible (Bouwer, 2002). In an aquifer system that feeds surface water, which is often the case in Sweden, a change in the groundwater levels could result in drainage of close by waterbody, like lake or rivers, which could have ecological consequences (Brunner, Cook, & Simmons, 2009).

2.1.2.3 Enhanced groundwater movement

Clogging is a common problem in infiltration systems which reduces the infiltration rate (Bouwer, 2002). The opposite problem could also arise since infiltration and pumping system increase the groundwater movement. As groundwater movement increase, the erosion rate increases, and therefore the hydraulic conductivity of the aquifer could increase over time (Gette-Bouvarot et al., 2015). Pumping of groundwater compresses the soils and make them

move towards the pumped well. Infiltration or recharge have the opposite effect, the soils expand and move away from the infiltration facility (Zhang et al., 2017). Over time this could lead to a change in the aquifer characteristic.

2.1.3 Short duration hydraulic tests

To describe the hydraulic properties of an aquifer hydraulic tests are performed. A short duration hydraulic test, often referred to as slug test, is when a volume of water or a displacement body is abruptly added to or removed from a borehole raising/or lowering the hydraulic head (h) temporally compared to the static water level (figure 1). The resulting pressure change creates type-curves with pressure and time. These curves can be used for evaluation of aquifer characteristics.

Slug and bailers are two commonly used methods. A slug is a heavy cylinder with a certain volume which can both raise (by inserting the slug in the well) or lower (removing the slug from the well) the hydraulic head. The bailer method only lowers the hydraulic head by insert the bailer under the static water level. The bailer is filled with water and is then rapidly removed (Hölting & Coldewey, 2019).

The theoretical background for slug test is that the time for equalization of pore water pressure in response to a change in hydrostatic head is inversely proportional to the hydraulic conductivity of the sediment. The time required for eliminating pressure differences is called the time lag. On a semi-logarithmic plot, the head ratio versus time will be linear. The slope of the line is proportional to the permeability of the aquifer (Hvorslev, 1951).

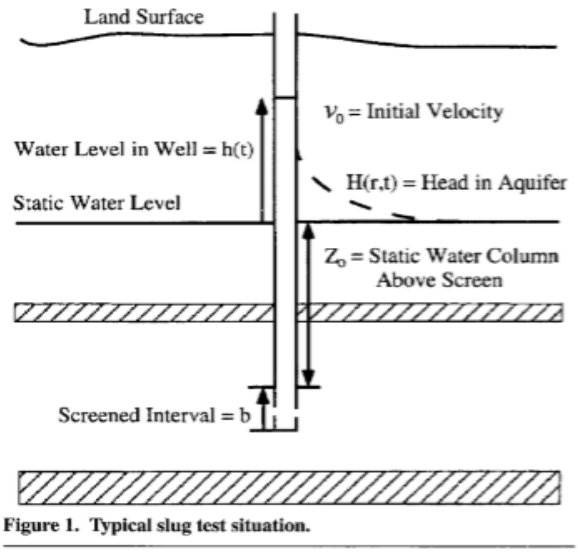

Figure 1. Typical slug test situation.

Figure 1. The configuration of a short duration hydraulic test taken from McElwee (2001). Application of a nonlinear slug test model. Retrieved from https://www2.scopus.com/inward/record.uri?eid=2-s2.0-0031149311&doi=10.1111%2fj.1745-6584.1997.tb00110.x&partnerID=40&md5=8f6c41705459be6ac41041c716cd04e7.

Hvorslev (1951), Cooper, Bredehoeft, and Papadopulos (1967) and Bouwer and Rice (1976) are the most widely used methods for slug test evaluation. All these three are linear theoretical models and assume aquifer homogeneity and isotropy. The Cooper et al. (1967) method is the

only method that accounts for storativity. It assumes a fully penetrating well, two-dimensional radial flow to or from the well in a confined aquifer (Mas-Pla, Yeh, Williams, & McCarthy, 1997). The Hvorslev and Bouwer and Rice methods are developed for usage on both fully and partially penetrating wells (Bouwer & Rice, 1976; Hvorslev, 1951). The Bouwer and Rice (1976) method was developed to be more suitable for unconfined aquifers and if the well screen is above the water table.

The most suitable method for evaluation of aquifer properties depends on aquifer characterisation (confined, unconfined), expected storativity of the aquifer, aspect ratio of the test interval and the radius of the well screen (Mas-Pla et al., 1997). The screen (or filter section) is the open or perforated interval of the well where groundwater can move from or into the well and aquifer.

Mas-Pla et al (1997) compared these three methods in a sandy aquifer and concluded that the Hvorslev and the Bouwer and Rice method are most representative for this type of aquifer and that these two methods resulted in similar hydraulic conductivities. This was thought to be due to that the only difference in the two methods is the form factor related to the well function. The Hvorslev method generally yielded lower hydraulic conductivities than the Bouwer and Rice method (Mas-Pla et al., 1997).

For evaluation of the hydraulic conductivity (K) Butler Jr, Bohling, Hyder, and McElwee (1994) reported that the Hvorslev method provided acceptable parameter estimates in the ratio of screen length to the radius of the screen between 3 and 300. Parameter estimates of hydraulic conductivities where within 20 percent of actual hydraulic conductivities (Butler Jr et al., 1994; Hyder, Butler, McElwee, & Liu, 1994). At larger aspect ratios and storage parameters Cooper et al. provides better estimates (Mas-Pla et al., 1997). The Bouwer and Rice method has been reported to estimate hydraulic conductivity parameters within 30 percent of the actual conductivity values in unconfined, isotropic and homogeneous aquifers (Hyder & Butler, 1995; Mas-Pla et al., 1997).

Short duration hydraulic tests are easier and less expensive to perform than pumping tests (Hölting & Coldewey, 2019; Mas-Pla et al., 1997). These are also proven valuable when testing is needed at contaminated areas because there is no extraction of groundwater needed (Hölting & Coldewey, 2019). Short duration hydraulic tests are thought to give a good estimation of spatial variability of hydraulic conductivity and hence the horizontal heterogeneity (Brauchler, Hu, Hu, & Ptak, 2012; Mas-Pla et al., 1997).

There are also methods developed for multilevel slug tests to analyse the vertical heterogeneity (Brauchler et al., 2010; Zemansky & McElwee, 2005). Zemansky and McElwee (2005) found that averaged multilevel slug tests showed hydraulic conductivities in the same magnitude as results from slug test conducted over the entire screen length. Jones (1993) found relationship between results from pump tests in the same magnitude of hydraulic conductivity as results from slug tests in unweathered till. Butler Jr and Healey (1998) found that, on average, slug test data yield lower hydraulic conductivity than pumping test within the same formation.

The drawback with slug tests is that they only sample on local scale around the well and the well function, installation and development may be dominant in results (L. Jones, 1993). When performing multiple slug tests with different initial heads the linear theoretical methods states that the type curves should coincide on a semi-logarithmic plot. If this is not the case, nonlinear effects influence the evaluated result. Nonlinear effect are effects related to other factors than the soil permeability. The nonlinear effects can be caused by turbulence because of the slug velocity, friction loss, radius change in the well bore and mobile fine fraction in the soil. Nonlinear effects are most pronounced in aquifers with high hydraulic conductivity (underdamped or oscillatory aquifer). Underdamped or oscillatory response is when the hydraulic conductivity is high enough to produce pulses (waves) by the velocity of the slug, as on a free water surface. Nonlinear effects can be of importance in medium and low hydraulic conductivity (overdamped or nonoscillatory) aquifers as well, for example if there is mobile fine fraction in the aquifer. Exactly how to deal with nonlinear effects is unclear (Zemansky & McElwee, 2005).

Nonlinear effect can be determined by conducting several slug tests with different initial head (H(0)). If the response is changing with initial head, there are nonlinear effects. If multiple slug test with the same initial head response in different ways, there is noise in the data, or the well is changing as tests are conducted. As the hydraulic conductivity increase toward over-damped or oscillatory response, velocity and acceleration of the inserted slug becomes significant for the result. If corrections are not made the velocity in the water column will decrease pressure and the head is underestimated. When mobile fine grain material is present Hvorslev model may not be valid (McElwee, 2001).

2.1.4 Transient pumping tests

Pumping tests are thought to be representative for the median hydraulic conductivity of an isotropic two-dimensional aquifer (Renard et al., 2000). Both slug tests and pumping tests deals with estimation of hydraulic properties of aquifer systems. While the slug tests (or short duration hydraulic tests) increase or decrease the hydraulic head in the well by adding or remove a smaller volume of water, pumping test involve groundwater withdrawal by larger quantities.

During a pumping test groundwater withdrawal, generally with a constant rate, is performed in a well. The responses in one or several other wells around the stressed well are recorded to determent the heterogeneity and connectivity in the aquifer system (Paradis, Lefebvre, Gloaguen, & Giroux, 2016). The influenced area of the tests is a function of the system hydraulic conductivity (or transmissivity), aquifer condition (unconfined/confined) and aquifer heterogeneity or diffusivity (speed of pressure disturbance is aquifer system) (Kruseman & De Ridder, 1994; Paradis et al., 2016). Aquifer parameter estimate determined by pumping test involve the median (mean or effective) hydraulic conductivity. The early response between the stressed well and the observation well (inter-well region) are most sensitive to parameter estimate (Gupta et al., 2006; Paradis et al., 2016; Renard et al., 2000). As the influenced area increases outside the inter-well region the influence of parameters within the inter-well region decrease (Paradis et al., 2016).

2.2 Geological and hydrogeological description

A relevant conceptual model of the stratigraphy (geology) and type of aquifer (hydrogeology, e.g. confined, unconfined) are key for the evaluation of the hydraulic properties. The following section describes a conceptual model of the sedimentology in different parts of Sweden. This aims to demonstrate differences between aquifer systems dependent on geographical location. An early and relevant hypothesis of the geological conditions will allow for confirmatory rather than exploratory investigations.

2.2.1 Quaternary geology and geological history in Sweden

The unconsolidated sediments in Sweden are mainly quaternary deposits from the latest ice-age (Kleman, Stroeven, & Lundqvist, 2008; Stroeven et al., 2016) and the most common soil type is till. Around 75 percent of all unconsolidated soils in Sweden are till ("Geology of Sweden," 2019). As mentioned in section 2.1 recharge to an aquifer is dependent on the infiltration capacity, the transmissivity of the aquifer, the type of aquifer and the heterogeneity of the aquifer (Bouwer, 2002; Pedretti et al., 2012). All these parameters are related to the sedimentology of an area. Different depositional environments and processes form different types of sediments and hence the aquifer character is related to these processes.

The conceptualisation of typical Swedish sedimentology and stratigraphy will be based on and further developed based on the geographical and ice dynamic sectors suggested by Stroeven et al. (2016). Glacier dynamics controls, to a large extent, the erosion and deposition patterns within an glacier (Kleman et al., 2008). In a cold-based glacier, the ice is frozen to the bed. The consequence of this is that the ice moves by internal deformation rather than sliding (Benn & Evans, 2014). This slows erosion rates down and increases the preservation potential of older sediments (Bergman, 2018; Kleman et al., 2008; Stroeven et al., 2016). A warm-based ice is above the freezing point at the bed interface and the glacier can slide. This has the opposite effect in that it enhance erosion rates and decrease preservation potential (Kleman et al., 2008; Stroeven et al., 2016).

In the following sections a general picture of the surficial sediments of Sweden and the processes involved will be presented. The aim is to give a picture of which type of aquifer system that can be expected to be found dependent on location in Sweden.

2.2.2 Glacial history of Sweden

During the quaternary period Sweden has been subjected to several glaciations. The last glaciation, the Weichselian, occurred between 115-11.7 thousand years ago (ka) (Anjar, 2012). During Weichselian several glaciation and warm periods, called interglacial or interstadial, occurred. Most of the older deposited sediments was removed during the Weichselian (due to the erosive power of glaciers) and hence most unconsolidated sediments found in Scandinavia are 115 ka or younger (Mangerud, Gyllencreutz, Lohne, & Svendsen, 2011).

The last glacial maximum (LGM) during the Weichselian occurred 26.5 to 20 thousand years ago and it covered all of Scandinavia, the Baltic states, western Russia, Northern Belarus, Poland, Germany, Denmark, Netherlands and all the way to Ireland (Stroeven et al., 2016). Before the LGM three major interstadial had occurred during the early and middle Weichselian,

where large parts of Sweden were ice free. These are the Brørup, Odderade and Ålesund interstadials. During the Brørup and Odderade interstadials, which occurred 100 and 80 ka, where characterized by almost ice-free conditions in entire Sweden. During the Ålesund interstadial (38-35 ka) most of southern and central Sweden where ice-free while the northern part where mainly below ice, except a small part of the east coast (Mangerud et al., 2011).

The late Weichselian is the phase of the LGM upon final deglaciation (Mangerud et al., 2011). During the Late Weichselian deglaciation there where several standstill and re-advances. One major re-advance occurred during a colder glacial period called Younger Dryas, 12 ka, which produced the Middle Swedish End-moraine zone. The glacial front was then positioned on the latitude of Lidköping (Johnson & Ståhl, 2010; Stroeven et al., 2016).

The glacial history of Sweden suggests that there could be several glacial and deglacial sequences in the stratigraphic records. However, the erosion by later glaciers has often erased older deposited sediments. Still, sediments have been found from earlier interstadials and glaciations where glacier dynamics has been favourable (Benn & Evans, 2014; Bergman, 2018; Hättestrand & Stroeven, 2002; Kleman, Borgström, Robertsson, & Lilliesköld, 1992; Kleman et al., 2008; Lagerbäck & Robertsson, 1988; Möller, 2006; Möller, Anjar, & Murray, 2013).

2.2.3 Conceptual sedimentological model of Sweden as a basis for aquifer characterisation

2.2.3.1 Northern Sweden (north of Luleå)

Most of northern Sweden have been cold-based upon final glaciation (Hättestrand & Stroeven, 2002; Kleman et al., 2008; Stroeven et al., 2016). Saprolites (a zone in the lower soil profile which represents deep weathering in the bedrock) in the stratigraphical record indicate low erosion rates during former glaciations. The lack of features indicative for thawed bed conditions and reshaping by glacial sliding further strengthens this theory (Bergman, 2018; Ebert, Hall, & Hättestrand, 2012; Hättestrand & Stroeven, 2002). Deposits of organic or non-glacial cold climate sediments have been found also indicating preservation of sediments deposited during interglacial cold periods, Brørup and Odderade (Gibbard, 1992). The northern part of Sweden has been glaciated during the longest time (Stroeven et al., 2016).

The central and north of Sweden was below an ice cap that was approximately 2-2,5 kilometers. This have led to considerable suppression of the buoyant lithosphere and hence post-glacial isostatic uplift as a consequence of unloading (Grånäs & Ising, 2008). The highest coastline (HK) is the line that represent the highest point where the land has been below sea level (Björck, 1995). The highest coastline in the northern Sweden is approximately 200 meters above (todays) sea level (MASL) (Påsse & Daniels, 2015). Because of this, glaciomarine sediments can be found far inland from todays coastline.

There are well developed deglacial landforms as well as inherited pre-late Weichselian glacial landforms such as Veiki moraine, drumlins, and eskers in the north of Sweden. During deglaciation stagnant ice could cover eskers and glaciofluvial deposits by a thinner layer of melt-out till (Lagerbäck & Robertsson, 1988). Towards the coastal areas De Geer moraines

indicate a calving ice margin. Further inland deglacial landforms are generally less developed (Stroeven et al., 2016).

Advance of a cold-based glaciers that override of frontal depositions and lakes can create considerable basal debris layer. This generates a thrust block moraine of sand, gravel and silt (Hambrey & Glasser, 2012). During deglaciation of a cold-based glacier the major landform recorded is lateral meltwater channels (Benn & Evans, 2014). This gives a simplified glacial advance and recession stratigraphy of thrust block moraine below clastic water-laid sediment. Bergman (2018) presented till deposition from three glaciations, Saale, middle and late Weichselian. These till units are often separated by organic or clastic water-laid sediments. This stratigraphy is well consistent with the above explanation. Late Weichselian till is generally only a thin sequence of 1-3 meters covering old glacial and non-glacial deposits (Stroeven et al., 2016). The moraine in the north of Sweden is generally sandy (Lagerbäck & Robertsson, 1988). Most of the aquifers above the HK are therefore thought to be unconfined and made up of sandy till. The till could have considerable thickness since it can represent three different glaciation cycles and be divided by water-laid and organic sediments (figure 2).

Below the HK the late-Weichselian deglaciation was maritime. Earlier, during the two glacial-interstadial cycles and the last advance before the LGM, the glaciation environment was terrestrial (Mangerud et al., 2011). Therefore, the model for sediment deposition according to Bergman (2018) would apply. Though, during the final deglaciation the thermal regime in these areas changed to warm-based which typically enhance erosion (Benn & Evans, 2014; Stroeven et al., 2016). Therefor sequences of advance and pre-late Weichselian deposits are not thought to be as continuous as further inland.

The De Geer moraines reveals a calving margin with proglacial water depth in excess of 150 meters during deglaciation (Lindén & Möller, 2005). Basal till is first deposited. As the glacier front recede subaqueous fan are deposited at the grounding line by sediment gravity flows. Suspended material is carried by water and deposited further away covering the earlier deposited sediments. These fine-grained sediments can be deposited along with drop stones from icebergs (Benn & Evans, 2014; Hambrey & Glasser, 2012). Fine-grained material continue to deposit and overgoes to mud and organic deposits as the ice front retreats further (Hambrey & Glasser, 2012). Isostatic uplift causes regression and the shoreline retreat causing reworking by waves and redeposition of the outwash material, such as sand (Påsse & Daniels, 2015). Below the HK aquifers are suggested to be confined and sediments below the confining layer are basal till and sediment gravity flows. Reworking and deposition of postglacial sands could create a two aquifer system with an upper unconfined aquifer of outwash sediments and sand above the confined aquifer (figure 2).

2.2.3.2 Central Sweden (south of Luleå to a line drawn between Norrköping-Karlstad-Strömstad)

The deglaciation in the central of Sweden was mainly terrestrial, except in the coastal areas and valleys below the HK connected to the coast. The HK in central Sweden is found between approximately 140 to 300 MASL. The most pronounced isostatic uplift is found in the province of Ångermanland and the least prounounced in the southern area, around Norrköping, Karlstad

and Strömstad (J. Lundqvist, 1969; Påsse & Daniels, 2015). Below the HK the deglaciation was in lacustrine to maritime environment, since the Ancylus lake developed to the Yoldia sea during the deglaciation (Möller, 2006).

The area of central Sweden is thought to have had a more polythermal and warm-based basal thermal regime. A polythermal glacier has a mixed basal thermal regime with temperatures both below and above the freezing point (Benn & Evans, 2014). The extensive record of striae, eskers and lineation indicate a domination of warm-based thermal regime (Stroeven et al., 2016). Therefore, compared to the northern part of Sweden, pre-late Weichselian landforms and deposits are rarer. Still, the mountains in the west are thought have been subjected to cold-based ice for considerable time leading to preservation of older glacial deposits (Hättestrand & Stroeven, 2002; Kleman et al., 1992; Möller et al., 2013). This has been concluded by the finding of organic layers which represent paleo-surfaces from interstadials (Kleman et al., 1992; Möller et al., 2013).

During the Weichselian glaciation the area was subjected to four interglacial and three interstadials (Mangerud et al., 2011). This makes the central part of Sweden the area where most glacial-interstadial cycles have occurred during the Weichselian glaciation. During the LGM central Sweden was cold-based. But upon the final deglaciation almost the entire central of Sweden was warm-based, except in the western mountain area (Stroeven et al., 2016). In central Jämtland and Ljungarn-Ljusnarn area larger ice-dammed lakes was developed leading to deposits of glaciolacustrine sediments (Benn & Evans, 2014; Stroeven et al., 2016).

Pre-late Weichselian deposits are considered erased from the sedimental record under the late Weichselian warm-based ice. Still, at the western mountain area pre-late Weichselian tills separated of paleosol has been found (Kleman et al., 1992). In these areas lacustrine and apron deposits interpreted as deposited during Marine Isotope Stage 3b (MIS 3b), the interstadial before LGM, has been found. These sediments are overlaid by basal till from LGM (Möller et al., 2013). The many glacial-interstadial cycles are therefore suggested to create a more complex stratigraphy in this area and at the mountain pre-late Weichselian deposits could be found under Late Weichselian deposits. In the northern and western part of central Sweden, the ice recession changed direction transverse across valleys causing a cease in deposition of glaciofluvial deposits since drainage in valleys occurred under shorter time spans (Kleman et al., 1992; J. Lundqvist, 1969). This also contribute to higher preservation of pre-late Weichselian sediments.

In the southern and eastern areas in central Sweden cold-based glacier did not prevail upon final deglaciation. Therefore, most of the sediment records are thought to be from the last deglaciation (Kleman et al., 2008). Larger esker systems generally follow valley system both in supra-aquatic and sub-aquatic depositional environments. These larger esker systems have often erased older sediments to the bedrock. Above the HK dammed-up ice lakes produced lacustrine deltas which some places developed to sandur systems. Where larger glacial lakes existed, sub-aquatic eskers covered with fine-grained deposits can be found (Benn & Evans, 2014; J. Lundqvist, 1969; Möller, 2006). Thick deposits of quaternary sediments in valleys are

covering the bedrock. Toward higher ground the deposits gets thinner and the heights are generally covered with a thinner unit of till (Möller et al., 2013).

Below the HK sub-aquatic eskers have developed to deltas during standstills in the ice recession (Benn & Evans, 2014; J. Lundqvist, 1969; Möller, 2006). These standstills can be seen by trace of marginal moraines in Uppsala (Rudmark, 2000). The sedimental models are generally the same as the model presented for the northern of Sweden below the HK. The difference is that more commonly, the pre-late Weichselian sediments have been eroded by the warm-based ice (Kleman et al., 2008; Stroeven et al., 2016). The sediment load is suggested to be higher due to higher erosion rate and higher discharge of water and more substantial proximal and distal deltas can build up (Hambrey & Glasser, 2012), figure 2.

2.2.3.3 Southern Sweden (from Scania to a line between Strömstad and Norrköping)

The southern parts of Sweden only experienced one glacial-interstadial cycle before the LGM (Mangerud et al., 2011). The deglaciation of southern Sweden was mostly slow and terrestrial with major standstills and minor re-advances, which have resulted in ice marginal formations. The thermal regime in southern Sweden during deglaciation was warm-based which affect the erosion. Still, at some places the basal condition remained cold-based during the complete deglaciation which resulted in limited glacial erosion (Stroeven et al., 2016). Southern Sweden has only had two interglacial during the Weichselian and has therefore been glaciated shorter time than the northern and central Sweden (Mangerud et al., 2011). The southern of Sweden will be sub-divided into four areas, Mt. Billingen, Southwestern area of Sweden, South central Sweden, and Scania.

2.2.3.4 Mt. Billingen

A colder period called Younger Dryas was initiated here. As a consequence a frontal advance took place (Johnson & Ståhl, 2010). The ice sheet retreat slowed down and oscillatory advances occurred creating the Swedish Middle End Moraine Zone (MSEZ) (Johnson, Wedel, Benediktsson, & Lenninger, 2019). The area west and east of Mt. Billingen has been subjected to processes related to the outburst of the Baltic Ice Lake, the development to the Yoldia Sea and later the Ancylus Lake (Andrén, Lindeberg, & Andrén, 2002; Björck, 1995). The development of the area started with a glacial phase. As the deglaciation took place the Baltic Ice Lake started to evolve (Björck, 1995). The lake was dammed-up and had no contact with the sea (Björck, 1995; Stroeven et al., 2016). When the deglaciation reached Mt. Billingen, an outlet was opened connecting the Baltic Ice Lake with the Atlantic Ocean, a phase called the Yoldia Sea. The following regression resulted in disconnection to the Atlantic and a new freshwater phase started, the Ancylus Lake which later on drained through Öresund and developed into the Baltic sea (Björck, 1995).

The history of this area makes the stratigraphy different from other areas in Sweden. Johnson (2010) Analysed sediment cores west of Mt. Billingen and found out that there were no pre-late Weichselian deposits in the sequences. The sea-level was 120-130 meter above todays sea level and during deglaciation mainly fine-grained glaciomarine sediments were deposited. Till is generally a rare sediment type in the area. Thick layers of glacial varved clays has then been deposited in areas below sea-level (Johnson & Ståhl, 2010; Johnson et al., 2019). As the ice

front reached the north of Mt.Billingen a connection between the ocean and the Baltic ice lake was opened. A drainage of the Baltic Ice Lake followed. Two drainage event is thought to have occurred but evidence of drainage deposits is lacking (Johnson et al., 2019). During the construction of E20 in Götene poorly sorted sand and gravel was found in between layers of varved marine clay indicative of an outburst event (Johnson, Ståhl, Larsson, & Seger, 2010). Outwash fans, some eskers and hummocky topography, which is irregular morainic topography associated with supraglacial origin (Benn & Evans, 2014), are found on inter-moraine flats. The sediment depth can be up to 50 meters but is generally 20-30 meters (Johnson & Ståhl, 2010; Johnson et al., 2010).

The area east of Mt. Billingen generally has a thin layer of till beneath the thicker fine-grained layer which is of both lacustrine and maritime origin. Before the opening of Mt. Billingen connection, the deposition was lacustrine at the ice front. After the Baltic ice Lake outburst, the conditions become glaciomarine (Fromm, 1976). The isostatic uplift de-connected the two areas and the lacustrine phase of Ancylus Lake was developed. During the final phase of the development of the Baltic Sea most of the area was above sea level. Only a bay in the area of Norrköping was still below sea level (Björck, 1995). At heights a thinner cover of basal sandy till was deposited (Fromm, 1976).

2.2.3.5 Southwestern area of Sweden (Åmål down to Varberg)

The relief of the west coast is thought to have shaped a landscape during deglaciation with drainage in longer valleys, calving bays, and archipelagos. The ice movement was down in fjords and fissure valleys. This left a rather shallow layer of till at the hill tops. The valleys acted as drainage channels (Hillefors, 1979). There has been several minor advances and standstills during the deglaciation (Plink-Björklund & Ronnert, 1999; Stroeven et al., 2016). A major standstill and ice-front advance mixed deposited glacial clay with till which produced clay moraine and also the pronounced end moraines seen in the west coast area (Hillefors, 1979).

The sedimentology of west coast of Sweden is characterised by maritime, glaciomarine deposits and larger end-moraine ridges. Generally, the presence of till is sparse compared to the rest of Sweden. The shallow deposits are dominated by bare rock and glacial and postglacial clays. Glaciofluvial deposits are more rare in this area than the rest of Sweden (Adrielsson & Fredén, 1987).

The glacial settings of the south western Sweden with warm-based ice and drainage in valleys suggests that preservation of old sediment is low (Benn & Evans, 2014; Hillefors, 1979). Therefore, sediments are assumed to be deposited during the last deglaciation phase. Since valleys acted as drainage channels glaciofluvial material is expected to be found there. During deglaciation the bottom layer of basal till or glaciofluvial material was deposited (Hillefors, 1979). At ice margins deltas were built up during standstills in the recession (Plink-Björklund & Ronnert, 1999). A major standstill and ice-front oscillation mixed deposited glacial clay with till which produced clay moraine and the pronounced end moraine seen in the west coast area. As the area becomes ice-free glaciomarine clay deposited (Hillefors, 1979).

As deglaciation continued the sea level decreased due to isostacy (Påsse & Daniels, 2015). Around 10000 years bp the sea level rise overcome the isostatic uplift and a transgression took place which reached its highest point around 7000 bp (Påsse & Daniels, 2015). The glacial clay was reworked at many places and post-glacial fine grained sediments was deposited (Adrielsson & Fredén, 1987). Due to the high deposition of clays covering high conductive glaciofluvial material, eskers or deltas are not as easily found by geomorphological features as in other parts of Sweden. The till on the west coast is generally sandy to silty in composition (Adrielsson & Fredén, 1987). The suggested dominated aquifer system is confined aquifer (figure 2).

2.2.3.6 South central Sweden (highlands in Småland)

The highlands in Småland is located in the middle of the south of Sweden are thought to be an area where the thermal regime of the ice sheet has been cold-based for a longer while during the last glaciation (Stroeven et al., 2016). The area has never been below sea-level and fine-grained sediments are therefore glacial, glaciolacustrine or lacustrine (Lemdahl et al., 2013). Larger and thicker layers of clay and silt as therefore rarer than in the coastal areas and hence confined aquifers are rare. The area was subjected to terrestrial and slow deglaciation (Stroeven et al., 2016).

Glacial topography such as ribbed moraine, drumlines, hummocky moraine and glaciofluvial deposits are common in the area (Magnusson, 2009; Möller, 2010; Möller & Murray, 2015). Ribbed (or Rogen) moraine genesis are not fully understood but it could be glacial reshaping pre-existing landforms and therefor an indicator of preservation of deposits from older ice sheets (J. Lundqvist, 1997; Möller, 2006). Other suggest that the landform is more polygenetic and the term only should be used as a descriptive, morphological term (Möller, 2010). Glaciofluvial deposits generally increase in frequency west of Växjö and is less frequent to the east (SGU, 2019). Glaciofluvial deposits are generally the top most sediment but could be overlaid by a layer of till (Magnusson, 2009).

2.2.3.7 Scania

Scania is the region in Sweden that has been glaciated during the shortest period (Ringberg, 1989). Most of Scania is located above the HK except areas near the coast. The area has never been cold-based (Stroeven et al., 2016). Scania has many glaciofluvial deposits and striae which indicate sliding and warm-based conditions (Hebrand & Mark, 1989; Ringberg, 1988, 1989; Stroeven et al., 2016).

What is unique for Scania is the widespread upper unit of till with high clay content. This is because the bedrock in Scania is different from other parts of Sweden which have resulted in production of more fine-grained tills. This unit is most common from the west coast to the higher areas in the central of Scania. In lowlands this unit grades into clay. This clay unit generally overlay one or two layers of clay and silt which is divided by a layer of gravel and sand (Berglund & Lagerlund, 1981). Underneath this unit sand and clay layers the lowest unit that is found which generally compose of another till layer (Ringberg, 1989).

On the east coast the glacial history is different from the west coast. The areas are subjected to processes connected to the development of the Baltic sea as described in section 2.2.3.4 (Björck,

1995; Hebrand & Mark, 1989; Påsse & Daniels, 2015). The shallow layers on the east coast are therefore often sand and gravel and at some places varved clays (Hebrand & Mark, 1989). Also, further inland, the eastern part of Scania was more subjected to damming up of ice lakes and therefore the building of deltas in lacustrine environments. Eskers and glaciofluvial deposits are more often exposed compared to the western part of Scania. Some eskers have eroded the bottom unit of moraine and are in direct contact with the bedrock, but a layer of till is usually beneath the glaciofluvial material (Hebrand & Mark, 1989; Ringberg, 1991). A general stratigraphically model from bottom is till, overlaid by deltaic or outwash sediments which could be overlaid by fine grained lacustrine sediments. When approaching the coastal areas, the till locally is overlaid by glaciofluvial deposits and glacial clay with a topmost thinner layer of outwash material such as sand (Daniel, 1986; Hebrand & Mark, 1989; Ringberg, 1991). The till on the east coast of Scania is generally clayey (Daniel, 1986).

2.2.3.8 Summary of conceptual model

Figure 2 suggests four basic and simplified stratigraphy's depending on the environment at glacier terminus and glacier thermal regime. Over the highest coastline the aquifers are generally unconfined. Where there have been glaciolacustrine environments confined aquifers can be found. Under the highest coastline confined aquifers are expected to be found. An upper unconfined aquifer could be found where there are outwash sediments and postglacial sands. For some locations, the stratigraphy will be very different because of different glacial history such as the areas around Mt. Billingen (section 2.1.4.4) with thick layers of clays in direct contact with the bedrock. Also, situations that deviates from the proposed model is the clay moraine (confining bed) in Scania (section 2.1.4.7) or areas which where glaciolacustrine such as at Ljungarn-Ljusnarn area described in section 2.2.3.2. Confined aquifers can hence be found without being under the HK or in a glaciolacustrine environment. The suggestion for construction of a conceptual model for a specific location is based on the determination of the ice dynamics during the deglaciation and the location in relation to the HK (under/over). Then one should define whether there are specific glacial events that could complicate the basic and simplified stratigraphy. Thereafter, modify the general stratigraphy presented in figure 2.

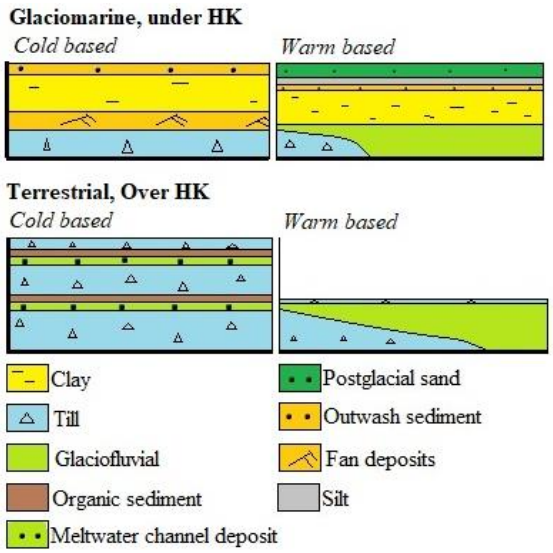

Figure 2. Four basic and simplified stratigraphy's which can be used for aquifer characterisation.

2.3 Case study Varberg

Infiltration, hydrogeology, and heterogeneity are key topics of this thesis and focus is on a case study for the Varberg tunnel project. Varberg is a smaller town located at the west coast of Sweden around 60 kilometers south of Gothenburg (figure 3). Varberg is a part of the infrastructure project "Västkustbanan". In this project a double train trac is built between Malmö and Gothenburg. In Varberg the train tracks will both go through a tunnel and in a trough. If the groundwater surface is above the tunnel or trough groundwater must be pumped out of the aquifer so the excavation does not get filled with groundwater. Pumping of ground water or infiltration of water creates a radius of influence and groundwater moves towards the pumping facility or away from the infiltration well along the hydraulic gradient (Fetter, 2001). The growth of the radius of influence depends on duration of the pump test, discharge rate, aquifer transmissivity (amount transferred water per time unit through the cross section of the aquifer) or hydraulic conductivity, aquifer heterogeneity, type of aquifer (confined or unconfined) and boundary conditions (Kruseman & De Ridder, 1994).

This case study is focusing on the last four parameters which do not depend on technical specifications. The case study will include a conceptual model of unconsolidated sediments in Varberg and in-situ measurement of the hydraulic conductivity by short duration hydraulic tests. The purpose was to provide guidance in relation to location and design of mitigation measure for the mitigation of pressure and flow focusing on infiltration and pumping.

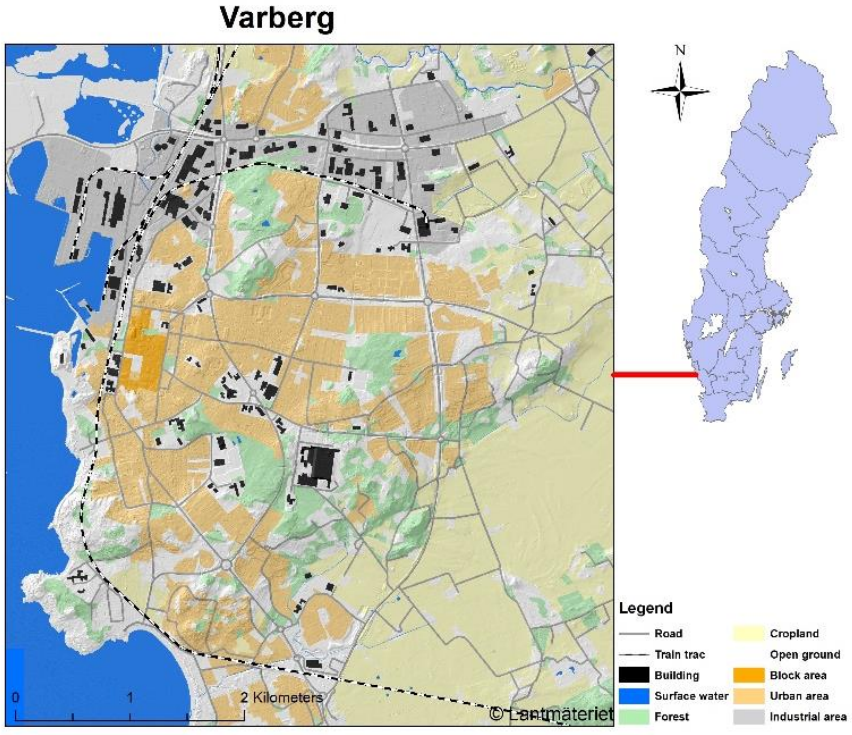

Figure 3. Overview map of Varberg city.

In the project “Varbergs tunnel” risks for environmental consequences have been estimated at a drawdown that exceeds 0.3 meters. During the maintenance of the train tracks groundwater drawdown are at some places thought to exceed 2 meters and at maximum during the construction 12 meters (Tyréns, 2016; Wååg & Niord, 2018). The juridical decision from Vänersborg’s Land and Environmental court (2018) states that infiltration is necessary and should be used where consequences from drawdown are estimated.

2.3.1 Geological and environmental description of Varberg

2.3.1.1 Climate, hydrology, and topography

Varberg has according to Köppens climate classification a warm-summer humid continental climate. Varberg has an annual precipitation between 800-900 millimeters and an annual mean temperature of 8-degree Celsius (SMHI, 2020). The annual evaporation is 400 mm and the potential are 600 mm per year. The potential evaporation is a measure of the airs ability to evaporate water compared to the evaporation which is an actual measure of the evaporation (SMHI, 2017). The city of Varberg is located on a gently sloping hill between two valleys with the lowest point 0 MASL and highest 54 MASL. In the middle of Varberg there is a smaller valley (figure 4). The valleys all trend northeast southwest or west-east direction. This is approximately the same direction as the ice movement were during the last deglaciation. The red line represents 15 MASL which is the highest coastline from the 7000 Bp transgression (Påsse, 1990). There are no larger streams in the area. Varberg is positioned by the Kattegatt ocean.

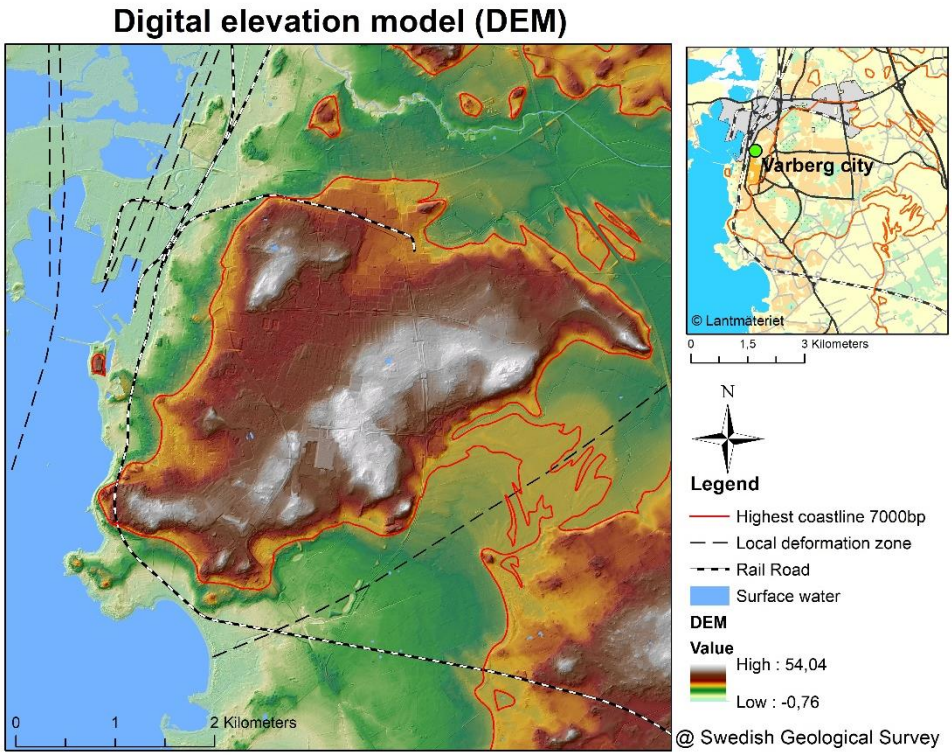

Figure 4. Topography, in meter above sea level, and the highest coastline 7000 bp.

2.3.1.2 Sediments and quaternary geology

Figure 5 shows the surface sediments found in Varberg. There is a local deformation zone going through the valley south of Varberg (Apelviken valley). Along this deformation zone further inland larger glaciofluvial deposits can be found at Grimeton and Rolfstorp (Påsse, 1990). The shallow sediments mostly consist of postglacial fine sand (or sand) and outwash sediments (gravel) (figure 5). At heights till or outwash till is the dominant sediment. Glacial clays can be found in patches at flatter areas. In the north-east part of the area moraine ridges can be found. Outwash sediments are concentrated to heights while postglacial fine sand is found in valley systems. At heights there is shallow sediment depths, between 0 to 5 meters. In valleys the sediment depth increases, and the thickest sediments are up to 30 meters. The Apleviken valley generally have a sediment depth of 10-20 meters (figure 5).

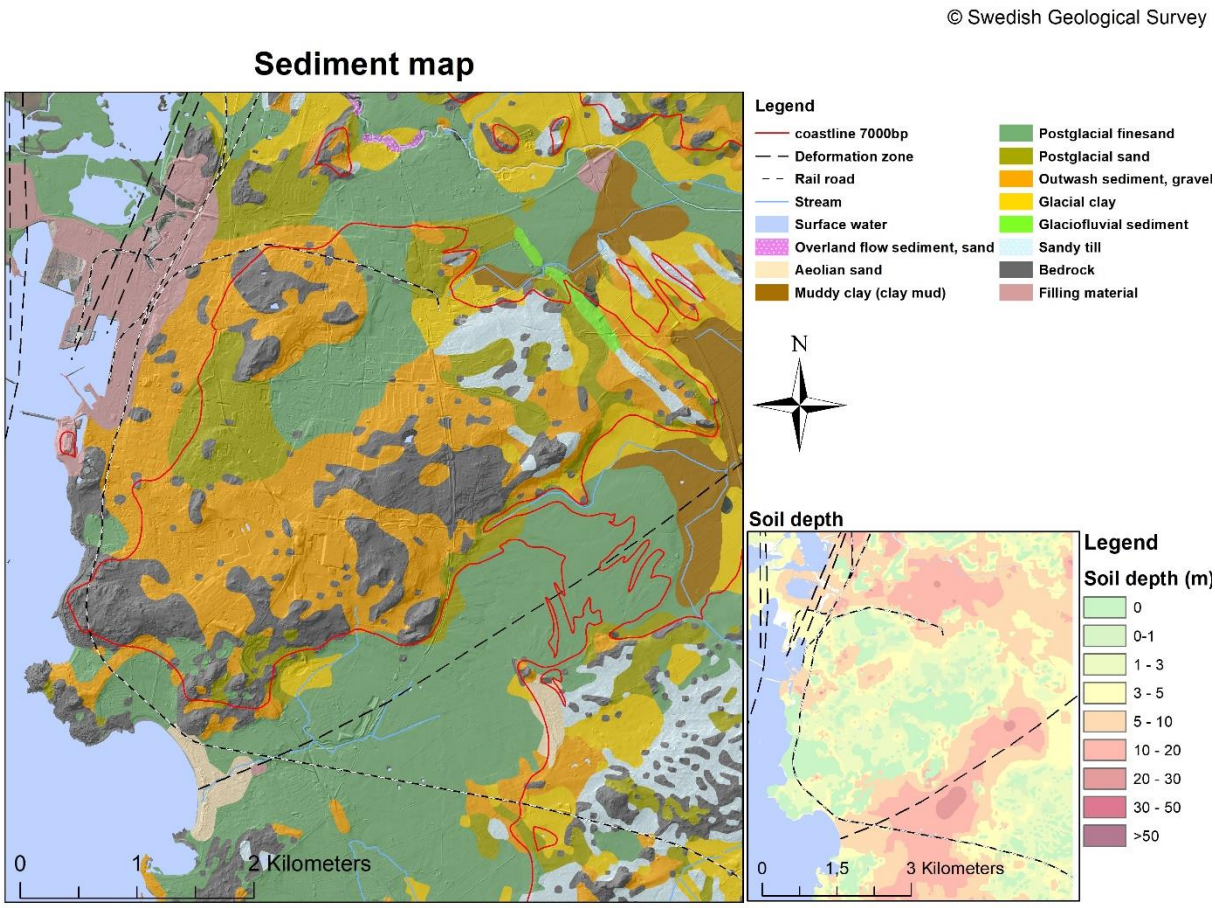

Figure 5. Surface sediments and sediment depth in Varberg.

The area of Varberg was deglaciated between 16-17 ka (J. Lundqvist, Lundqvist, & Lindström, 2011; Stroeven et al., 2016). During the deglaciation, the Varberg area was below sea-level. At the time the coast line was 75 meters above present shore level (Påsse & Daniels, 2015). The deglaciation was in a marine environment but turned terrestrial around 15 kilometers further inland where the land was higher (Hillefors, 1979). The thermal regime of the ice was mainly warm-based (Hillefors, 1979; Stroeven et al., 2016). The simplified and basic ice-recession stratigraphy for a glaciomarine, warm-based ice under the HK in figure 2 would therefore be suggested for the Varberg area.

There are several ice marginal formations in the area indicating standstills and re-advances of the glacier. These formations are occurring from the sea up to the border to the highlands. The area are a part of the Halland Coastal end-moraine zone (J. Lundqvist & Wohlfarth, 2001). Terminal moraines such as De Geer moraines has also been found within the proximity of Varberg (V. Bouvier, M. D. Johnson, & T. Påsse, 2015). Marginal formations are formed perpendicular to the ice front and in Varberg they have been described as consisting of glaciofluvial sediments, till and in some part clays (Hillefors, 1979; Påsse, 1990). Glaciotectonized material has been found in these ridges, suggesting ice frontal advance (Påsse, 1990). The warm-based ice with a calving ice margin caused high meltwater rate and sediment load (Hillefors, 1979; Stroeven et al., 2016). During marine deglaciation, the sediment loaded water in channels are deposited as subaqueous fans on the basal till. Where rapid deposition occur eskers can be buried as cores below fan forms, turbidites sediment flows and rhythmites (Benn & Evans, 2014). As the ice retreated fine-grained suspended sediments were deposited and covered older sediment structures (Påsse, 1990). This creates a confined aquifer.

As the deglaciation reached the highland (approximately 15 kilometers inland) valleys drained the hills. This resulted in fast ice movement within the valleys. At the terminus large glaciofluvial deposits were built up (Hillefors, 1979). When the glacial front got to the HK ice-proximal deltas was produced in the valleys. As meltwater was continuing to feed the valley with sediment ice-distal aprons could be developed (Hillefors, 1979; Påsse, 1990).

Offshore suspended materials was deposited in the deeper calmer waters (S. J. Jones & Jones, 2015; Påsse, 1990). Icebergs transported from the ice front could deposit rain-out diamicton on the fine-grained sediment (Hambrey & Glasser, 2012; Hillefors, 1979). As the deglaciation continues isostatic uplift initiates a regression (Påsse & Daniels, 2015). During the regression wave action reworked the deposited fine-grained material of glaciomarine clay and silt (S. J. Jones & Jones, 2015; Påsse, 1990). The area was completely deglaciated at 13200-13300 years ago (Påsse, 1990).

10 000 years ago the isostasy was slower than the sea-level rise followed by a transgression that continued until 7000-8000 years ago (Påsse & Daniels, 2015). The shore displacement was around 15 meters above todays sea-level. Lower areas around Varberg was below sea level and beach processes reshaped the area. Several beach terraces can be seen around Varberg indicating different ancient shorelines (Påsse, 1990). A regression followed which has continued ever since and is still ongoing (Påsse & Daniels, 2015). During the last transgression most of the heights in Varberg was above sea-level (red line in figure 4 and 5).

The hill tops in Varberg is thought to have acted as an ice divide and drainage occurred in the valleys and depressions in the bedrock (Hillefors, 1979; Påsse, 1990). At slopes turbidity currents are thought to have redistributed sediments and inhibited deposition of fine-grained materials such as clay and silt (Evans & Benn, 2004). During the regression wave action are suggested to have been more powerful in erosion and redistribution at slopes and at heights while on flatter and lower areas experienced lower energy erosion. This led to higher redistribution of sediments at hillsides.

By reworking of clay by wave actions and beach deposition younger sandy or silty post glacial sediments cover glacial clays in the valleys (Påsse, 1990). Therefore, below 15 MASL an upper unconfined sandy to silty aquifer could be separated by a clay layer to a lower confined aquifer with till or glaciofluvial material. On the coastal plain of Varberg area few larger glaciofluvial deposits have been found. Smaller, 1-2 meter thick, layers of glaciofluvial sediments which are horizontally widespread have been found below the glacial clays (Påsse, 1990). Since the glacier dynamics where warm-based pre-late Weichselian deposits are thought to be erased and glaciofluvial deposits could be in direct contact with the bedrock (J. Lundqvist, 1969; Möller, 2006). The processes acting after deglaciation have concealed much of the geomorphological features and the marine clay have covered glaciofluvial material which makes it hard to visually find features compared to areas which are above the HK.

2.3.1.3 Bedrock

The Varberg area is dominated by 1700 million years old intrusive rocks (Göransson, Bergström, Shomali, Claeson, & Hellström, 2008). The bedrock in Varberg where formed during a long period, 800 million years, and have been subjected to at least two orogenic events. The Gothian orogeny occurred 1750 to 1550 million years ago and the Sweconorwegian orogeny, 1150 to 900 million years ago. During these events the bedrock in Varberg has been subjected to profound deformation and metamorphosis (Lundquist & Kero, 2008). Granodioritic-granitic gneiss is the most common rock in Varberg (figure 6). There are only minor areas of Gneiss with other compositions. There are also some smaller areas of gabbroid-dioritoid. The other major rock type is charnokite. Charnockite consist of hypersten and orthoclase which indicate metamorphosis under high pressure and temperature (Lundquist & Kero, 2008).

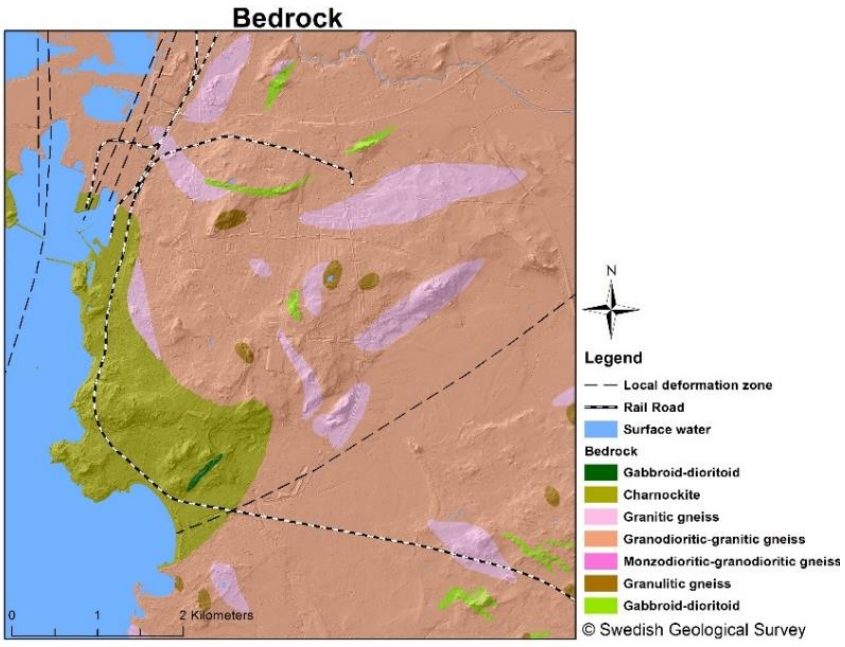

Figure 6. Bedrock in Varberg.

2.3.2 Earlier performed short duration hydraulic tests in Varberg

There have been several short duration hydraulic tests performed in the Varberg area (figure 7). Tyréns (2016) performed several short duration hydraulic tests along the train track in Varberg. This will be referred to as the first testing campaign. 46 wells where tested whereas 39 of these where wells drilled to the bedrock (in this thesis the focus is on the lower confined aquifer). The method used for the short duration hydraulic tests was infiltration. Water was added into the well to raise the head and the recovery was measured. Where the recovery was fast the Bailer method was used to remove water and lower the head. The evaluation method used was Hvorslev (1951), equation 4.

$$K = \frac{r^2 \times \ln\left(\frac{L}{R}\right)}{2 \times L \times T_0} \quad (4)$$

Where K is the hydraulic conductivity, r is the radius of the well, L is the screen length, R is the radius of the filter and T_0 is the time lag. The tests used in this thesis from the first testing campaign is showed in table 1.

Table 1. Results from short duration hydraulic tests performed during the first testing campaign.

Renen	**K (m/s)**
14T3090	3.5×10^{-5}
14T3091	1.6×10^{-4}
14T3092	5.8×10^{-6}
14T3065	4.5×10^{-5}
14T3100	1.1×10^{-5}
Southern trough and tunnel	
14T713	2.4×10^{-6}
14T7040	4.1×10^{-6}
14T7041	4.2×10^{-5}
14T7046	3.7×10^{-6}
14T7047	2.4×10^{-7}

2019 Golder Associates (Wiklund et al., 2019) performed short duration hydraulic tests. These tests are referred to as the second testing campaign. The head in the well was lowered by a drainable pump and the recovery to the static water level was measured with pressure transducer and piezometer. The recovery curves were evaluated in Aqutesolv with Hvorslev (1951) method. The results from the tests are presented in table 2. The data from wells in the southernmost area (Vareborg) where evaluated in this thesis. In figure 7 the wells from earlier performed short duration hydraulic tests are presented. Results from these wells were used in this thesis.

Table 2. Results from short duration hydraulic tests performed during the second testing campaign.

Southern trough and tunnel	**K (m/s)**
U04G11	2.1×10^{-7}
U04G16	1.6×10^{-4}
U04G38	2.5×10^{-3}
U04G40	1.5×10^{-6}

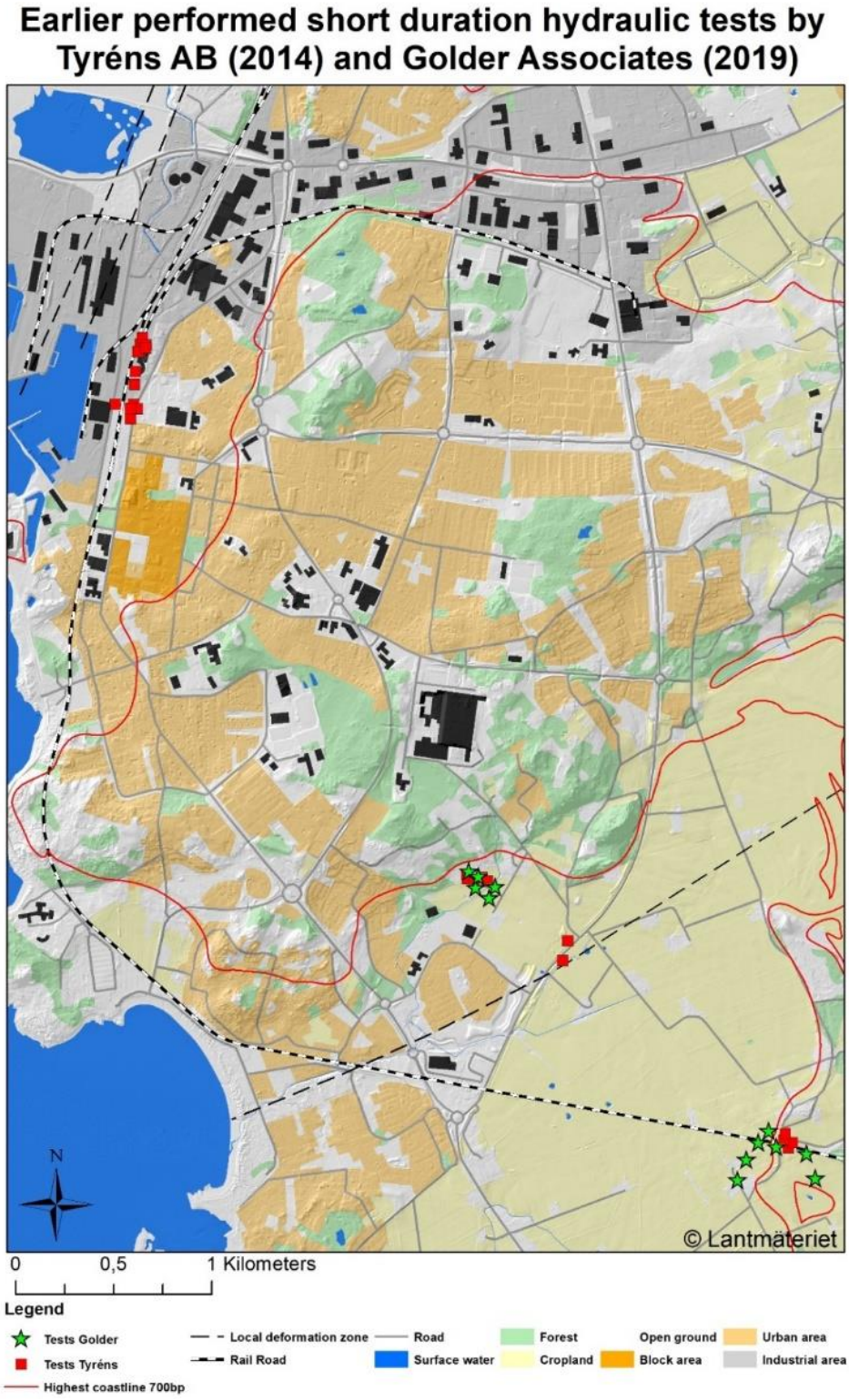

Figure 7. Overview of earlier performed short duration hydraulic tests.

2.3.3 Earlier performed transient pumping test in Varberg

The first testing campaign performed transient pumping tests along the future train trac in Varberg and 2019 the second testing campaign did several pumping tests. The following text describe 5 of these pump tests that are relevant for this thesis.

At the area Renen, in figure 8, the pumped well and observation wells used during the pumping test are showed. The pumped well had a filter placed 10-12 meters beneath the ground surface with the filter bottom at the sediment-bedrock interface. The dashed line displays the outline radius of influence during the pumping test. Well 14T3085 was pumped and six well measured a drawdown. Well 14T3087 is drilled into the bedrock which is 9.5 meters below the ground surface which is overlaid by silt. The well casing is 12 meters. All the influenced wells are deeper than 8 meters below the surface and in the vicinity of the pump well (except well 14T3090U). The closest surrounding wells outside of the influence area are shallower than the wells that was influenced (7 meters deep or shallower).

The pump test was initiated the 12th of November 2014 with a discharge of 8 litres per minute (l/min). The 15th of November the pump lost power and was shut off. The 19th of November the pump was started again with a higher discharge of 14 l/min and continued until the 24th of November. The evaluation method used was Hantusch-Jacob. The evaluation of the drawdown measured a hydraulic conductivity of 1-2×10^{-5} m/s with an assumed aquifer thickness of 5 meters.

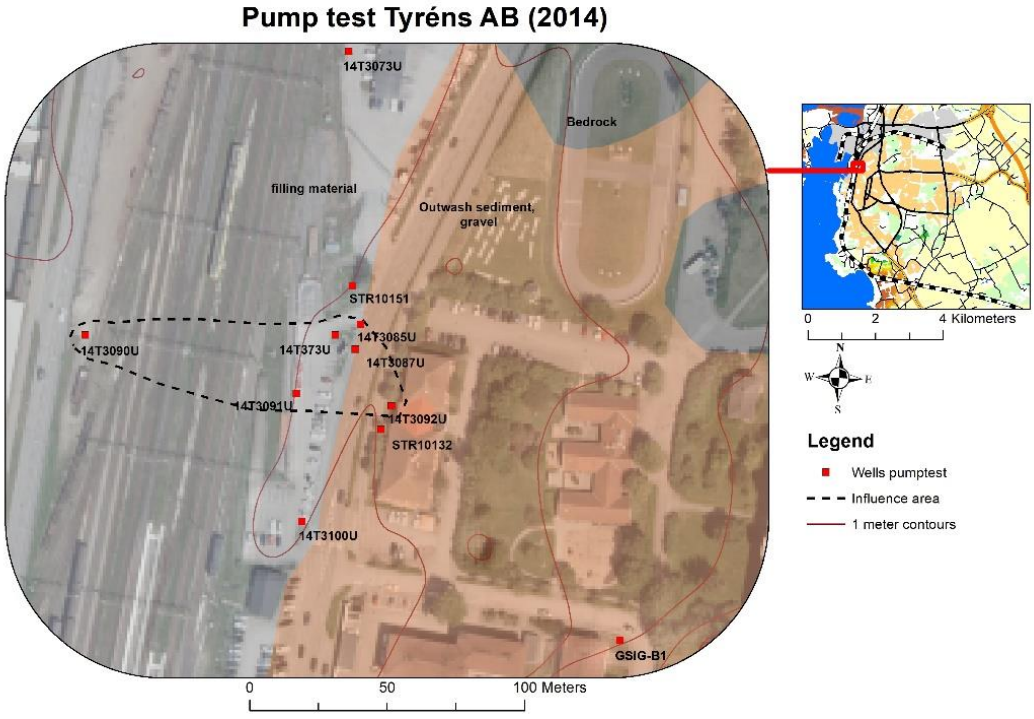

Figure 8. Pumping test performed at Renen. Copyright 2020 by Lantmäteriet (background map) and Swedish Geological surveys (surface sediments).

Figure 9 shows the wells that responded to pumping in well 14T720FO by the first testing campaign at Southern trough and tunnel. All observation wells and the pumped well are positioned in the lower aquifer. The test where carried out between the 2nd to the 9th of June 2014 with a discharge of 37 l/min. There was only one well that did not show a drawdown, well 14T711. Evaluation of the recovery curves and the drawdown measured a hydraulic conductivity of 1×10^{-4} to 2×10^{-4} m/s with an assumed aquifer thickness of 3 meters.

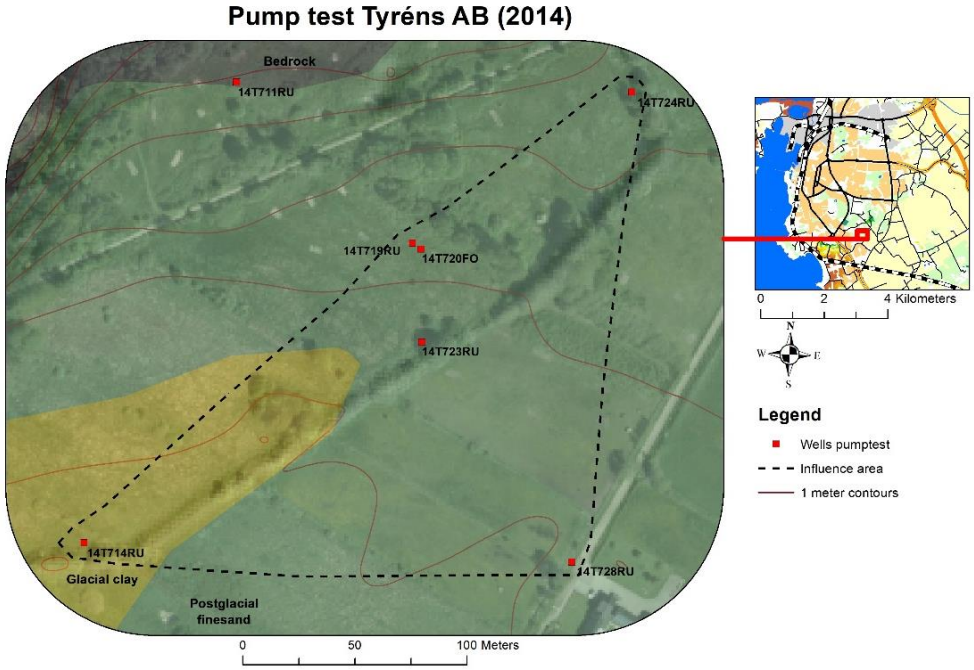

Figure 9. Pumping test at Southern trough and tunnel. Copyright 2020 by Lantmäteriet (background map) and Swedish Geological surveys (surface sediments).

During the second testing campaign pumping tests where performed at Österleden (figure 10). Only three observation wells showed drawdown, wells U12G36, 14T7035 and U19G30. The discharge throughout the pump test varied due to problems with silt that clogged the pump and that the pump had a low capacity. The method used for evaluation of the transmissivity was time-distance evaluation to minimize the influence of the unsteady pump rate. The transmissivity measured a value of 3.2×10^{-5} m^2/s.

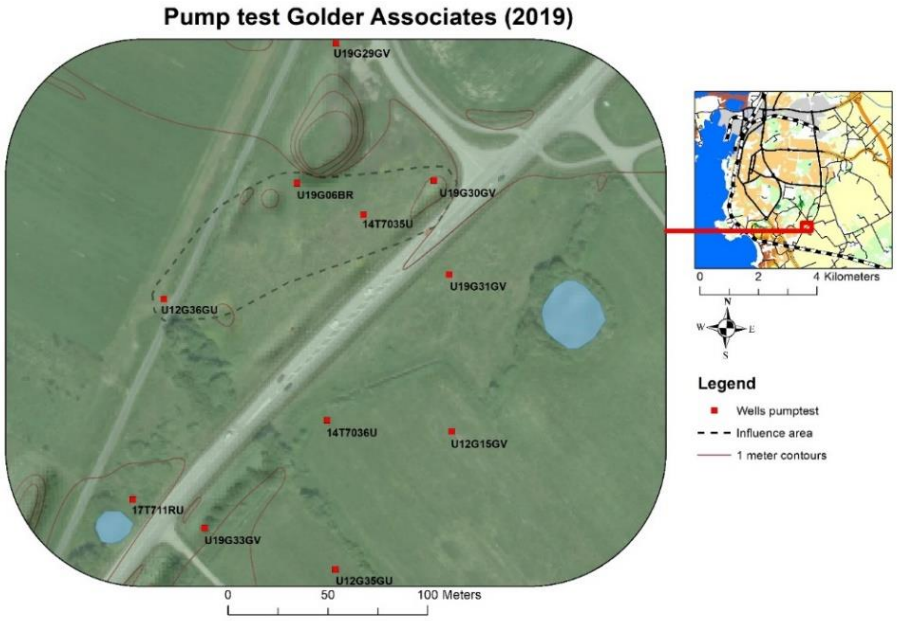

Figure 10. Pumping test at Österleden. Copyright 2020 by Lantmäteriet (background map).

Figure 11 show the influence area from pumping test in Vareborg performed during the second testing campaign. Well U19G08BR was used as pump well. The first testing campaign performed another pump test in 2014 in well 14T8033 with wells 14T8028, 14T8026 and 14T8025 as observation wells. All the observation wells were influence by the pumping during the test. The second testing campaign measured an average transmissivity of 3×10^{-5} m^2/s whereas during the first testing campaign measured a transmissivity of 4×10^{-5} m^2/s. During the second testing campaign more observation wells where used and hence the value is thought to represent the hydraulic characteristics for a larger part of the system.

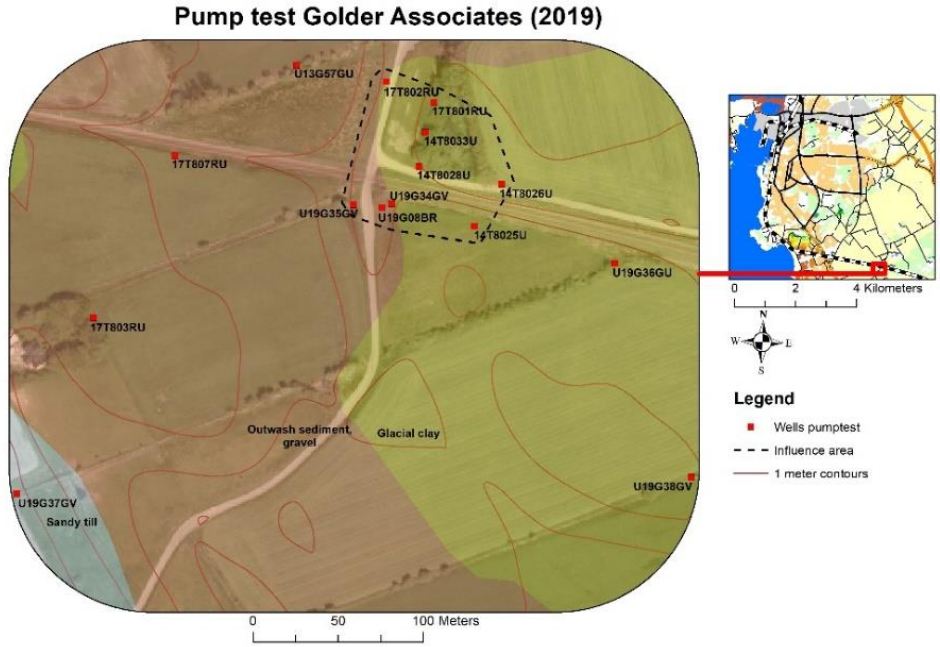

Figure 11. Pumping test at Vareborg. Copyright 2020 by Lantmäteriet (background map) and Swedish Geological surveys (surface sediments).

3. Materials and method

3.1 Description of deposits (sediments) to be Analysed

The investigation areas were chosen based on expected hydrogeological settings or type of aquifer. The radius of influence depends to a large extent on the type of aquifer where the borehole is situated (Kruseman & De Ridder, 1994). According to the quaternary geology presented in section 2.2.1.2 and figure 2, the lower, more flat areas (below 15 MASL) are described by a two-aquifer situation with a lower confined and an upper unconfined. The lower aquifers were expected to consist of glaciofluvial sediments and till. The glaciofluvial deposits are expected to have a hydraulic conductivity over 3.3×10^{-5} m/s, with a composition of sand and gravel as can be seen in table 12 and 13 (Hölting and Coldeway, 2019; Domenico, 1998). The till was expected to have a lower hydraulic conductivity due to it being poorly sorted and consisting of finer grain sizes. Domenico (1998) suggested a hydraulic conductivity for till between 1×10^{-12}- 2×10^{-6} m/s (table 12). The till in Varberg is generally sandy and the hydraulic conductivities for till are expected to be in the higher span (Påsse, 1990).

When reaching 15 MASL which is the highest point where the 7000 Bp transgression reached, old sediment has been eroded and new beach sediments have been deposited (Hillefors, 1979; Påsse, 1990; Påsse & Daniels, 2015). These sediments are expected to vary between a hydraulic conductivity for silt to sand (table 12).

In figure 12 a suggested conceptual model of the sedimentology, based on section 2.2.1.2 and figure 2, and the aquifer system is presented. The figure suggests a cross-section of a valley system. The red squares show the suggested condition where the confined aquifer terminates at the hillside. The aquifer is thought to go from confined to leaky in this situation. The pink square represents a confined situation in the central valley where glaciofluvial deposits are suggested to be found. Under the cross-section a map over the Apelviken valley is presented with squares that shown where the different environments in the cross-section is suggested to be located (figure 13). The short duration hydraulic tests that were performed aimed at detecting and characterizing the different environments. Also, the aim was to find contacts between the depositional environments in the horizontal direction along the slope of the bedrock. In-situ measurement was carried out at Renen (figure 8) to describe difference between the unconfined and confined aquifers.

.

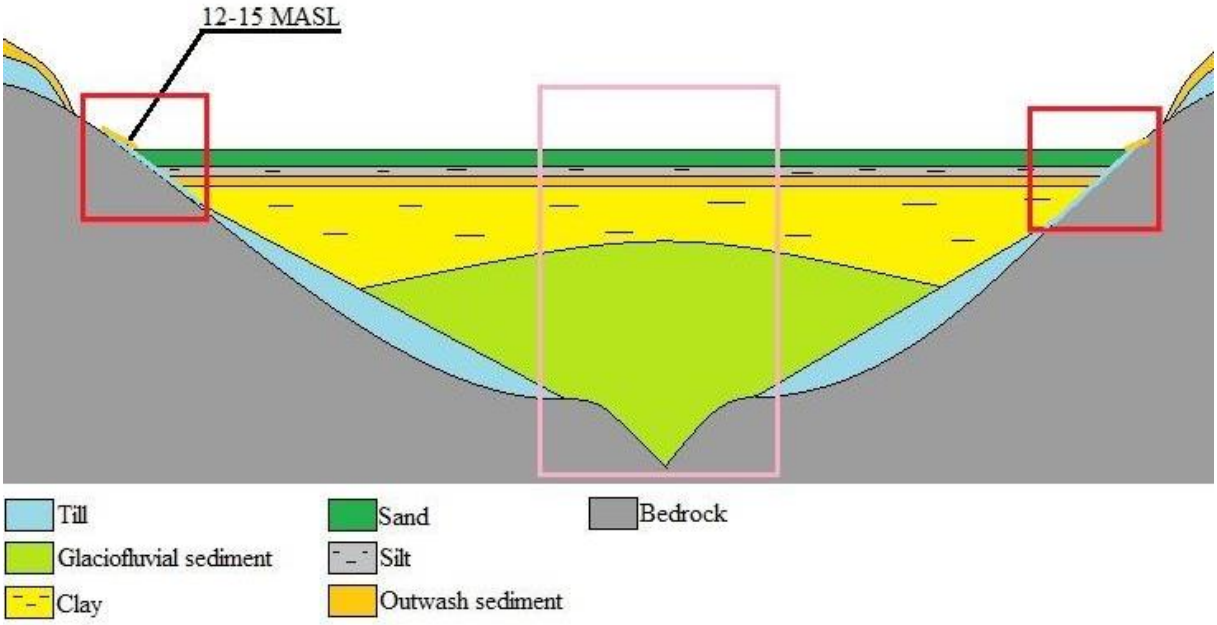

Figure 12. The conceptual model of sediments and aquifer system at the investigation sites as a cross-section of the valley system. Red squares represent aquifers which are confined to semiconfined (Vareborg and Southern trough and tunnel). The pink square represents the confined aquifer at Österleden.

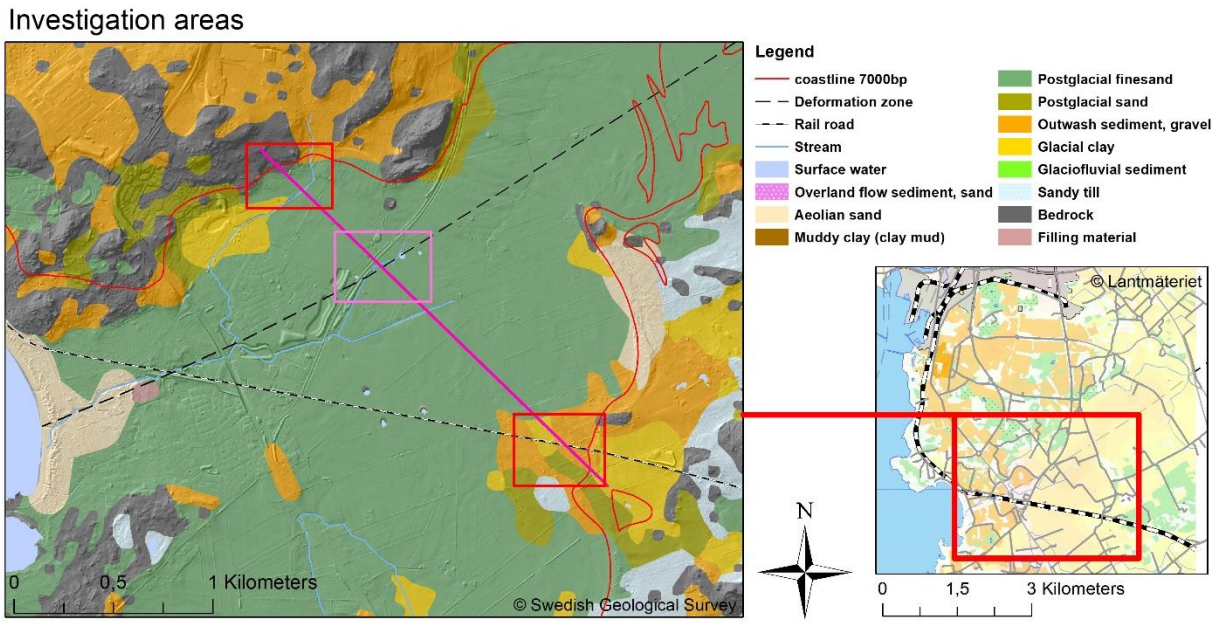

Figure 13. Displays the cross-section from aerial view. Red squares are the semi-confined investigation areas (Vareborg and the Southen trough and tunnel). The pink square is the confined investigation area (Österleden).

3.2 Field testing methods

The short duration hydraulic tests were performed between the 14th of November to the 13th of December 2020. Four field techniques, rising head with pump, slug, infiltration, and bailer where used to measure the saturated hydraulic conductivity (K) in 18 wells. Several field methods where used to evaluate if the results from different methods were consistent. The second reason is the evaluation of nonlinear effects (McElwee, 2001).

32 short duration hydraulic test had already been made by the first and second testing campaign. To assess if the results from different actors consist some of the already tested wells was tested again.

Before test started all wells inner radius and well height above or below the ground surface where measured. The depth to the water table and depth of the well was then measured with a piezometer. Pressure transducers (divers) where used in all wells to measure the pressure change.

3.2.1 Rising head test by pumping

A drainable pump with the capacity to pump water from a depth of 7 meters was used. The discharge during pumping was measured by count with a stopwatch the time it took to fill a 1 litre bucket with water. Water was pumped until the well was empty (in unconfined shallow aquifer) or water surface was below the pump, then the pump was turned off. If the inflow to the well was too high to pump the well dry or down below the pump, pumping continued until a satisfying drawdown had been achieved or until steady state flow, which means that pressure do not change with times (Bourdet, 2003). The recovery time was measured with a pressure transducer. All the equipment where left in the well throughout the test. This to avoid disturbance and to avoid that the diver moves during the recovery. During testing at investigation site Renen, water that had been pumped up was collected in 20 litre cans because of groundwater contamination. A disadvantage with this method that is important to point out is that the h_o is hard to exactly control.

3.2.2 Slug test-, infiltration-, and Bailer methods

To be able to do multiple tests, assess nonlinear effects (McElwee, 2001) and to compare results from different field methods slug and infiltration was used. Also, bailer was used for 1-inch wells.

A slug was used with the length (l), diameter (d) and volume (V) of 0.9 meter (m), 0.4 m and 0.0011 cubic meter (m^3), respectively. The theoretical hydraulic head change (h_o) caused by the slug is calculated by equation 5 (Kruseman, 1994). The theoretical h_o is for a HDPE wells with an inner radius (r_e) of 0.029 m is 0.42 m and for the steel pipes with an inner radius of 0.0255 m is 0.54 m.

$$h_o = \frac{V}{\pi r_e^2} \qquad (5)$$

The slug was instantaneously inserted in the well and left in until recovery of the static water level occurred. Then it was rapidly removed from the wellbore and the recovery time was

measured. Equation 5 for a 1-inch bailer with the volume of 0.000177 m^3, the radius of 0.0127 m and a length of 0.35 m results in an initial head displacement of 0.35 centimeters.

The infiltration method was used at the investigation site "Renen". Since there was a risk of contaminants in the groundwater the pumped water had to be collected in cans then poured back into the well. Due to safety precautions the water could not be moved to other containers and hence the water was poured back into the well without controlling the volume added. Were wells could be filled to the top of the well the increase in h_o could be theoretical calculated by knowing the depth to the static water level and the radius of the well.

3.2.3 Evaluation of field saturated hydraulic conductivity

3.2.3.1 Preparation of pressure data

Before the test initiates the initial pressure (p_i) downhole is constant. As the head is decreased or increased the pressure changes according to the change in the water column above the pressure sensor (figure 14). The recovery of the head is a function of time (t). The drawdown pressure response (Δp) of the test is calculated by equation 6 (Bourdet, 2003).

$$\Delta p = p_i - p(t) \qquad (6)$$

The pressure difference between the borehole and the aquifer produces a flow to or from the borehole (Hvorslev, 1951). The build-up pressure change for each time step (Δp) is calculated by equation 7, from the flowing pressure when time (t) is zero, p(t=0) (Bourdet, 2003).

$$\Delta p = p(t) - p(t = 0) \qquad (7)$$

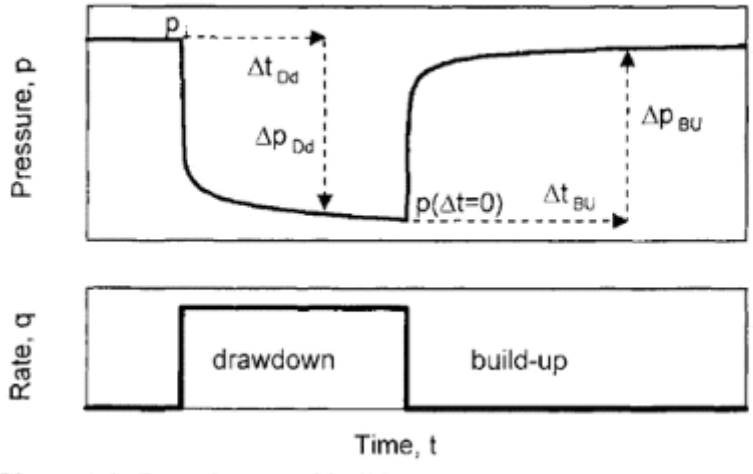

Figure 14. Pressure change because of a drawdown and equalization curves taken from figure 1.1 in Bourdet (2003). Well Test Analysis: The use of Advanced Interpretation Models. Retrieved from Elsevier Science.

As the recovery of the drawdown reach quasi-steady state (the recovery only dependent on the hydraulic conductivity of the porous media) the build-up pressure change is equal for each time step and the pressure recovery curve displays a straight line (Bourdet, 2003). The slope of the straight line is proportional to the hydraulic conductivity (Hvorslev, 1951).

The pressure data is expressed in millibar (mbar) by the pressure data logger. The initial displacement h_o (or $p(\Delta t=0)$) was set to time 0 in Excel. The build-up pressure was calculated by equation 7 for each timestep. The data was transformed to meter from water column (pressure) by the International System of Units (SI) which state that 1 centimeter of water at 4 degree Celsius (°C) equals to a pressure of 98.0665 Pascal (Pa) under the assumption that the water density is 1000 kg/m^3 (equation 8). This equals to 0.980665 mbar per centimeter (Thompson & Taylor, 2008).

$$\frac{\Delta p\ mbar}{0.980665\ mbar \times 100cm} = H\ meters \qquad (8)$$

If multiple test where performed in the well the pressure data from the tests where plotted as normalised head (h/h_o) versus time to assess impact of nonlinear effects (McElwee, 2001).

The basic time lag is calculated according to Hvorslev (1951). Hvorslev (1951) suggested that if there are no errors present during pressure equalization the total flow required for pressure equalization depends primarily of the permeability of the soil. The time it takes for equalization of the pressure difference between the well and the porewater pressure because of a change in head in the well is called basic time lag, equation 9.

$$\frac{t}{T} = \ln \frac{H_o}{H} \qquad (9)$$

Where t/T is the time lag ratio, H_o is the initial head displacement and H is the head displacement per time unit. If the assumptions for Hvorslev (1951) method are fulfilled the semi-logarithmic plotted recovery pressure data and time should display a straight line and the basic time lag correspond to a head ratio of 0.37.

3.2.3.2 Evaluation of hydraulic conductivity in Aqtesolv

The Hvorslev (1951) method was used for evaluating of the field data. The Hvorslev method states that the rate flow (q) to or from the well at any time (t) is proportional to the hydraulic conductivity (K). The Hvorslev method is under the assumption that the aquifer is isotropic, infinite in thickness and extent. Further, the aquifer is incompressible and artesian condition is prevailed or that inflow or outflow is small enough to not cause change in groundwater level or pressure (Hvorslev, 1951). In this evaluation an additional assumption will be that the aquifer thickness is the same as the screen length. Hvorslev neglect S_s in the formula under the assumption that the storage coefficient effect is insignificant (Koussis & Akylas, 2012). The method of Hvorslev is a straight forward method and do not consider nonlinear effect, velocity or acceleration, equation 10 (Hvorslev, 1951).

$$K = \frac{A}{F(t_2 - t_1)} ln \frac{H_1}{H_2} \qquad (10)$$

Where K is the hydraulic conductivity, A is the cross-section area of the standpipe and F is the intake shape factor. The validation of the data was made by a semi-logarithmic plot of head versus time. There are several situations producing deviation from linear theoretical models (McElwee & Zenner, 1998). The program Aqtesolv Pro (Duffield, 2007) will be used for evaluation.

For instantaneous initiation in high K aquifers the pneumatic method is most reliable but was not used in this work. Hence, the translation method for evaluation was used when there was noisy data in the early part of the test. In this method the noisy data at slug initiation is ignored in the evaluation and the h_o is selected where the pressure displays a straight line (Butler Jr & Healey, 1998).

A critical unknown property of the lower confined aquifer is the lack of data of the aquifers thickness which is needed for Hvorslev (1951) method. In this work the evaluation of the data the aquifer thickness is assumed to be the same as the screen length. This assumption is based on the theoretical fact that a slug test only tests the absolute vicinity of the screen (Fabbri, Ortombina, & Piccinini, 2012). A sensitivity analysis for the aquifer thickness parameter for 50 percent (%) of the screen length (l), 150 % and 600% of the screen length was made for the highest, median and lowest measurement at each investigation site. These values for parameter sensitivity (s) estimation are chosen based on that most screen lengths are 1 meter and that data from cone penetration test (CPT) from the second testing campaign suggests that the aquifer thickness seldom exceed 6 meters. The sensitivity was measured by equation 11.

$$s = \frac{Precentage\ change\ in\ input}{Precentage\ change\ in\ output} \qquad (11)$$

3.3 Compilation and analysis of field saturated hydraulic conductivity

The basics of the analysis of the saturated hydraulic conductivity data is that in a lognormal isotropic medium the geometric mean is the exact upscaled hydraulic conductivity (effective hydraulic conductivity) in a two-dimensional medium (Renard et al., 2000). The variability of hydraulic conductivity tends to exhibit lognormal distribution and therefore the central tendency can be represented by the geometric mean (or median) (Gupta et al., 2006). The assumption for this analysis is that the transient pumping tests represent the upscaled hydraulic conductivity (geometric mean) of the system tested. The variability of field data from short duration hydraulic test was assumed to be lognormally distributed and hence the central tendency (median) would for an isotropic homogenous medium equal the geometric (effective) hydraulic conductivity from transient pump tests. The Weibull formula (equation 12) for probability distribution (P) was used. The values ranked from highest to lowest (Svensson & Sällfors, 1985).

$$P = \frac{N+1-m}{N+1} \qquad (12)$$

Where N is number of measurements and m is the rank from highest to lowest measured hydraulic conductivity. The hydraulic conductivity data was plotted lognormally against P. The median in the data will be compared to the value of hydraulic conductivity evaluated from the transient pump test.

For this analysis results from both earlier performed short duration hydraulic tests and results from the field short duration hydraulic test was used (table 1 and 2). The results from rising head test with pump was used in first-hand. If the result from the rising head test with pump was indicating errors, results from slug, infiltration or Bailer tests will be used.

4. Results

4.1 Field saturated hydraulic conductivity

Table 3 displays wells that where tested in both testing campaigns and during the field work. Well 14T80325 to 14T8033 are a comparison between the first testing campaign, and the second. Wells 14T3056 to 14T3073 are comparison between field test made in this thesis and the first testing campaign (marked in grey). One well measured 130 times larger hydraulic conductivity for the first testing campaign compared to the second one (well 14T8026). The largest values for the other measurement are between 1.1 to 2.8 times larger.

Table 3. Displays wells that have been tested during both testing campaigns and in this thesis. The darker grey areas are hydraulic conductivities measured during the field work.

Well	K (m/s), second testing campaign	K (m/s), first testing campaign	Ratio
14T8025	2.6×10^{-7}	4.9×10^{-7}	1.9
14T8026	1.2×10^{-8}	1.6×10^{-6}	130.1
14T8028	4.3×10^{-6}	6.7×10^{-6}	1.6
14T8033	4.2×10^{-5}	5.3×10^{-5}	1.3
14T3056	1.0×10^{-3}	1.1×10^{-3}	1.1
14T7035	4.6×10^{-7}	1.3×10^{-6}	2.8
14T3073	4.7×10^{-6}	3.3×10^{-6}	1.4

During the field test three well construction types were used. Two- and one-inch steel pipes with perforated screen section and high-density polyethylene (HDPE) wells. The latter well type is installed in a borehole and filled with sand.

4.1.1 Unconfined aquifers

4.1.1.1 Renen

Rising head tests with pump and infiltration tests (falling head test) for all wells were made (figure 15). The pump that was used had no check valve (prevent backflow in the hose) installed and hence the rising head test got a sharper gradient in the beginning of the test due to that water in the hose went backwards after turning the pump of (figure 15). This error in the measurement are thought to not affect the result in aquifers with lower conductivity. While with higher transmissivity and faster recovery this effect will influence the result to a lager extent (U09G97, 14T335 and U09G83). The resolution of the transducer was two seconds, except for in well U09G97 where it was set to one second. 14T335, U09G97 and U09G84 have the sharpest gradient in the recovery curve. Due to high transmissivity in well U09G84 there was a problem to produce a larger drawdown. 14T335 had only 1.31 meters from the well bottom to the static water level and U09G97 had a sharp edge in the well which the pump got stuck on. Hence, a smaller drawdown was used in these wells.

There was disturbance in the test of U09G97 due to that the pump got stuck in the well and during attempt to remove the pump the transducer where moved around. Also, the well was clogged during the falling head test and recovery was not achieved.

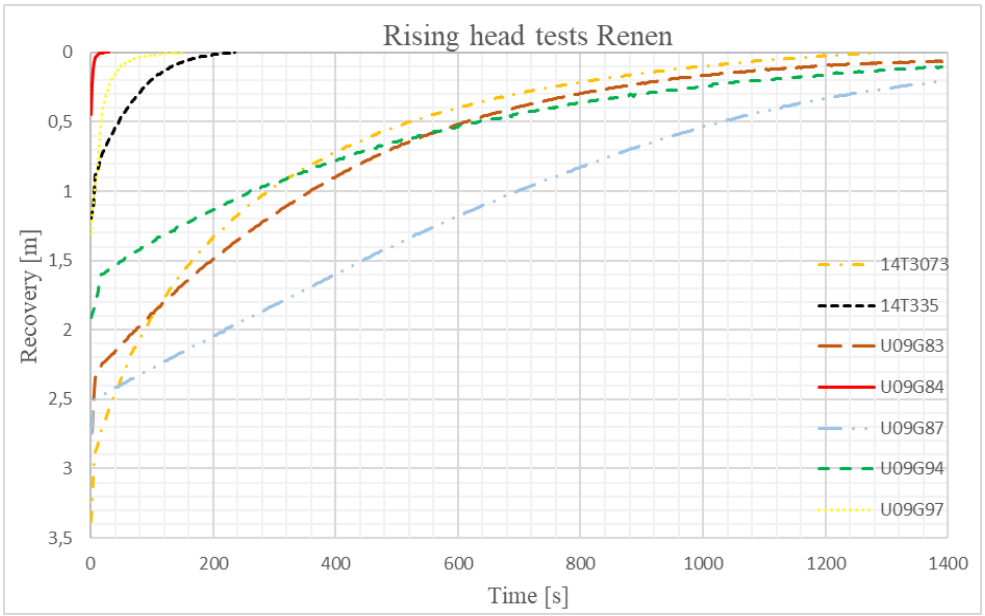

Figure 15. Rising head tests at Renen.

The recovery curves from falling head test can be seen in figure 16. Well U09G97 is excluded due to that the recovery of the head did not occur. The falling head test display the same appearance as the rising head test that U09G84 and 14T335 have the sharpest gradients in the recovery.

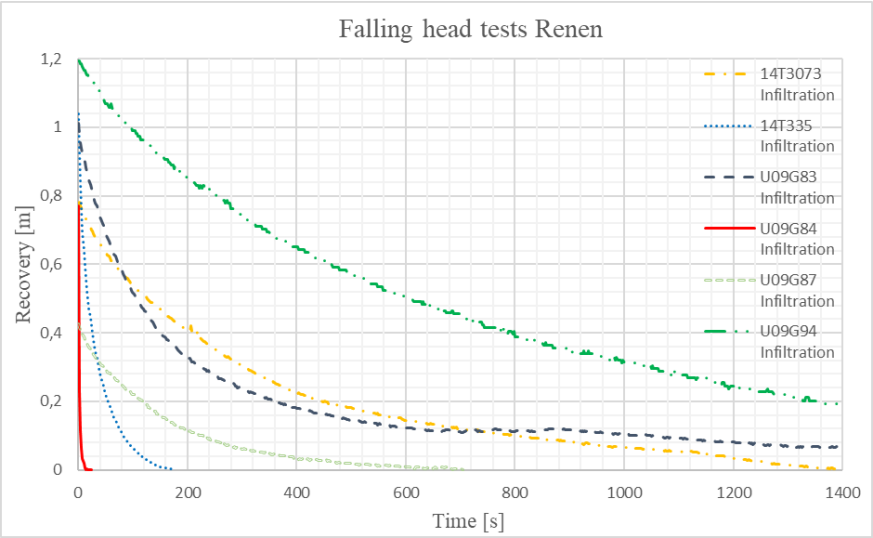

Figure 16. Falling head test Renen.

Figure 17 show the semi-logarithmic normalized heads and time for all wells which measured a hydraulic conductivity lower than 6×10^{-6} m/s. The solid lines are rising head tests with pump while the dashed are falling head tests (infiltration). The black dotted line is the basic time lag (0.37). Most of the test are displayed as straight lines. Both wells U09G94 and U09G87 are slightly concave downward. The falling head test for well U09G83 are not a straight line. This could be due to filter package drainage since the screen are above the static ground water level (Bouwer, 1989). For wells without nonlinear effects the both different tests would display identical recovery curves on the semi-logarithmic plot. The recovery curves from U09G87 are the well which displays most impact of nonlinear effects. In this well 60 part per million (ppm) of gas was measured with a photoionization detector (PID). This can decrease the effective pore space and effect the measured hydraulic conductivity (Hvorslev, 1951). In the other wells there was no gas detected. The PID was not used in U09G94 and U09G97.

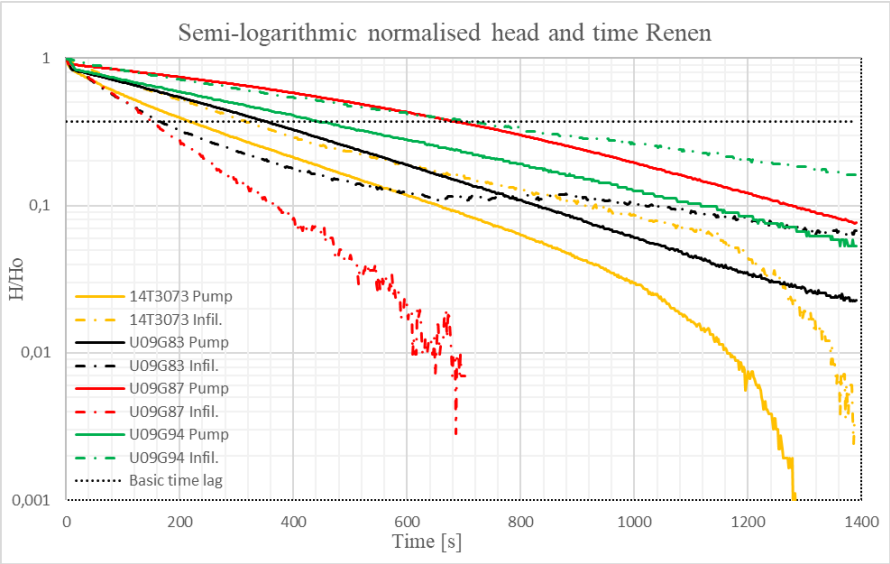

Figure 17. Display the semi-logarithmic normalized heads and time for all wells which measured a hydraulic conductivity slower than 6×10^{-6} m/s. Both the falling head (infiltration) and the rising head (pump) for each well is shown.

Figure 18 displays the semi-logarithmic plot for U09G83, U09G97 and 14T335 which have hydraulic conductivities of 6×10^{-5} m/s or higher. U09G84 have the sharpest gradient and the rising head and falling head tests are well agreed. Results from 14T335 deviates more from each other.

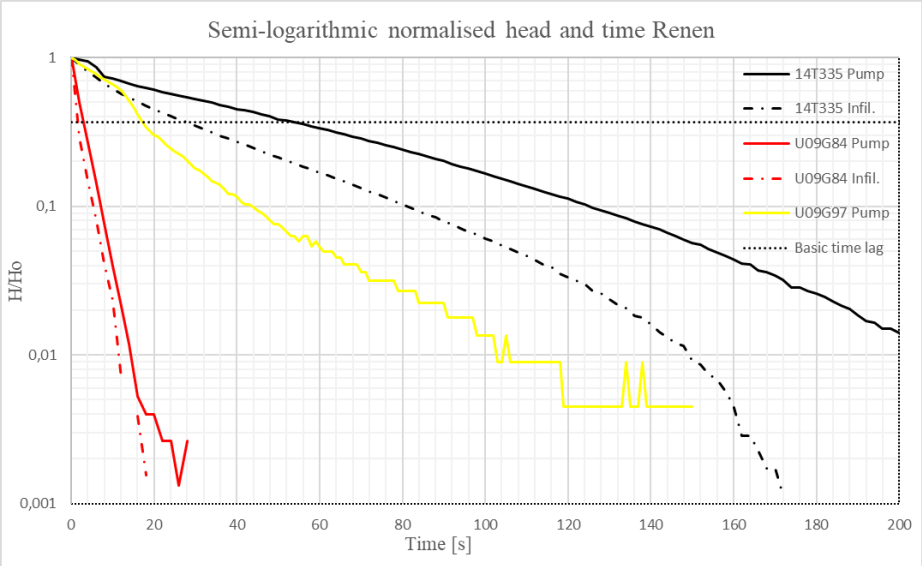

Figure 18. Displays the semi-logarithmic plot for U09G83, U09G97 and 14T335 which have hydraulic conductivities of 6×10^{-5} m/s or faster.

Table 4 shows the hydraulic conductivities calculated in Aqtesolv. In well U09G84 the highest hydraulic conductivity was measured at 4.4×10^{-4} m/s which deviate clearly from the results from other wells. Also, well U09G97 measured a higher conductivity than the rest of the wells with a hydraulic conductivity of 7.0×10^{-5} m/s. All other measurements are within an order of magnitude.

Table 4. Show the calculated hydraulic conductivities for the rising head tests (pump) and falling head tests (infiltration) at Renen. MASL is the ground surface above sea level. GW (masl) is the groundwater surface above sea level. GW (m) is the meter below or above the ground surface. L/R is the aspect ratio between the screen length and the radius of the screen.

Well	MASL	GW (MASL)	GW (m)	L/R	Pump, K (m/s)	Infil. K (m/s)	Well construction
14T3073	2.1	1.2	-0.92	34	4.7×10^{-6}	4.5×10^{-6}	2” HDPE
14T335	3	1.1	-1.88	34	3.0×10^{-5}	4.5×10^{-5}	2” HDPE
U09G83	2.1	0.8	-1.31	103	2.3×10^{-6}	1.9×10^{-6}	2” HDPE
U09G84	2.1	0.6	-1.53	39	4.4×10^{-4}	4.4×10^{-4}	2” Steelpipe
U09G87	2.4	1.1	-1.32	103	1.1×10^{-6}	4.0×10^{-6}	2” HDPE
U09G94	2	0.5	-1.47	39	3.2×10^{-6}	2.2×10^{-6}	2” Steelpipe
U09G97	2.2	0.7	-1.54	39	7.0×10^{-5}	-	2” Steelpipe

Table 5 displays the initial head displacement, the measured hydraulic conductivity and the method used for multiple tests. The infiltration method was always carried out after the rising head with pump test (called pump in table 5). The result display higher K-values for a larger

initial head displacement, except in well U09G87 where the smaller displacement yielded the highest K-value. The smallest initial head displacement yielded 33.4 to 1.6 percent lower K-values. The lowest head displacement for well U09G87 measured a 363.6 percent higher K-value then the larger displacement. There was no trend dependent on method used or dependent on order of test.

Table 5. Displays the hydraulic conductivity (m/s) dependent on initial head displacement (h_o). The percentual change between the highest and lowest initial head is shown in column 4 (% change).

Well 14T3073	h_o (m)	K (m/s)	% Change	Method
	3.9	4.7×10^{-6}		Pump
	0.9	4.5×10^{-6}	-5.1	Infiltration
14T335				
	1.8	4.5×10^{-5}		Infiltration
	1.31	3.0×10^{-5}	-33.4	Pump
U09G83				
	2.2	2.3×10^{-6}		Pump
	1.25	1.9×10^{-6}	-17.0	Infiltration
U09G84				
	0.8	4.5×10^{-4}		Infiltration
	0.45	4.4×10^{-4}	-1.6	Pump
U09G87				
	2.8	1.1×10^{-6}		Pump
	1.25	4.0×10^{-6}	363.6	Infiltration
U09G94				
	2	3.2×10^{-6}		Pump
	1.4	2.2×10^{-6}	-33.3	Infiltration

4.1.2 Semiconfined (leaky) aquifers

4.1.2.1 Southern trough and tunnel

All the tested wells displayed artesian condition with the groundwater level (GW) above ground surface. Figure 19 displays all rising and falling head tests (for larger initial head displacements) except 17T706. The falling head tests are slug tests. The well 14T728 measured a depth in field from the well top to bottom of 6.55 meters. According to the field data from the construction of the well it should be 8.92 meter deep. There has not been any earlier performed slug test but from pump test during the first testing campaign the hydraulic conductivity was estimated to be 1×10^{-4}. 14T728 is therefor thought to be clogged and the result not reliable.

As can be seen in the figure the recovery is steep between 2 to 3 meters and then there are no further recovery. In field full recovery in well 14T714 did not occur. The transducer did show a recovery from 0.5 meters drawdown as can be seen in figure 19. The drawdown corresponds relatively well with the theoretical initial head displacement of 0.54 meters. There is a risk that the measurement with the piezometer in field is wrong since the recovery was not detected. Still, the measurement of hydraulic conductivity in well 14T714 should be used with caution. During the falling head test in 17T714 (slug) water poured out of the well due to high static water level in the well. The initial head displacement was 0.1 meter lower than the theoretical initial head displacement of 0.42 meters.

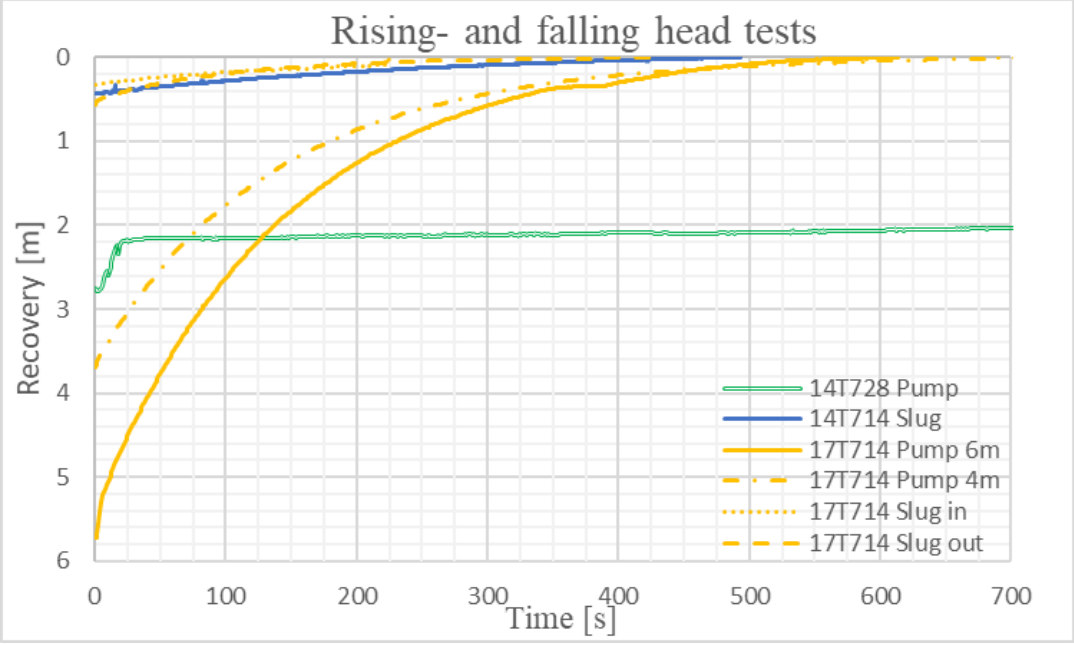

Figure 19. Rising- and falling head tests for larger initial head displacements.

In figure 20 recovery curves from well 17T706 are presented. The transducer resolution of two seconds was to coarse for the fast respond in the well. During falling head test (slug) water was poured over the edge of the well because of high static water level. The result from the slug must hence be read with caution. Disturbance during slug initiation seems to have affected the transducer and produced a higher initial head displacement than the theoretical initial head displacement. For the rising head test with pump two different pumps where used with different

capacities. Only 0.15-meter drawdown was achieved with a stronger pump (pump 2) until steady state. The recovery after switching of the pump was too fast for the transducer to record and hence the flat appearance in the diagram.

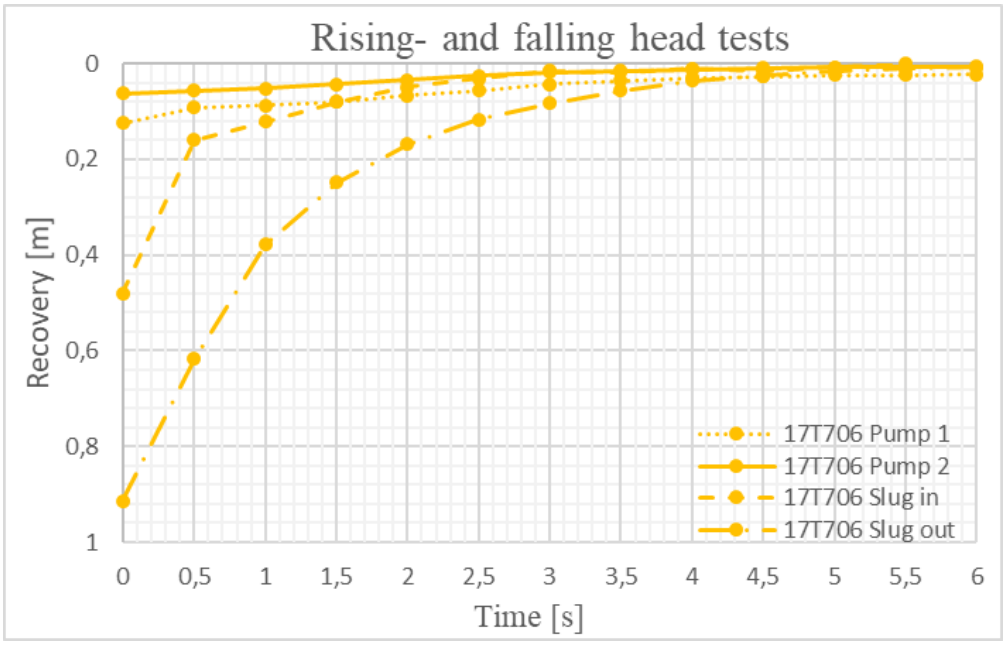

Figure 20. Rising- and falling head test in well 17T706 (smaller initial head displacement).

Figure 21 displays semi-logarithmic head ratio and time for well 17T714. Both rising head test with pump displays similar appearance. The recovery curve from slug removal displays a sharper gradient in the beginning of the test. The slug tests display more deviations from each other than the rising head test with pump.

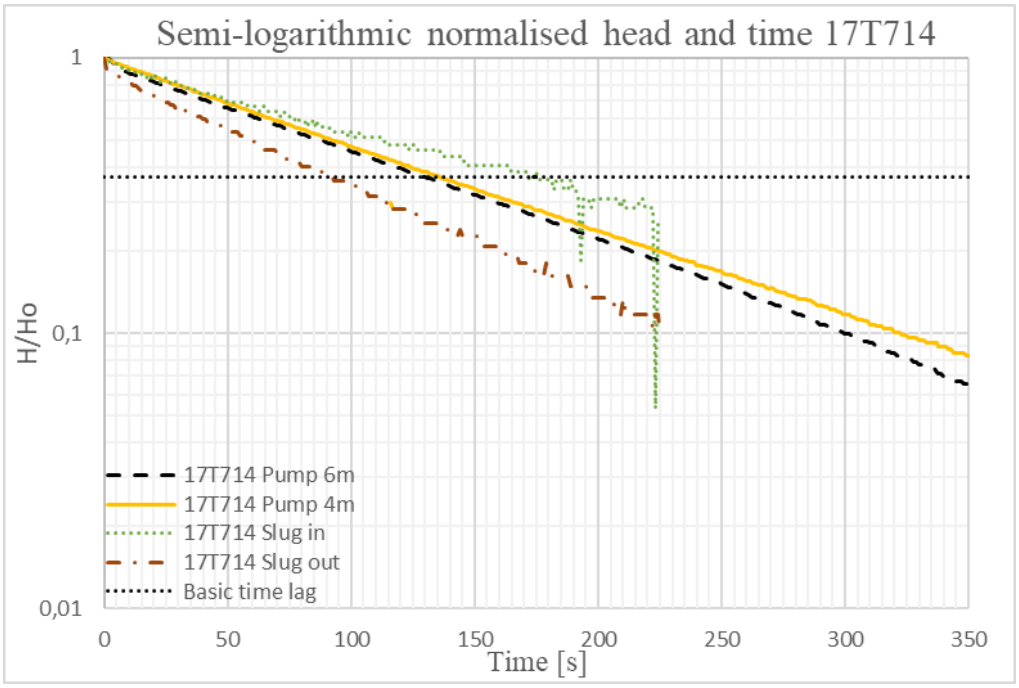

Figure 21. Multiple tests on a semi-logarithmic head ratio diagram for well 14T714.

Semi-logarithmic head ratio and time for well 17T706 is presented in figure 22. The well displays high impact of nonlinear effects. The slug tests do show straight lines after approximately 1 second. The rising head tests with pump are hard to evaluate according to Hvorslev (1951). The Cooper-Jacob straight line method of the drawdown curve was therefore used as evaluation method.

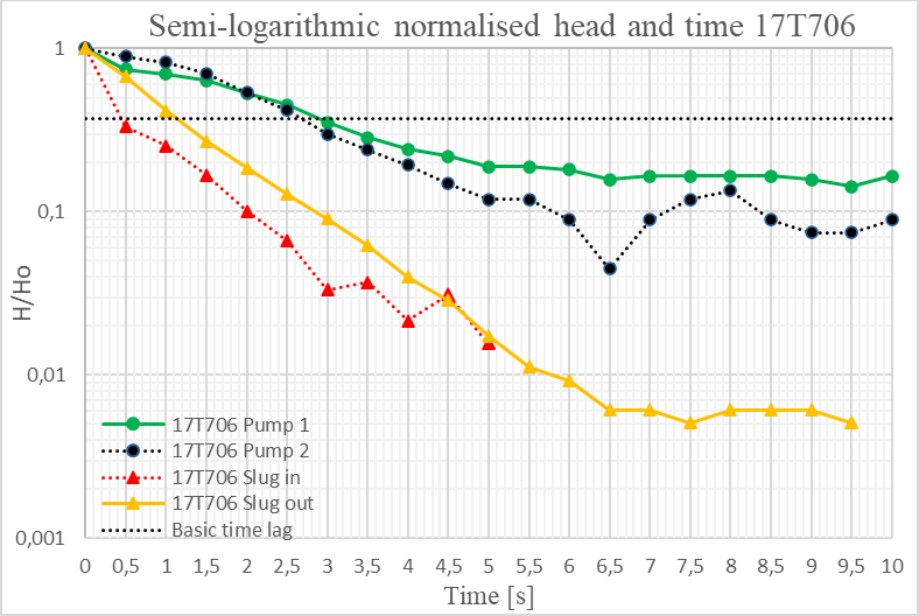

Figure 22. Multiple tests in a semi-logarithmic head ratio diagram for well 17T706.

In Table 6 calculated hydraulic conductivities are shown. Recovery curve in well 14T728 indicate clogging since the well do not recover completely. Well 17T706 measured high hydraulic conductivities 1.8×10^{-3} m/s. The 6-meter drawdown measurement is used for well 17T714 and the slug removal measurement for well 17T706. The slug removal for 17T706 was chosen because this displayed the longest straight line on the semi-logarithmic plot and the Hvorslev (1951) method was used (figure 22).

Table 6. Show the calculated hydraulic conductivities for the rising- and falling head tests (slug and pump) at southern trough and tunnel. MASL is the ground surface above sea level. GW (masl) is the groundwater surface above sea level. GW (m) is the meter below or above the ground surface. L/R is the aspect ratio between the screen length and the radius of the screen.

Well	MASL	GW (MASL)	GW (m)	L/R	K (m/s)	Field method	Well construction
14T728	9.5	9.5	0	75	7.8×10^{-8}	Pump	2” Steelpipe
17T714	8.9	9.6	+0.72	34	1.4×10^{-5}	Pump	2” HDPE
14T714	8.5	9.1	+0.56	39	3.8×10^{-6}	Slug in	2” Steelpipe
17T706	9.2	10.1	+0.90	69	1.8×10^{-3}	Slug out	2” HDPE

Table 7 present the multiple tests carried out at Southern trough and tunnel. The slug tests were performed first. Well 17T714 measured highest hydraulic conductivity for the largest initial head displacement for rising head with pump. Slug removal (slug out) did measure the highest K-value almost 23 percent higher than the 6-meter drawdown with pump. Well 17T706 had

high hydraulic conductivity and a drawdown was almost not possible to produce. The lower initial head displacement for the pump measured lower hydraulic conductivities. During the slug initiation (slug in) water flowed over the edge of the well. This happened for slug initiation in both wells.

Table 7. Displays the hydraulic conductivity (m/s) dependent on initial head displacement (ho) for well 17T714 and 17T706. The percentual change from the highest initial head is shown in column 3 (% change).

17T714			
Ho (m)	**K (m/s)**	**% Change**	**Method**
6	1.4×10^{-5}	0	Pump
4	1.3×10^{-5}	-5.9	Pump
0.42	1.0×10^{-5}	-25.0	Slug in
0.42	1.8×10^{-5}	22.7	Slug out
17T706			
0.42	2.0×10^{-3}	0	Slug in
0.42	1.8×10^{-3}	-14.2	Slug out
0.12	1.0×10^{-3}	-49.0	Pump
0.06	1.1×10^{-3}	-46.6	Pump

4.1.2.2 Vareborg

The field test was performed during the second testing campaign and evaluated in Aqtesolv in this thesis. Figure 23 displays wells with a faster recovery time, under 2000 seconds. The appearance of the recovery curves for several test deviate from a normal appearance, especially in well U19G37. For three of the tests there is a disturbance in the middle of the recovery (well 14T78028, U19G35 and 14T8033).

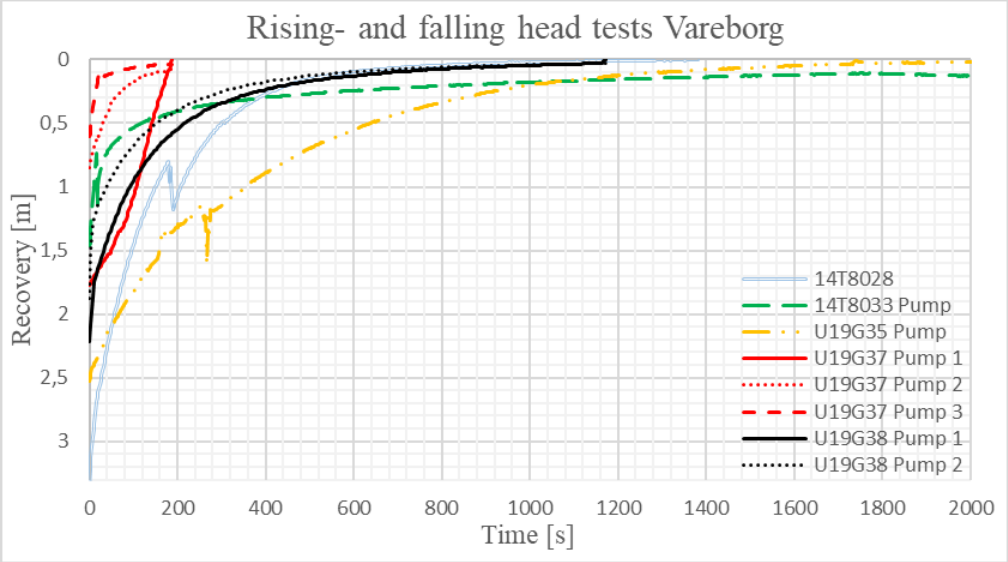

Figure 23. Rising- and falling head tests for short recovery time (<2000 seconds).

Figure 24 shows wells with longer recovery times, over 2000 seconds. In well 14T8025 and 14T8026 infiltration was used as field method since the wells were 1-inch wells. This well had a longer recovery time than 10000 seconds.

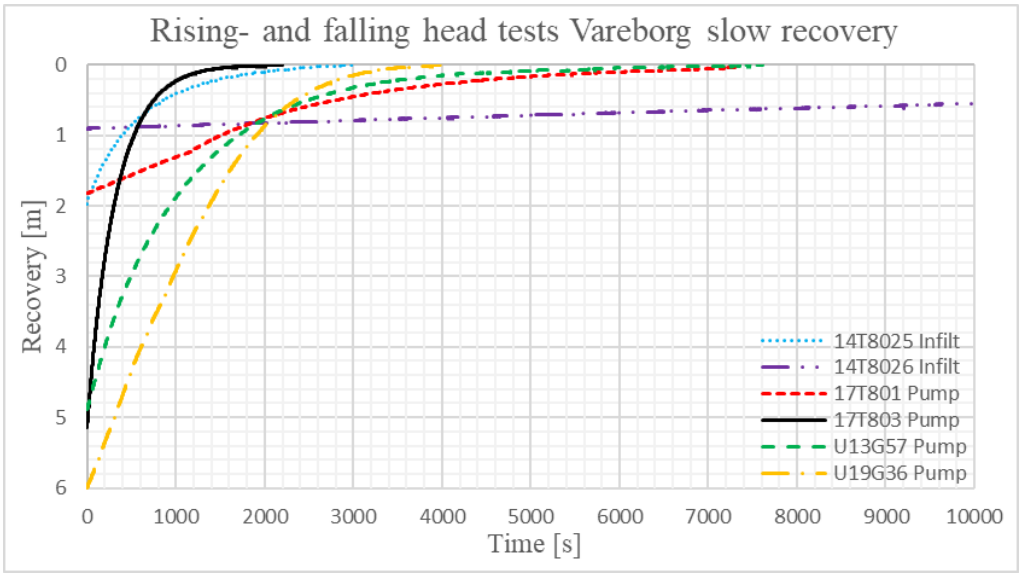

Figure 24. Rising- and falling head tests for long recovery time (>2000 seconds).

In figure 25 all measurement with longer recovery times than 2000 seconds are showed on a semi-logarithmic plot. All semi-logarithmic recovery curves display straight lines except well

U19G36. Well U19G36 are slightly concave downward. This well was pumped to steady state and the Cooper-Jacob straight line method was used for evaluation.

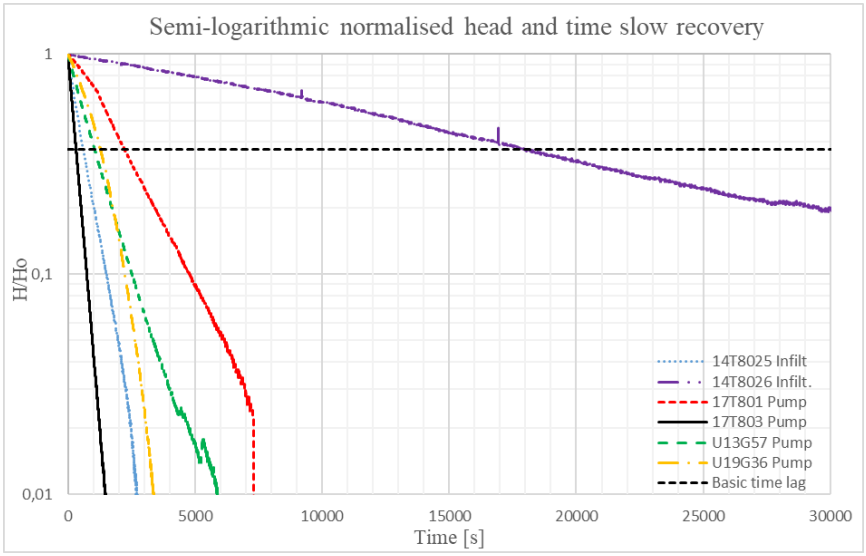

Figure 25. Rising- and falling head tests on a semi-logarithmic plot for long recovery time (>2000 seconds).

In figure 26 the semi-logarithmic head ratio plot is displayed for measured hydraulic conductivities that recovered within 2000 seconds. There is only well U19G35 that displays a continuous straight line (except the disturbance). Both test for U19G38 are concave upward but follow each other well. The appearance of the recovery curves in well 14T8028 and 14T8033 are because the wells where pumped to steady state. Cooper-Jacob straight line method for evaluation was used on the drawdown curve for these two wells. Well U19G37 displays fundamentally different recovery for the three rising head test that was made. The second test displayed the straightest line.

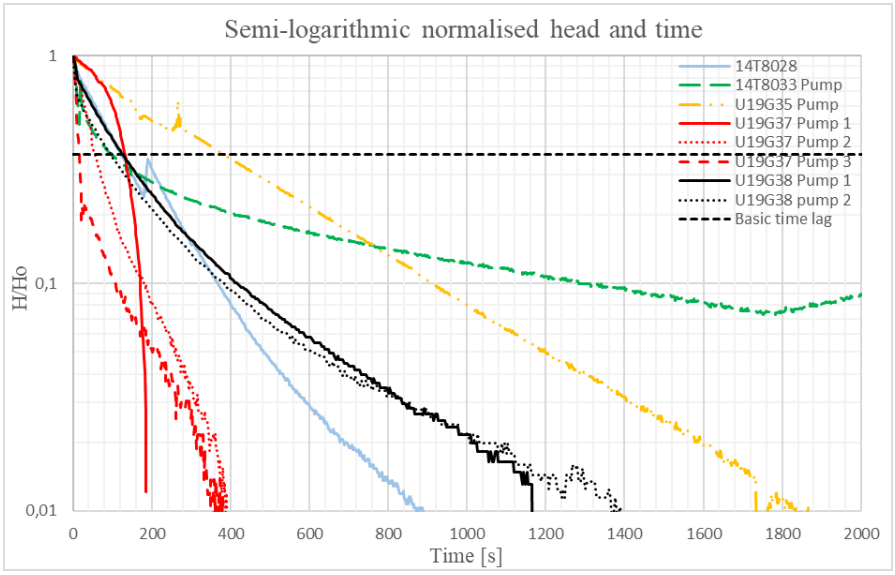

Figure 26. Rising head tests on a semi-logarithmic plot for short recovery time (<2000 seconds).

Table 8 present measured hydraulic conductivities for Vareborg. Wells 14T8025, 14T8026, 17T801 and U19G36 measure lower hydraulic conductivities than the other wells which are all between 1.6×10^{-6} m/s to 3.3×10^{-5} m/s. Well 14T8028, 14T8033, 17T807 and U19G36 was pumped to steady state and the drawdown curve where evaluated with the Cooper-Jacob method. The first testing campaign assumed an aquifer thickness of two meters. This thickness was used to calculate the hydraulic conductivity.

Table 8. Show the calculated hydraulic conductivities for the rising- and falling head tests (slug and pump) at Vareborg. MASL is the ground surface above sea level. GW (masl) is the groundwater surface above sea level. GW (m) is the meter below or above the ground surface. L/R is the aspect ratio between the screen length and the radius of the screen. For measurement were the Cooper-Jacob method was used transmissivity in column 7 was divided with the aquifer thickness (2 m) to obtain the hydraulic conductivity in column 6.

Well	MASL	GW (MASL)	GW (m)	L/R	K (m/s)	T (m^2/s), CooperJacob	Well construction
14T8025	15.5	14.9	-0.65	197	2.6×10^{-7}		1” Steel pipe
14T8026	15.8	14.9	-0.92	157	1.2×10^{-8}		1” Steel pipe
14T8028	16.0	16.0	0.00	39	3.0×10^{-6}	6.1×10^{-6}	2” HDPE
14T8033	15.6	14.7	-0.86	39	3.3×10^{-5}	6.5×10^{-5}	2” HDPE
17T801	15.7	15.0	-0.72	39	9.1×10^{-7}		2” Steel pipe
17T803	13.2	12.6	-0.64	39	5.4×10^{-6}		2” Steel pipe
17T807	14.4	12.9	-1.49	39	2.2×10^{-5}	4.4×10^{-5}	2” HDPE
U13G57	14	13.6	-0.40	39	1.6×10^{-6}		2” Steel pipe
U19G35	16	144	-1.62	39	4.2×10^{-6}		2” Steel pipe
U19G36	15.4	14.9	-0.48	39	8.6×10^{-7}	1.7×10^{-6}	2” Steel pipe
U19G37	12.8	12.1	-0.75	39	2.2×10^{-5}		2” Steel pipe
U19G38	16.2	15.0	-1.01	39	1.0×10^{-5}		2” Steel pipe

4.1.3 Confined aquifers

4.1.3.1 Österleden

Figure 27 displays recovery curves for rising head test performed at Österleden which measured hydraulic conductivity under 1×10^{-5} m/s. There is a clear difference in recovery in wells U19G29, U12G36 and 17T711 compared to the other wells with steeper recovery curves. In well U19G32 the Bailer method had to be used in field since the well was a one-inch well hence the smaller drawdown.

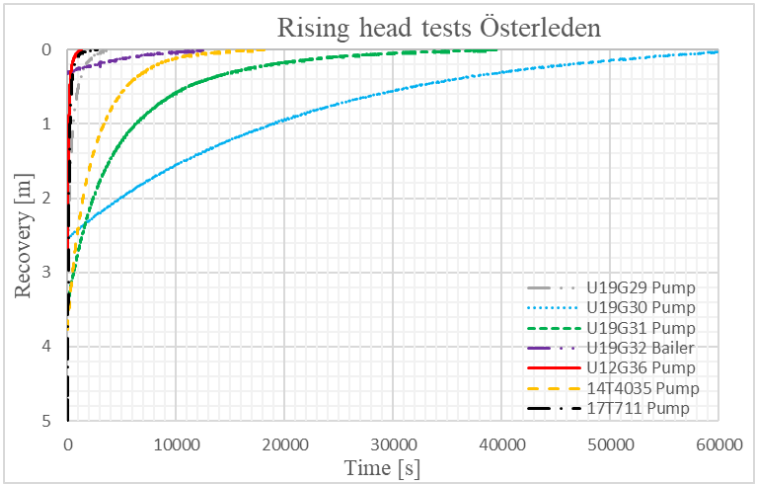

Figure 27. Rising head tests Österleden.

In the following figures (28, 29 and 30) the rising head test with drawdowns smaller than 1.5 meters and a recovery time faster than 100 seconds are presented.

The recovery curves for the slug tests in well U19G33 (figure 28) display different initial heads. The theoretical initial head change is 0.54 meters. The slug removal from the first slug test (slug 1 out) was the only test that recorded an initial head change that agreed with the theoretical calculated initial head. All the other slug test displays a fast decline in head the first five seconds (from approximate 1 meter to 50 centimeters) then the recovery slows down and follows the recovery curve of the rising head test with pump.

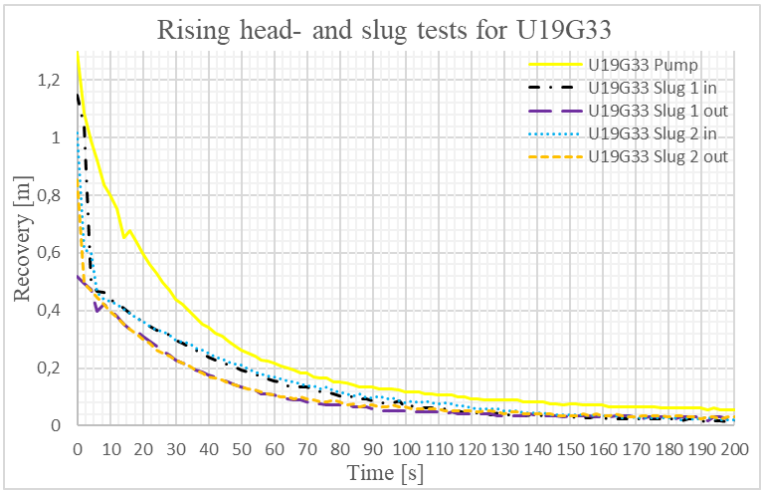

Figure 28. Rising head - and slug tests in well U19G33.

Figure 29 shows underdamped response in well 14T7036. The response indicates an aquifer with very high hydraulic conductivity. Hvorslev (1951) method was not possible to use on this well due to oscillatory response. Therefor, the method for oscillatory response by Butler Jr (1998) was used. During the rising head test with pump in the same well the pump went broken and lost power. When the pump was turned off the recovery had started, and the recovery curve had flattened out.

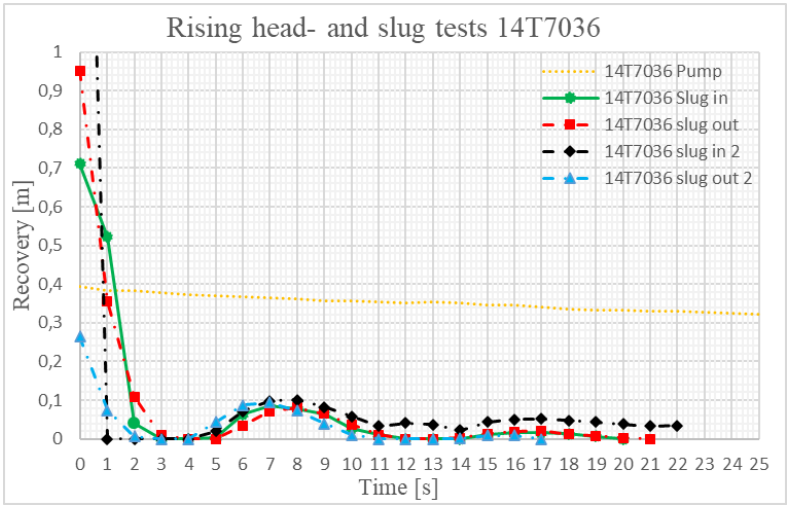

Figure 29. Rising head test and slug tests in well 14T7036.

Figure 30 shows aquifer tests in well U12G35. The response in this well was rapid and the resolution on the transducer was too coarse for the slug test which makes the tests hard to evaluate. Still, the response indicates an aquifer with high hydraulic conductivity. The Butler Jr (1998) method was used for comparing with the Hvorslev method. Due to the low resolution the curve matching was not exact, and the obtained hydraulic conductivity was between 1×10^{-3} to 5×10^{-3} m/s with the Butler Jr (1998) method. Since the appearance of the response in figure 30 are slightly oscillatory the hydraulic conductivity measured with the Hvorslev could be lower than the actual hydraulic conductivity. The Hvorslev method measured a hydraulic conductivity of 2.3×10^{-4} m/s (table 9).

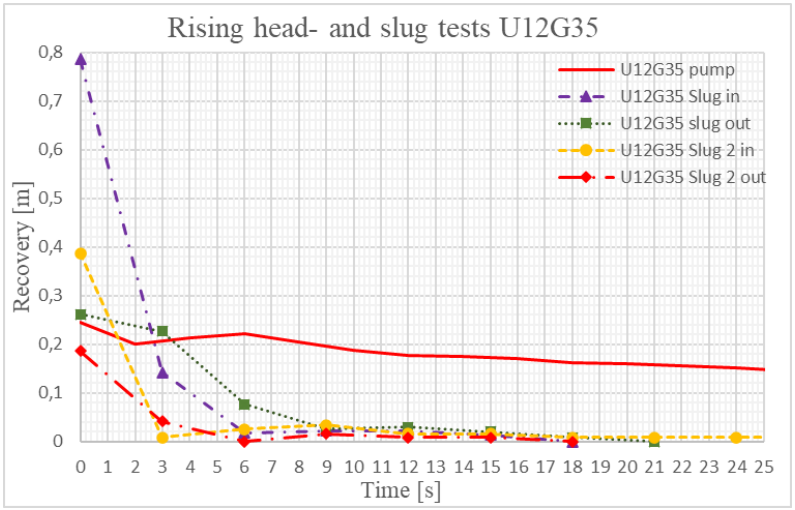

Figure 30. Rising head test and slug tests in well U12G25.

Figure 31 shows the semi-logarithmic plot for rising head test that measured hydraulic conductivities slower than 1×10^{-5} m/s. All displays straight lines. The appearance of U19G32 could be due to that the resolution of the transducer was too high compared to the recovery rate.

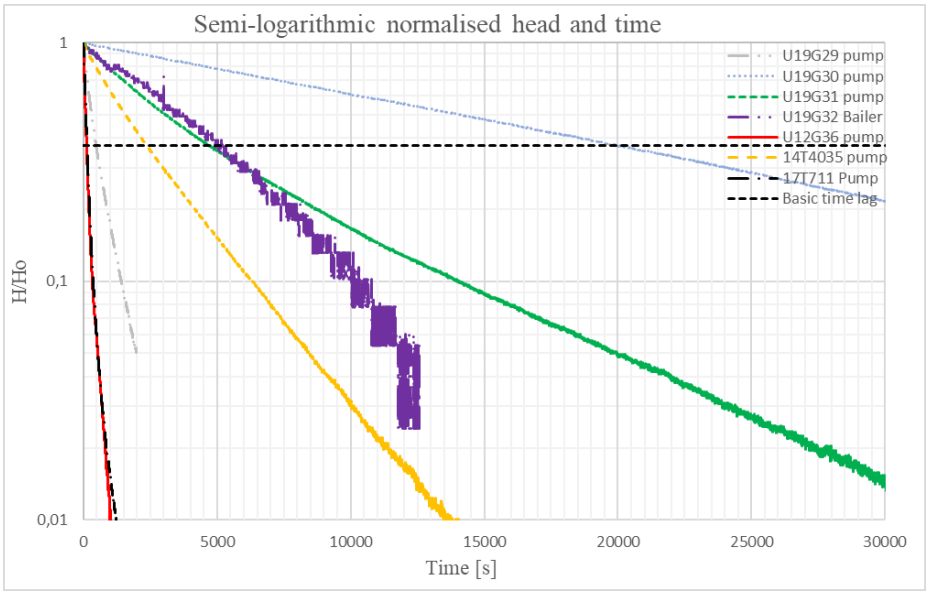

Figure 31. Display the semi-logarithmic plot for all wells measuring hydraulic conductivity under 1×10^{-5} m/s.

Figure 32 display semi-logarithmic plots of multiple tests (rising head test and slug test) for well U19G33. The slug test displays a double straight-line effect for three of four tests. The rising head test (pump) do not display the same appearance. If this where related to the wellbore skin effect the appearance would be the same for all the tests (Moench, 1998). The inclinations of the straight lines after the disturbance in the beginning was used for evaluation.

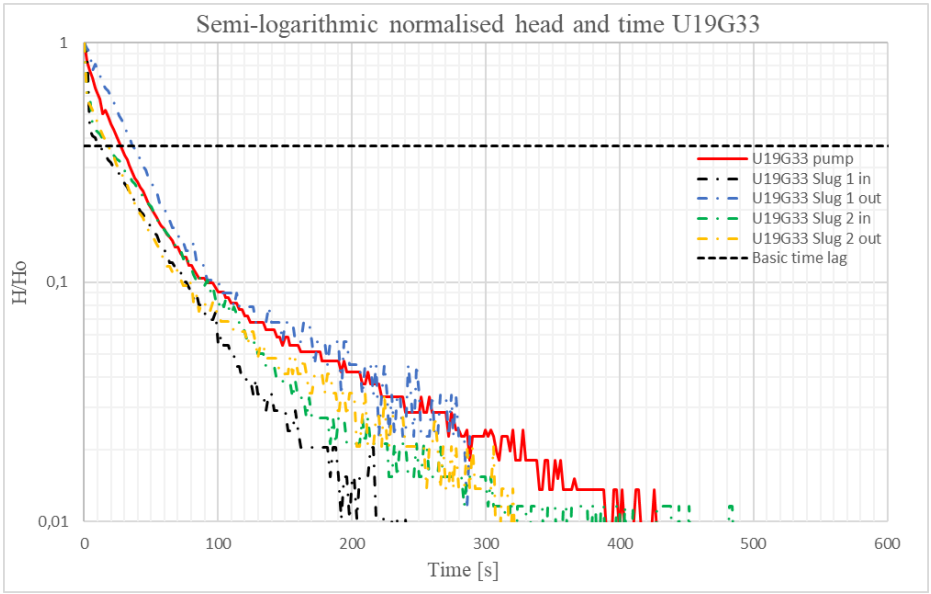

Figure 32. Multiple tests in well U19G33.

Figure 33 displays rising head test and slug test for measured hydraulic conductivities higher than 9×10^{-5} m/s. 14T7036 displays oscillatory response. U12G35 show a slight increase after

the recovery. The transducer resolution was set to coarse in this well and hence with a finer resolution the response could be different than seen in figure 33. Both rising head test with pump shows a different result with a flatter recovery curve. The hydraulic conductivity was high enough to not be able to produce a drawdown larger than 0.1 meter in U12G35 and the recovery was too fast to get any records. The only test from well U12G35 that could be evaluated was the slug removal from the first test round (purple line in figure 33). The appearance in the rising head test by pump in 14T7036 was due to that the pump broke and lost power and the head started to recover during the pumping of the well.

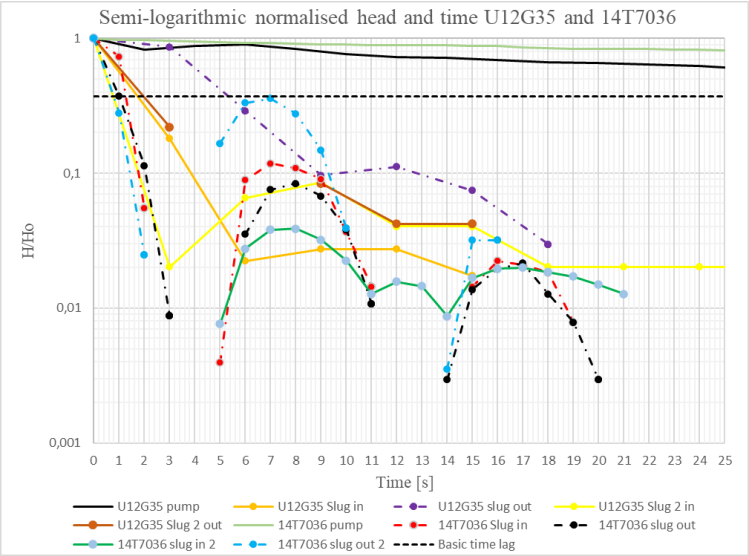

Figure 33. Semi-logarithmic head ratio plot for multiple testing in well U12G35 and 14T7036.

In table 9 the evaluated hydraulic conductivities are presented. Wells U12G35 and 14T7036 measured high hydraulic conductivities compared to the other wells in the investigation area. For well 14T7036 the measured hydraulic conductivity from the slug test was used. In well U12G35 the Cooper-Jacob method measured a transmissivity of 2.2×10^{-4} m^2/s.

Table 9. Show the calculated hydraulic conductivities for the rising- and falling head tests (slug and pump). MASL is the ground surface above sea level. GW (masl) is the groundwater surface above sea level. GW (m) is the meter below or above the ground surface. L/R is the aspect ratio between the screen length and the radius of the screen.

Well	MASL	GW (MASL)	GW (m)	L/R	K (m/s)	Method	Well construction
U19G31	9.4	9.8	+0.38	39	2.4×10^{-7}	Pump	2” Steel pipe
14T7036	9.1	8.7	-0.45	34	2.7×10^{-3}	Slug	2” HDPE
U12G36	9.7	9.6	-0.09	39	1.4×10^{-5}	Pump	2” Steel pipe
17T711	9.0	9.0	-0.02	34	1.6×10^{-5}	Pump	2” HDPE
U19G33	8.9	8.5	-0.38	39	5.1×10^{-5}	Pump	2” Steel pipe
U19G32	9.2	9.0	-0.19	71	9.4×10^{-8}	Bailer	1” Steel pipe
U19G29	9.1	9.1	-0.02	39	2.5×10^{-6}	Pump	2” Steel pipe
U19G30	9.8	9.9	+0.08	39	8.6×10^{-8}	Pump	2” Steel pipe
U12G35	9.2	8.4	-0.76	39	2.3×10^{-4}	Slug	2” Steel pipe
14T7035	9.6	9.9	+0.30	39	4.6×10^{-7}	Pump	2” Steel pipe

Table 10 present multiple tests performed at Österleden. All slug test where performed first and than the rising head test with pump. All the slug test yielded lower hydraulic conductivity then the rising head test with pump for well U19G33, which had a larger initial head displacement. The slug method measured 36.9 to 6.3 percent lower hydraulic conductivities. The insertion of the slug yielded K-values that deviated more from the rising head test with pump compared to the removal of the slug, around 30 percent compared to 10 percent respectively.

Due to problems with the pump in well 14T7036 enough drawdown where not produced and the measurement is not reliable since the recovery started before the pump was turned off. Therefor, the method yielded a mush lower K-value than the other methods. The slug test yielded oscillatory response. The first slug test measured lowest hydraulic conductivity. Since no comparison can be made for different initial head displacement the change from the mean (3.0×10^{-3} m/s) are showed. The initiation of the slug measured the highest deviation from the mean. Here it should be mentioned that the measured initial head displacement in field deviated extremely from the theoretical. At the most the measured initial displacement where more than two times larger than the theoretical displacement (0.95 m).

Table 10. Displays the hydraulic conductivity (m/s) dependent on initial head displacement (h_o) for well U19G33 and 14T7036. The percentual change from the highest initial head is shown in column 3 (% change). For well 14T7036 the percentual change is shown as deviation from the mean value since no different h_o where used.

U19G33			
Ho (m)	**K (m/s)**	**% Change**	**Method**
1.2	5.1×10^{-5}	0	Pump
0.54	3.5×10^{-5}	-32.0	Slug in
0.54	4.8×10^{-5}	-6.3	Slug out
0.54	3.2×10^{-5}	-36.9	Slug in
0.54	4.6×10^{-5}	-9.8	Slug out
14T7036		**% Change from mean**	
0.42	2.6×10^{-3}	-10.5	Slug in
0.42	2.8×10^{-3}	-4.8	Slug out
0.42	3.7×10^{-3}	19.8	Slug in
0.42	2.7×10^{-3}	-9.5	Slug out
0.40	7.6×10^{-6}		Pump

4.2 Sensitivity analysis for aquifer thickness

Table 11 displays a sensitivity (s) analysis for different screen length (or aquifer thickness). As can be seen, if the aquifer thickness is assumed to be the same as the screen length the sensitivity is high for an aquifer thickness that is thinner than the screen length. This would result in an overestimation of the hydraulic conductivity of around 400 percent. The parameter sensitivity is lower for an underestimation of the aquifer thickness (the screen length is shorter than aquifer

thickness). For a 200 percent thicker aquifer than the screen length the hydraulic conductivity will be underestimated by 0 to 15 percent, but most common under 10 percent. With an increased aquifer thickness the sensitivity of parameter estimate decrease.

The sensitivity analysis for the aquifer thickness parameter (Table 11) displayed that a percentual change of the input of 200 to 600 percent generally do not generate more than 10 percent change in the output. With an increase of 600 percent compared to a 200 percent increase in aquifer thickness the hydraulic conductivity generally do not change. Hence, the sensitivity is lower for a 600 percent change in the input parameter. If the aquifer thickness is smaller than the screen length the output parameter will change more dramatically. A 50 percent change in the aquifer thickness would result in a change of 300 to 500 percent in the output. This implies that the analysis is sensitive to a change in the aquifer thickness that is thinner than the screen length. For aquifer thickness that exceeds the screen length there is lower sensitivity. Therefore, the usage of the screen length is suggested to be acceptable since the thickness of the aquifers during the first testing campaign in the investigation areas are reported to exceed 2 meters.

Table 11. Sensitivity analysis for aquifer thickness. Column 2-5 displays the measured hydraulic conductivities for different aquifer thickness between 50 percent of the screen length (l) to 600 percent. Column 6-8 displays the percentual change in hydraulic conductivity dependent on the change in aquifer thickness. Column 9-11 displays the sensitivity (s) which is a measure of the difference (in precent) of the percentual change in the input to the output (equation 11).

Well	50% (l)	100% (l)	200% (l)	600% (l)	50% change	200% change	600% change	S 50%	S 200%	S 600%
U09G83	4.14×10^{-6}	2.07×10^{-6}	1.67×10^{-6}	1.67×10^{-6}	200 %	-19.3%	-19.3%	400.0%	-9.7%	-3.2%
U09G97	1.00×10^{-4}	9.50×10^{-5}	7.82×10^{-5}	7.82×10^{-5}	138.9%	-17.7%	-17.7%	277.9%	-8.8%	-2.9%
U09G84	9.40×10^{-4}	5.00×10^{-4}	3.83×10^{-4}	3.83×10^{-4}	206.6%	-15.8%	-15.8%	413.2%	-7.9%	-2.6%
14T728	1.59×10^{-7}	8.04×10^{-8}	7.67×10^{-8}	6.62×10^{-8}	197.8%	-4.6%	-17.7%	395.5%	-2.3%	-2.9%
17T714	3.19×10^{-5}	1.28×10^{-5}	1.28×10^{-5}	1.28×10^{-5}	249.2%	0.0%	0.0%	498.4%	0.0%	0.0%
17T706	3.51×10^{-3}	1.87×10^{-3}	1.50×10^{-3}	1.50×10^{-3}	187.7%	-19.8%	-19.8%	375.4%	-9.9%	-3.3%
U19G30	1.69×10^{-7}	8.68×10^{-8}	7.18×10^{-8}	7.18×10^{-8}	194.7%	-17.3%	-17.3%	389.4%	-8.6%	-2.9%
U19G29	5.82×10^{-6}	2.91×10^{-6}	2.02×10^{-6}	2.02×10^{-6}	200.0%	-30.6%	-30.6%	400.0%	-15.3%	-5.1%
U19G33	8.81×10^{-5}	4.41×10^{-5}	3.63×10^{-5}	3.05×10^{-5}	199.8%	-17.7%	-30.8%	399.6%	-8,8%	-5.1%
14T8025	5.28×10^{-7}	2.64×10^{-7}	2.26×10^{-7}	2.26×10^{-7}	200.0%	-14.4%	-14.4%	400.0%	-7.2%	-2.4%
U19G35	8.47×10^{-6}	4.23×10^{-6}	3.49×10^{-6}	2.93×10^{-6}	200.2%	-17.5%	-30.7%	400.5%	-8.7%	-5.1%
U19G38	1.86×10^{-5}	9.29×10^{-6}	7.84×10^{-6}	7.84×10^{-6}	200.2%	-15.6%	-15.6%	400.4%	-7.8%	-2.6%

5. Discussion

In this section compilation of the measured hydraulic conductivity will be presented to demonstrate the spatial variability and variance of the hydraulic conductivity in the investigation areas. The spatial variability of the field data will be used to explain or correct the conceptual model in figure 12. The difference of the variance, spatial variability and the results from the pumping tests will be presented and their differences and similarities will be discussed in relation to aquifer heterogeneity. Further, with this compilation of the data the heterogeneity and connectivity in the aquifer system will be discussed as a guidance on location and design of infiltration facility.

In figure 44 the lognormal distribution of the hydraulic conductivity is presented. To get a general view of what kinds of sediments that were tested intervals of hydraulic conductivities representative for a certain sediment (table 12) where included in figure 44. The hydraulic conductivity values for unconsolidated rock suggested by Domenico (1998) was used (table 12)(Şen, 2015). These will be used for classifying hydraulic conductivities in figure 34 to 43.

Table 12. Interval of hydraulic conductivities for different types of sediments by Domenico (1998).

Unconsolidated rock materials	K (m/s)
Gravel	3×10^{-4}- 3×10^{-2}
Coarse sand	9×10^{-7}- 6×10^{-3}
Medium sand	9×10^{-7}- 5×10^{-4}
Fine sand	2×10^{-7}- 2×10^{-4}
Silt	1×10^{-9}- 2×10^{-5}
Till	1×10^{-12}- 2×10^{-6}
Clay	1×10^{-11}- 4.7×10^{-9}
Unweather marine clay	8×10^{-13}- 2×10^{-9}

In addition, the classification of aquifer permeability (hydraulic conductivity) of Ad-hoc Airbeitsgruppe hydrogeologic (1997) is used (Hölting & Coldewey, 2019). This classification suggests a low permeable aquifer (or aquitard) below 1×10^{-6} m/s, moderate permeability aquifer between 1×10^{-6} m/s to 3×10^{-5} m/s and a high (or good) permeable aquifer over 3×10^{-5} m/s (table 13).

Table 13. Aquifer permeability (hydraulic conductivity) classification (Hölting & Coldewey, 2019).

Aquifer permeability	K (m/s)
Good (high)	$> 3\times10^{-5}$
Moderate	$1\times10^{-6} – 3\times10^{-5}$
Low	$< 1\times10^{-6}$

5.1 Short duration hydraulic tests

Hydraulic conductivity estimation did not change as more test were carried out in a continuous way. The change in measured hydraulic conductivity as testing continued varied from both higher and lower compared to the first test. There was no indication that different methods

rising head with pump, slug and infiltration gave continuously higher or lower measured hydraulic conductivity than other methods (table 5, 7, 10). The measured hydraulic conductivity did show a dependence on the initial head displacement (table 5, 7, 10).

In the evaluation of the repeatability of short duration hydraulic tests at investigation area Renen, the highest initial head displacement yielded the highest hydraulic conductivity except for one well, U09G87 (table 5). The result where independent of method used, the order of tests and seemed to only be dependent on the initial head displacement. According to McElwee and Zenner (1998) the critically damped region in a Hvorslev plot show dependence on initial head displacement. The result indicate that this is the case for the critically damped region but also for the overdamped region as well (table 5). McElwee and Zenner (1998) found that a larger initial head displacement yielded a lower hydraulic conductivity. In the result in table 5, the opposite is found, a larger initial head displacement yields a larger hydraulic conductivity. The difference in measured hydraulic conductivity for the lowest initial displacement were generally not larger than 30 percent lower than the largest initial head displacement (table 5). The exception, well U09G87, the largest initial head resulted in a hydraulic conductivity of 30 percent of the lowest initial head (table 5). This could be due to gas in the pores which decrease the effective porosity and measured hydraulic conductivities (Hvorslev, 1951). At Renen there is contamination of trichloroethylene which is a volatile chlorinate hydrocarbon (Martí et al., 2014).

The trend of lower measured hydraulic conductivities with smaller head displacement could also bee seen at Southern trough and tunnel and Österleden (table 7 and 10). There was one measurement in well 17T714 (table 7) and one in 14T7036 (table 10) that deviated from this trend. These two measurements yielded 22 and 19 percent higher hydraulic conductivities than the largest initial head displacement.

A setback with the analysis was that there were generally no more than two initial head displacement for comparison. With more measured head displacement for each well the confidence in the analysis would be higher. For example, McElwee and Zenner (1998) continuously used four initial head displacements between 1-5 meters. Also, Kulessa, Hubbard, Williamson, and Brown (2005) reported that sensitivity Analyses of curve fitting processes and repeatability of slug test tend to be of minor influence on parameter estimate compared to geometrical and hydrological parameter uncertainties between the borehole and the aquifer system.

The slug tests generally yielded a much higher or lower initial head displacement compared to the theoretical initial head displacement. This could be seen in well U19G33, 14T7036 and U12G35 at Österleden investigation area (figure 28, 29 and 30) and for slug removal in well 17T706 and 17T714 (figure 19 and 20) at Southern trough and tunnel. For slug initiation in well 17T706 and 17T714 this relationship could not be seen. This was due to that the initial head displacement being higher than the edge of the well and hence water poured out of the well at slug initiation. Both 14T7036 and U12G35 (figure 29 and 30) measured high hydraulic conductivity (table 9). The deviation of the head displacement compared to the theoretical head displacement suggest that there is impact of acceleration and the velocity of the slug. McElwee

(2001) wrote that as the hydraulic conductivity increase toward the overdamped region the velocity of the water column will decrease the pressure and the head will be underestimated. Results from both Österleden and Southern trough and tunnel suggest the opposite. The pressure seemed to increase, and the head is overestimated rather than underestimated.

The head for several slug initiation test overestimated the initial head with two times the theoretical head (figure 20, 28, 29 and 30). This could be due to the velocity of the slug (McElwee, 2002). Further, McElwee and Zenner (1998) did compare nonlinear numerical model estimation of K-values to a linear model. The result was that the linear model estimated K-values between 0.23 to 73 percent of the estimated values with the nonlinear numerical model. The deviation from the nonlinear model increased with increased initial head displacement. Hence, measurement of hydraulic conductivities which displays variability dependent on initial head displacement and are in the underdamped response could deviate more from actual hydraulic conductivities (figure 29 and 30).

Also, in this investigation wells which were in the underdamped region (figure 19, 20 and 28) displayed deviation from the theoretical initial head displacement which McElvee (2001) discussed only for the overdamped case. The position of the transducer is reported to influence the measured hydraulic conductivity, with a higher distance from the static water column the hydraulic conductivity risks being underestimated (Butler Jr, Garnett, & Healey, 2003). Butler et. al. (2003) reported that for transducer position 6.116 meters below the static water level could produce underestimation of hydraulic conductivities with a factor of 2.03 times. Transducers positioned within 0.5 meters from the static water table would make the correction for acceleration of the water column unnecessary. In this work the pressure transducer have generally positioned more than 6 meters from the static water level. Hence, the result from slug test performed in this work could be effected by the change of the effective water column as a consequence of radius change and acceleration of water, called the **β** parameter (Butler Jr et al., 2003; McElwee, 2001; McElwee & Zenner, 1998). Here it should be noted that the measured hydraulic conductivity between slug tests and rising head tests with pump (table 7 and 10) did not show any extreme differences compared to reported acceptable parameter estimates by Butler Jr. (1994) of 20 to 30 percent within actual hydraulic conductivities.

5.2 Field saturated hydraulic conductivity and variability

5.2.1 Unconfined aquifer

5.2.1.1 Renen

Figure 34 shows the spatial distribution of hydraulic conductivity. Short duration hydraulic tests in well 14T3090, 14T3091, 14T3092, 14T30100 and 14T3065 where performed during the first testing campaign (table 1). The other measurements where performed during the field work.

The higher hydraulic conductivities are concentrated to two areas, around wells 14T3091, 14T3090 and 17T335, U09G84 to 14T3065. The bedrock interpolation indicates that wells 14T3091 and 14T3090 are positioned in a depression in the bedrock whereas the bedrock becomes shallower to the east, north and south. The bedrock generally slopes towards the west

with some depressions and ridges in the bedrock trending in west-east direction. The area around 17T335, U09G84 and 143065 are not, according to the bedrock interpolation, positioned within a bedrock depression. The sediment depth is rather shallow at wells 17T335 and U09G84 (around 3 meters) and deepens towards 14T3065 to 8 meters. In the digital elevation model in figure 34 a ridge could be detected just north of these wells.

There are no low permeabilities (hydraulic conductivities) measured in the area (slower than 1×10^{-6} m/s) (table 13). Well U09G84 and 14T3091 measured the highest hydraulic conductivities of 4.4×10^{-4} m/s and 1.6×10^{-4} m/s (table 4 and 1), respectively. All other wells which measured high permeability was in the span of 3.0×10^{-5} to 4.5×10^{-5} m/s. During the pump test the radius of influence was highly unsymmetrical indicating that the connectivity to the south and the north is lower than the east-west direction (figure 34). This appearance can also be seen on the result from the short duration hydraulic tests. Both wells 14T3090-91 measured high permeability while those to the south and north measured moderate permeability.

The interpolated groundwater contours indicate a net groundwater flow towards the west (figure 34). The groundwater contours are interpolated by the groundwater level in MASL in table 4. The resolution of the groundwater contours is rather coarse, and therefore the groundwater flow should not be discussed in detail dependent on this result.

The gray line trending south-north (figure 34) represents the boundary between filling material (west) and natural deposited sediments (east). The filling material complicates the interpretation of the aquifer characterisation since original sediments has been removed to an unknown depth and the type of filling material deposited is unknown.

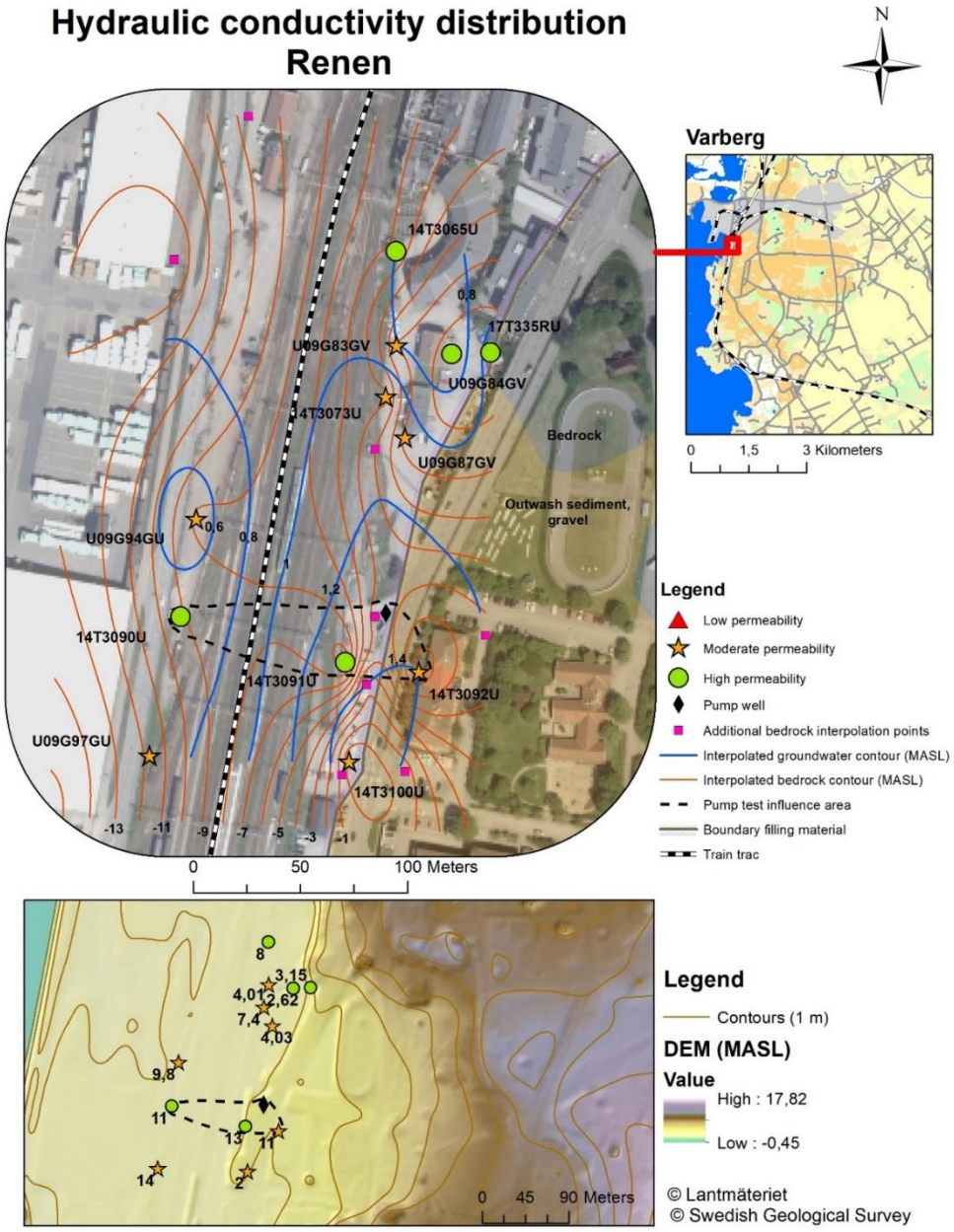

Figure 34. The upper map shows spatial variability of permeability (hydraulic conductivity) at Renen. The hydraulic conductivity is divided into three classes, low, moderate, and high permeability (Hölting & Coldewey, 2019) for determination of the behaviour of the aquifer (table 13). The lower map shows the surface elevation or digital elevation model (DEM), the surface contours with 1-meter equidistance and the well depths.

Figure 35 displays a scatterplot with the bedrock surface (defined as the bottom of the well). The values are within the range of moderate to good permeability. There are five wells that measure good permeability, 17T335, U09G84, 14T3065, 14T3090 and 14T3091. The bedrock (screen position) are located at 0, -0.5, -6, -9 and -10 MASL, respectively. All other wells measure permeabilities in the moderate span.

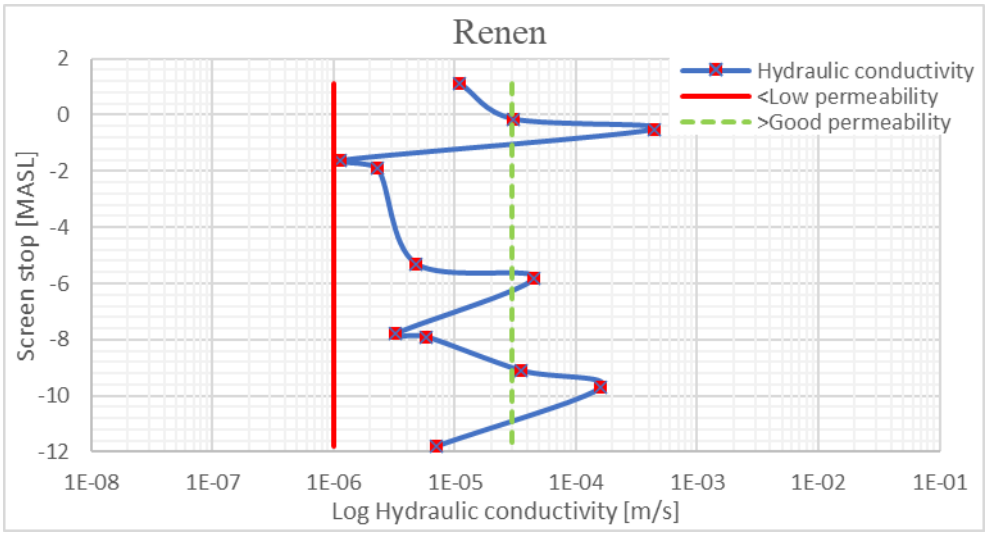

Figure 35. A scatter plot with the hydraulic conductivity in m/s and the bedrock surface in MASL.

At Renen wells with good permeability was clustered but not always within bedrock depressions. The areas of good permeability are considered oblong and stretched in the west east direction perpendicular to the bedrock slope (figure 34). This agrees with the conceptual model of Varberg with a drainage pattern from the hills downward (Hillefors, 1979). Also, well 14T3090 and 14T3091 are positioned in a bedrock depression with higher hydraulic conductivity (figure 34 and 35). This seems to be a continuous structure and could be a potential deformation zone. This situation agrees with the conceptual model in figure 12 with material with higher hydraulic conductivity in bedrock depression and deformation zones.

During the first testing campaign a drilling was performed and the stratigraphy was described. Coarser material within the filter section of the pumped well (figure 34) was found within the depression and was covered with 4-5 meters of sandy silt. The coarser material where interpreted as gravely till. During the first testing campaign the situation where interpreted, in the vicinity of the pumped well, as a lower leaky aquifer. The interpolated bedrock in figure 34 strengthen the theory from the first testing campaign. The bedrock could act as a barrier boundary (Fetter, 2001) by delineating well 14T3091-91 within the bedrock depression. The outline of the radius of influence from the pump test performed during the first testing campaign also coincide with the interpolated bedrock depression. This indicate that the wells outside of the influence area (14T3073, U09G83, U09G84, U09G87, 14T3065, 17T335 and 14T3100) from the pump test is positioned within another aquifer where the silt layer and the bedrock act as barrier boundaries within the aquifer system (Fetter, 2001).

This does not mean that the aquifers are not connected. The unconfined aquifer could act as a recharge boundary to the confined aquifer since the groundwater movement seems to be from

the east to the west (figure 34). From CPT tests (cone penetrating tests) during the second testing campaign the areas north of the bedrock depression was found to be an unconfined aquifer with direct contact to the bedrock. The two- aquifer situation is hence restricted to the bedrock depression and to the west side of the train trac. The filter screens in U09G94 and U09G97 at the west side of the train trac is below the silt layer interpreted during the first testing campaign.

Sediment classification of the upper unconfined aquifer from the first testing campaign (in well 14T3073) was interpreted as silty sandy till (figure 34). In the upper aquifer in the vicinity of the pump well sediment where interpreted as sand. This could be a representative sediment for the unconfined upper aquifer for the measurement in the moderate permeability span. The upper unconfined aquifer is suggested to transcend to a leaky aquifer or confined aquifer at the west side of the train trac. The unconfined aquifer could therefor act as a recharge boundary for the confined aquifer. The higher hydraulic conductivities could be smaller drainage channels as discussed by Hillefors (1979). It should be noted that during the first testing campaign the upper 1.5 meters of sediments where reported as filling material. The shallower wells are therefor not certain of being representative for natural deposited sediments.

5.2.2 Semiconfined (leaky) aquifers

5.2.2.1 Southern trough and tunnel

Short duration hydraulic tests where performed in well 14T713, 14T7040, 14T7041, 14T7046 and 14T7047 during the first testing campaign and in well U04G11, U04G16, U04G38 and U04G40 during the second testing campaign. Wells with high permeability is concentrated to the central part of the area (figure 36). Well U04G38 (table 2) and 17T706 (table 6) had a hydraulic conductivity between 1-2.5×10^{-3} m/s. This indicate that there could be some sort of glaciofluvial material. Wells U04G16 and 14T7041 had slower conductivities with 1.6×10^{-4} and 4.2×10^{-5} m/s, respectively (table 1 and 2). The highest permeabilities are measured in the deeper part of the bedrock bottom (figure 36).

During the pumping test well 14T7041 and 17T714 was not used as observation wells and hence the connection to these wells are unknown. Wells 14T714 and 14T728 indicate clogging during field work. The radius of influence from the pumping test further points to that the measured conductivities are wrong. The pumped well was positioned 25 meters northeast of U04G38 with a depth of 8.5 meters. The filter of the well is one meter and is positioned 1.7-2.7 MASL (figure 36). The filter of the pumped well is then positioned around 11 meter above the deepest influenced well and 2 meters under the highest positioned well (upper north east corner of the influence area). The radius of influence is stretched in the southwest-northeast direction.

Due to small amount of data from groundwater levels the groundwater surface could not be interpolated. From well 17T706 the hydraulic gradient is sloping toward 17T714 with a groundwater level of 10.1 MASL and 9.6 MASL, respectively (table 6).

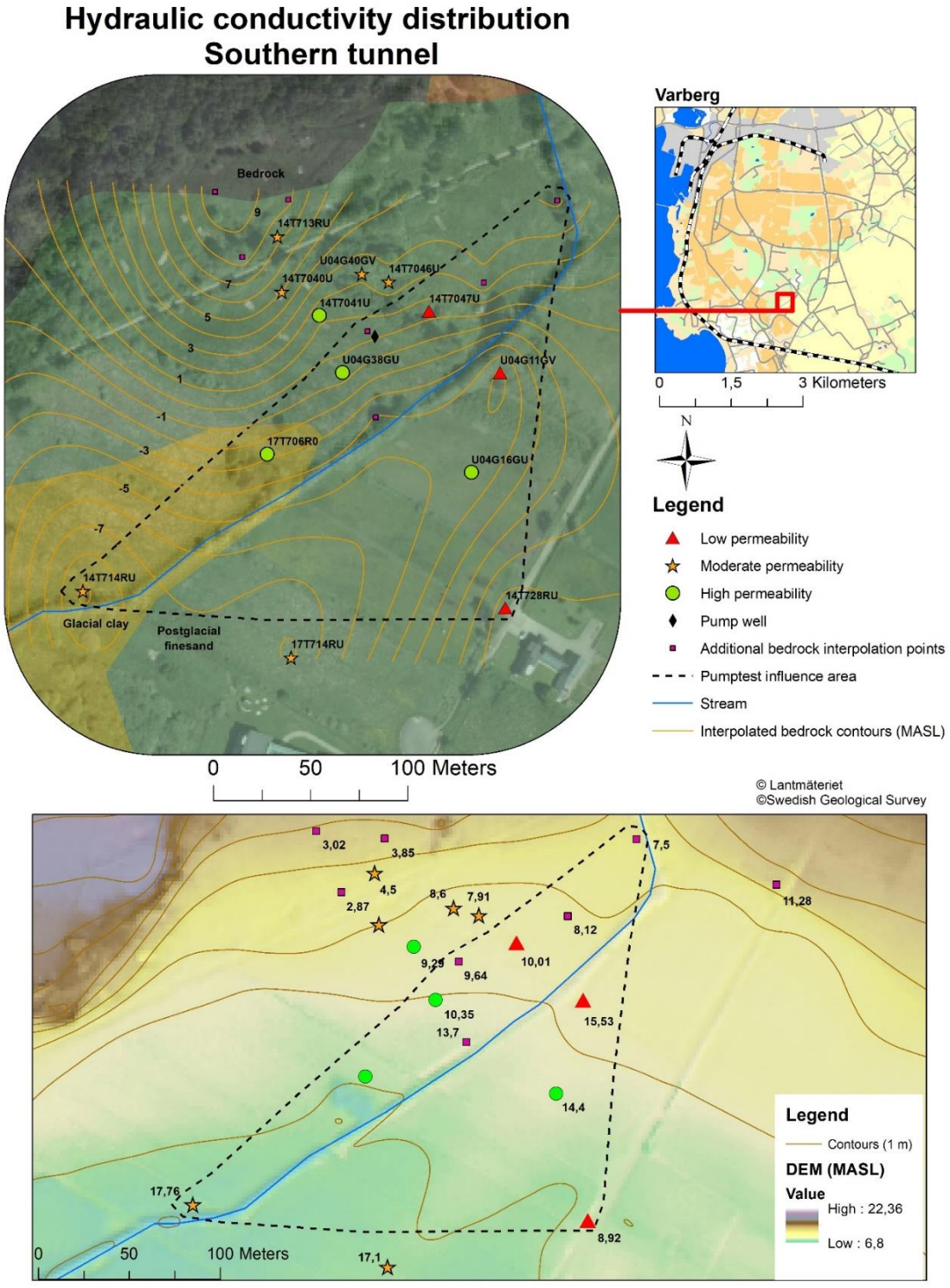

Figure 36. The upper map shows spatial variability of permeability (hydraulic conductivity) at Southern trough and tunnel. The hydraulic conductivity is divided into three classes, low, moderate, and high permeability (Hölting & Coldewey, 2019) for determination of the behaviour of the aquifer (table 13). The lower map shows the surface elevation or digital elevation model (DEM), the surface contours with 1-meter equidistance and the well depths.

In figure 36 the ground surface within the investigation area are 4 meters higher at the highest point compared to the lowest (from 9 to 12 MASL). The lowest to the highest point of the bedrock (here defined as the bottom of the well or screen end) are, for comparison, -10 to 8 MASL (figure 37). The uppermost part, between 2-7 MASL, the result shows medium permeability (between 1×10^{-6} to 3×10^{-5} m/s). Below 0 MASL the general trend is higher hydraulic conductivities (good permeability) between 0 to -5 MASL. Two measurements deviated from this trend with low permeabilities in well 14T728 and 14T7047 which are positioned in the eastern part of the area (figure 36). Here it should be mentioned that the result from 14T728 are uncertain since clogging are suspected. Under -5 MASL the hydraulic conductivity decreases again toward moderate permeability. There is one well, U04G11 that deviates with a lower permeability at -5.33 MASL.

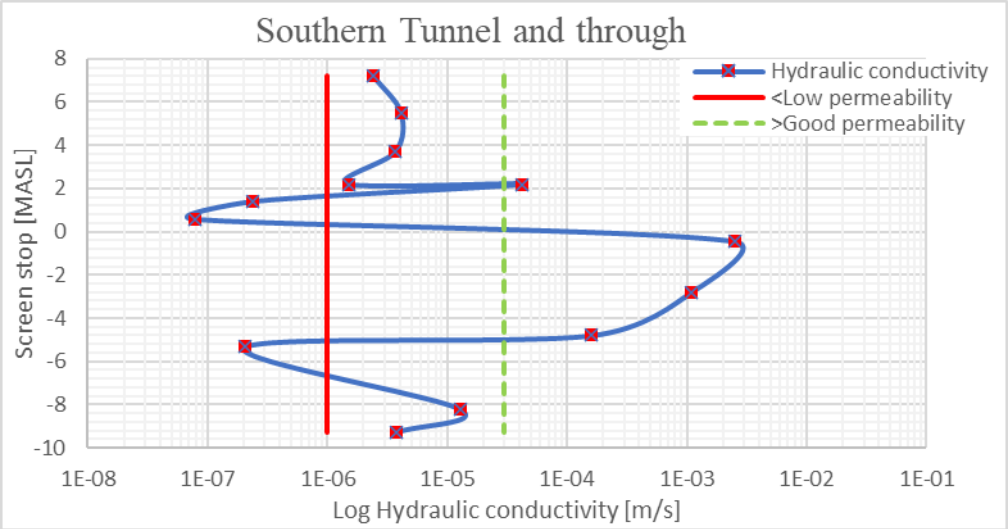

Figure 37. Displays a scatter plot with the hydraulic conductivity in m/s and the bedrock surface in MASL.

The red squares in the conceptual model in figure 12 represent the expected deposition to be found within the area. Within the larger depression in the bedrock good permeable material was found (figure 36 and 37). This could be a possible deformation zone. Larger glaciofluvial material was supposed according to the conceptual model to be in direct contact with the bedrock (figure 12). The Well U04G11 which is positioned lower than the wells that measured good permeability, as can be seen figure 37, measured low hydraulic conductivity. This indicate that either there is material deposited before the glaciofluvial sediments that have not been eroded or it represents a boundary between fine-grained deposits and glaciofluvial deposits (figure 12). At well 17T714, where the bedrock is some meter deeper than the wells that measured good hydraulic conductivity, moderate hydraulic conductivity was measured (table 6). Here the measured hydraulic conductivity also was lower which further indicate that there could be lower permeability material (till) beneath the glaciofluvial material. Well 17T714 could also represent a transition boundary between the glaciofluvial material and the till.

Both 14T714 and 14T728 measured lower conductivities (table 6 and figure 36). Well 14T728 never reached full recovery (figure 19). These wells are thought to be clogged since during the pump test performed during the first testing campaign these wells responded well which can be

seen in the influence area in figure 36. From the pump test the measured hydraulic conductivity was estimated to $1\text{-}2\times10^{-4}$ m/s. Therefore, the measurement from short duration tests are considered unreliable and the wells could have higher hydraulic conductivity.

The first testing campaign reported a sandy gravel in the screen section of the pumped well (figure 36). The upper aquifer was reported as silty sand with a 1.5-meter thickness. Between the unconfined and confined aquifer there was a clay layer with the thickness of 6-7 meters. At well 14T713 (figure 36) the material within the filter section reported was silty to sandy till. This agrees well with the measured hydraulic conductivities (table 1, 2 and 6).

The first testing campaign reported a 3-meter-thick glaciofluvial deposit and according to the bedrock interpolation the surface is at 0 MASL at the pumped well (figure 36). At the pump well this represent glaciofluvial deposits between 0-3 MASL, clay between 3-9 MASL and silty sand 9-10 MASL. In the well east of 14T7047 clay was identified during the first testing campaign at 6.2 MASL and silt at 3.5 MASL. In well 17T706 clay where found at 4.0 MASL. In figure 37, which presents the scatter plot between filter position (bedrock surface) and the hydraulic conductivity, the wells that measured good permeability have screens below 3 MASL which agree with sediment samples taken in the first testing campaign. In the chatter plot, between 3-9 MASL, no well measured hydraulic conductivity within the low permeability range (figure 37). The measurements between 2- 8 MASL are positioned along the bedrock slope in the northern part of the area (figure 36). This indicate that the clay layer gets thinner as the bedrock gets shallower and at well 14T713, which have a screen section located at 8-9 MASL, the clay layer is expected to be not more than 1 meter. The wells that measured moderate permeability is therefore thought to be positioned in the till unit below the confining unit as shown in the conceptual model in figure 12. This result also indicate that all the measured wells are positioned in the under aquifer. The result suggests that the glaciofluvial material is horizontally widespread, around 180 meters, between well 14T7041 to well 14T728. This structure of glaciofluvial deposits in the Varberg area are also mentioned by Påsse (1990), which strengthen interpretation of the result. Toward the northeast the glaciofluvial deposits gets narrower and the formation is suggested to go in between well U04G11 and 14T7041. This is suggested due to the appearance of the radius of influence in figure 36.

The deposits that have been identified in the conceptual model in figure 12 are the till layer below the confining unit and the contact between the till and glaciofluvial deposit. From the results the suggestion is that the glaciofluvial material have eroded older sediment to the bedrock, but tills can also be found between the bedrock and the glaciofluvial deposit.

5.2.2.2 Vareborg

Vareborg do not show hydraulic conductivities higher than 3.3×10^{-5} (table 8). The interpolated bedrock contours indicate a hill in the central area with a gentle slope to the west, south and north (figure 38). To the east the interpolation suggests a steeper gradient of the bedrock. The interpolated groundwater contours give the same appearance with a gentle slope to the west, and a hydraulic gradient an expected groundwater movement in the same direction. Toward the east (between well 14T8025, 14T8026 and U19G36) the groundwater levels produce a relatively flat surface. The spatial variability is higher at Vareborg compared to Southern trough

and tunnel. The hydraulic conductivity seems to vary rather local without continuous areas with K values in the same range (figure 38).

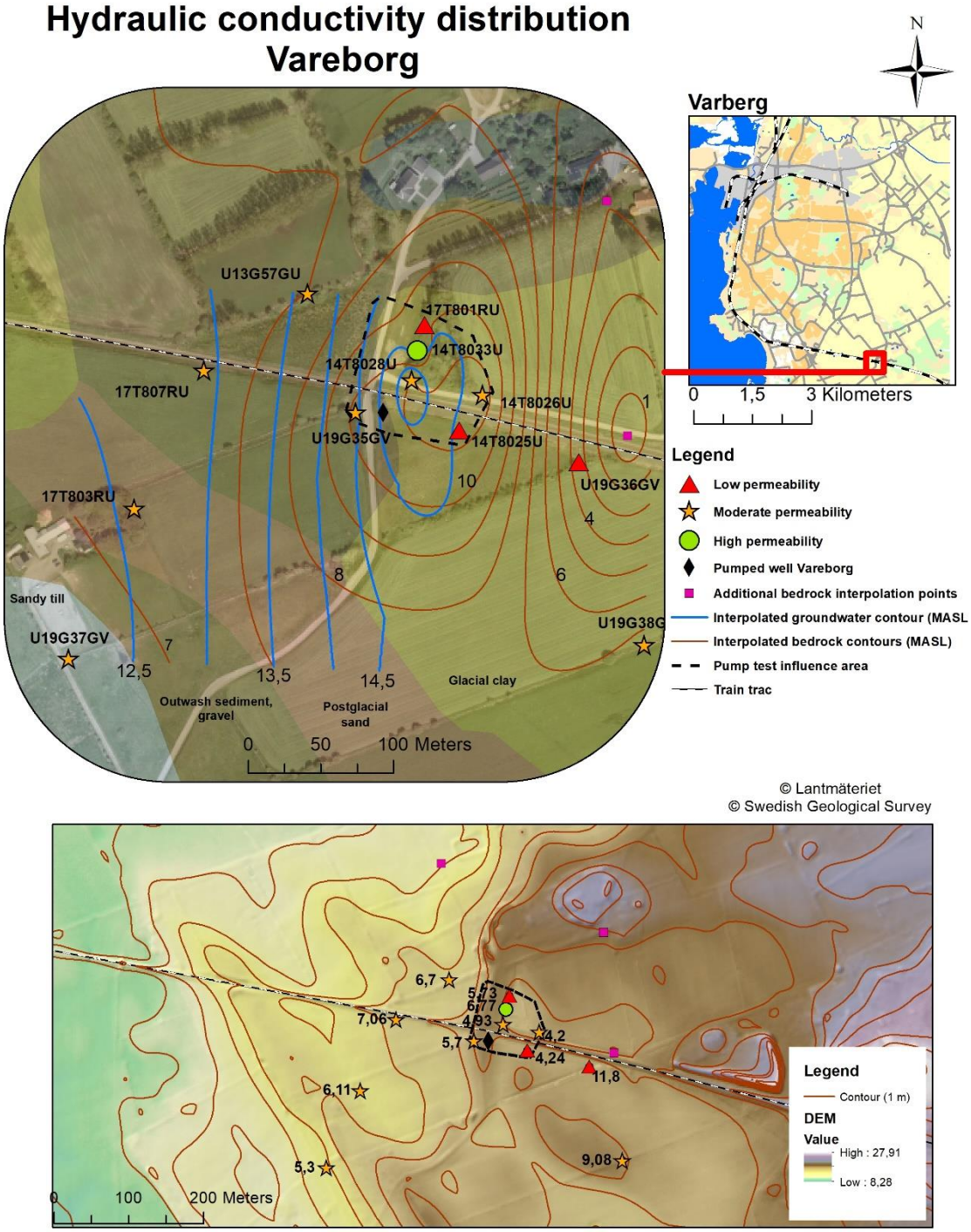

Figure 38. The upper map shows spatial variability of permeability (hydraulic conductivity) at Vareborg. The hydraulic conductivity is divided into three classes, low, moderate, and high permeability (Hölting & Coldewey, 2019) for determination of the behaviour of the aquifer (table 13). The lower map shows the surface elevation or digital elevation model (DEM), the surface contours with 1-meter equidistance and the well depths.

There is only a 3-meter difference in surface height in Vareborg (figure 38). The bedrock differs from 3 to 11.5 MASL (figure 39). Between 10-12 MASL the hydraulic conductivity varies between moderate permeability to low permeability. Below 10 MASL the hydraulic conductivity is mainly within the moderate permeability span. One measurement, in well 14T8033, the permeability is classified as good.

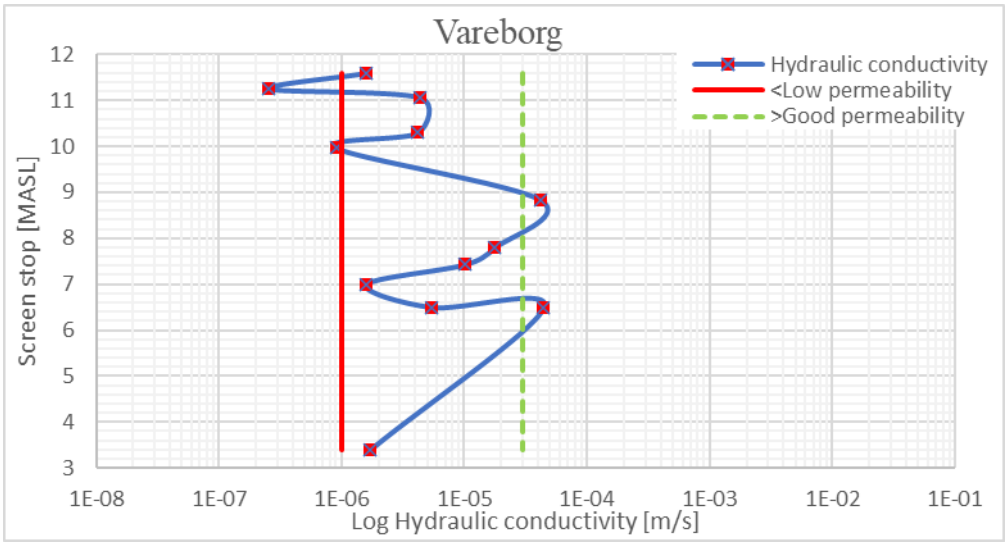

Figure 39. Displays a scatter plot with the hydraulic conductivity in m/s and the bedrock surface in MASL.

Figure 40 present a combined bedrock surface and hydraulic conductivity plot of Vareborg and Southern trough and tunnel since these two areas was the same type of aquifer (figure 12). Vareborg do not show as deep bedrock as Southern trough and tunnel. The upper part of Vareborg shows two measurement within the low permeability span. This was not seen in the area Southern trough and tunnel. The hydraulic conductivity over 2 meters above sea-level are generally indicating mainly moderate permeability for both areas.

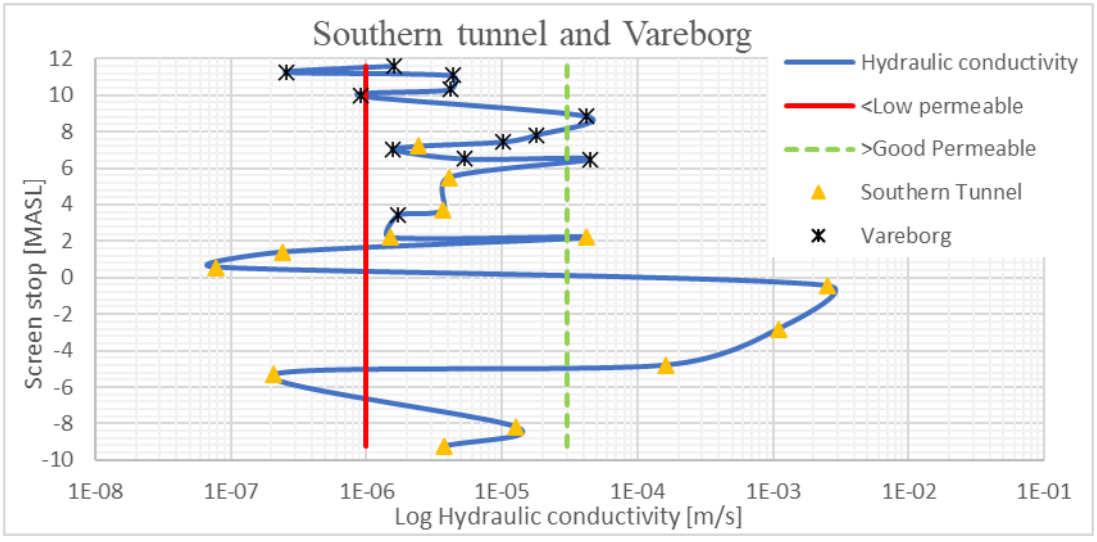

Figure 40. Displays a combination scatter plot for Southern trough and tunnel and Vareborg with the hydraulic conductivity in m/s and the bedrock surface in MASL.

At Vareborg the variability from the lowest measured hydraulic conductivity to the highest is lower than Southern trough and tunnel and trough (table 14). This is due to that there are no higher hydraulic conductivities identified at Vareborg (figure 38). Still, the hydraulic conductivity seems to change more locally than in Southern trough and tunnel. Both low permeability, moderate permeability and good permeability can be found within a rather small area (figure 38). This compared to Southern trough and tunnel (figure 36) where measured values of low, moderate, and good permeability generally are not found together. Rather, measurement within the same category is generally clustered. In figure 39 which shows the scatter plot between the screen depth (bedrock surface) and hydraulic conductivity at Vareborg there are no major formations indicating larger glaciofluvial deposits with increasing depth. The appearance of the spatial variability of K (figure 38) and the change of the hydraulic conductivity with deeper bedrock (figure 39) cannot be explained by the conceptual model in figure 12. In the first testing campaign sediment during the installation of well 14T728 was interpreted. Here, a clayey till was suggested. This sediment type has not been found in the other investigation areas. Hence, another possible explanation for the depositional process is presented below.

Northeast of the Apleviken valley some geomorphological features has been mapped by the Swedish Geological Surveys (SGU). These features can be seen in the black square in figure 41 (A) and highlighted in blue in (B). These can also be seen in the sediment map in figure 5. These features where found during the reconstruction by the highway (E6) and where described by Påsse (1990). The ridges are perpendicular to the direction of the ice movement and Påsse (1990) interpreted them as end-moraines. The moraine ridges contained glaciotectonized material, clay, till, and sand. It was found that the moraine ridges of till could overgo to glaciofluvial sediments. The ridges where generally 50 to 200 meters apart and the throughs in between the ridges where filled with younger fine-grained sediments. At the surface of the ridges outwash sediments where generally found.

V. Bouvier et al. (2015) described end-moraine formations in the Varberg area and Halland province as De Geer moraines. These are smaller push moraines formed sub-aquatic as ice-marginal formations. These are regular spaced ridges which has been found to be between 150-300 meters apart and the spacing is likely to represent ice-marginal retreat rates. De Geer moraines are generally found in the northern of Sweden and in the Middle Sweden end-moraine zone but also, as mentioned, in Varberg (V. Bouvier et al., 2015).

In figure 41 the pink square in (A) shows the digital elevation model with a hillshade to make surface features clearer. Three distinct ridges with the same direction as those described by Påsse (1990) is detected in the pink square (Vareborg). The blue lines in (B) highlight these features. The ridges are spaced 150 to 200 meters from each other which is in agreement with the De Geer moraines explained by V. Bouvier et al. (2015). In figure 41 (C) the measured wells in Vareborg are shown in relationship to the ridges. The ridges are generally perpendicular to the 7000 Bp highest coastline (red line) and therefore the ridges are thought not to be beach terraces. As can be seen in figure 41 (C) the all wells are positioned within this ridge system.

Also, the most southern part of the southern ridge formation where mapped by the Swedish Geological Surveys as a moraine (SGU, 2019).

Therefore, the interpretation is that all these ridges in Vareborg are end-moraines. These could be a part of the Halland coastal end-moraine zone described by J. Lundqvist and Wohlfarth (2001) or De Geer moraines as earlier have been found in the Varberg area by V. Bouvier, M. Johnson, and T. Påsse (2015). This could be the reason for the more complex spatial distribution of hydraulic conductivity at Vareborg. The buildup of these ridges has rearranged and deformed older deposited sediments and mixed them with younger sediments. According to Påsse (1990) these ridges could compose of a mixture between fine-grained sediments, till and glaciofluvial material, which could explain the more local variability of hydraulic conductivity at Vareborg. This implies that the origin and deposits at Vareborg are considerable different than sediments found at Southern trough and tunnel. The conceptual model in figure 12 are suggested to not be applicable at Vareborg. The sediments in the ridges could differ from the ones in the troughs.

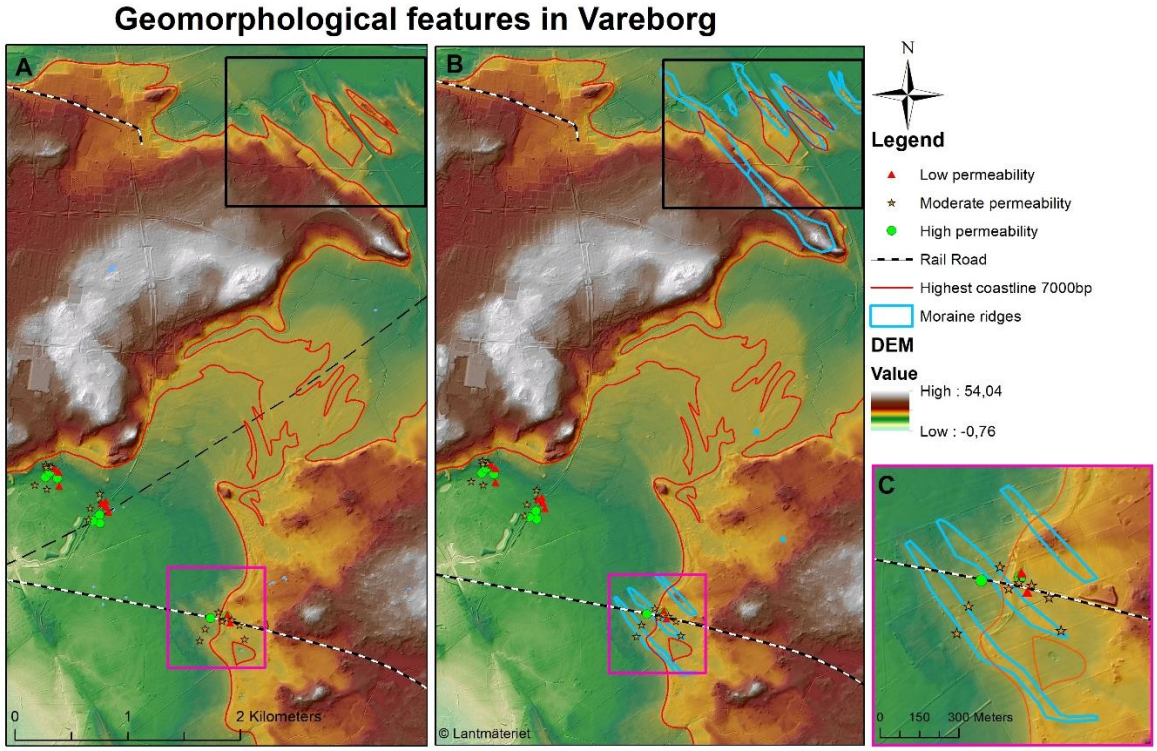

Figure 41. Shows the digital elevation model with a hillshade. (A) Shows only the DEM and the hillshade. Geomorphological features described and mapped by SGU (Påsse, 1990) are shown in the black square. The pink square are the investigation area Vareborg where simmilair geomorpholocial fetures can be identified. (B) Shows the ridge formations with outlines. (C) Displays a close up picture of Vareborg.

5.2.3 Confined aquifers

5.2.3.1 Österleden

The highest conductivities are centered in the southern part of the area (figure 42). Well U12G35 measured a hydraulic conductivity of 2.3×10^{-4} m/s and well 14T7036 a conductivity of 3.0×10^{-3} m/s (table 9). The interpolated bedrock contours indicate a sloping bedrock surface

from north to south which agrees with the local deformation zone (SGU, 2020). Well U19G33 measured a hydraulic conductivity of 5.10×10^{-5} m/s (table 9). All wells within or in the vicinity of the deformation zone measured K values representative for a good permeable aquifer except well U19G32 (figure 42). Wells measuring low hydraulic conductivity are within the same are. The same appearance applies on good hydraulic conductivity (figure 42).

The interpolated groundwater contours indicate a major groundwater movement from north to south with a northwestern movement in the northern part of the area (figure 42). This is the same pattern as the curvature of the bedrock. A digital elevation model is not shown in the map due to that the area is flat. The elevation ranges from 9.1 to 10.5 MASL.

The pumped well during the pumping test where positioned 25 meters northwest of well 14T7037 (figure 42). The radius of influence displays an unsymmetrical appearance with higher connectivity toward the west and east. This appearance could be an artifact due to that the length to observation wells to the south was much longer (14T7036).

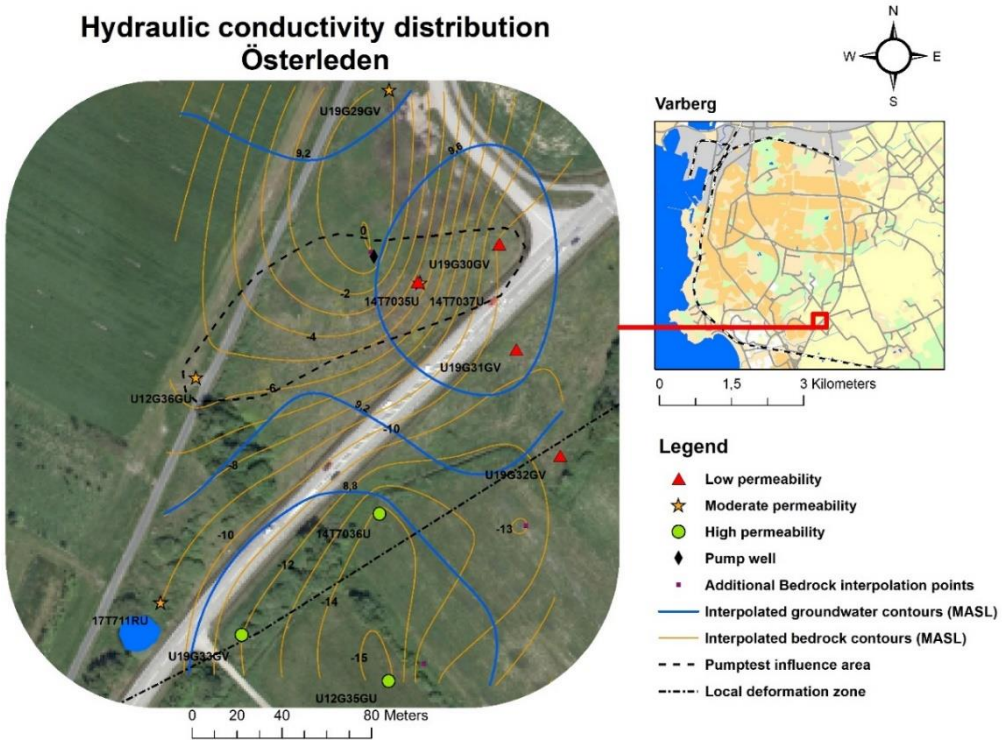

Figure 42. The map shows spatial variability of permeability (hydraulic conductivity) at Österleden. The hydraulic conductivity is divided into three classes, low, moderate, and high permeability (Hölting & Coldewey, 2019) for determination of the behaviour of the aquifer (table 13).

The bedrock at Österleden differs from -1 to -15 MASL (figure 43). Below -5 to -9 MASL moderate permeability was measured. Between -4 to -5 MASL low permeability was measured. Between -10 to -12 MASL three measurement within the low permeability span has been measured. The low permeabilities was also found within the same area (figure 43). From -12 MASL and down to -16 MASL (the deepest well) material with good permeability was found.

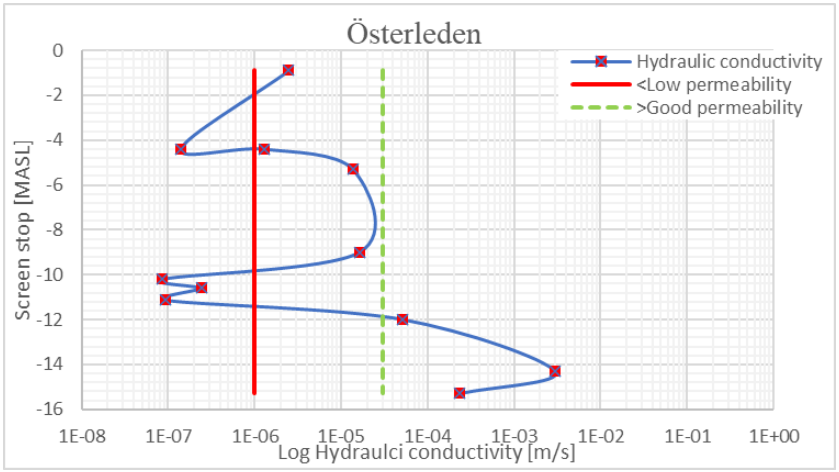

Figure 43. Displays a schatter plot with the hydraulic conductivity in m/s and the bedrock surface in MASL for Österleden.

Österleden is positioned in the middle of the valley system. The sediment depth is much deeper here than at Southern trough and tunnel. Sediment with the highest hydraulic conductivity if found at the deepest part of the bedrock which both figure 42 and 43 display. Also, at in figure 42 wells measuring good permeability are found in the vicinity of the local deformation zone (SGU, 2020). The result at Österleden are therefore in agreement with the conceptual model in figure 12. Well U19G32 is the only well in the vicinity of the deformation zone that do not measure good permeability. Field data from the installation of the well reported low discharge which indicate that there is lower hydraulic conductivity around this well. To determine whether the well is positioned within the deformation zone and within the glaciofluvial formation measurement could be taken further to the southeast of well U19G32. The well that were supposed to be tested during the field work within this position had been removed due to cultivation in the area.

Hebrand and Mark (1989) pointed out that glaciofluvial deposit in Skåne has eroded to the bedrock and eskers are in direct contact with it. The result indicate that this could be the case in Varberg as well. Results from Österleden (figure 42), Southern trough and tunnel (figure 36 and 37) and Renen (figure 34 and 35) indicate that glaciofluvial material are deposited in bedrock depressions.

5.3 Median hydraulic conductivity and effective hydraulic conductivity

Table 14 display that all pumping tests measured a higher hydraulic conductivity then the median K measured by short duration hydraulic tests. The median K value deviate most from the K obtained from the pumping tests in the investigation area Southern trough and tunnel. The pumping test K value is 26 times larger. The investigation area Renen show the least deviation between the median K compared to the K obtained from the pumping tests with a ratio of 2.2. All areas except Southern trough and tunnel have effective K values that are similar, within the range of 1×10^{-5} to 2×10^{-5} m/s. All the median K values received from short duration hydraulic tests are within the range of 2.5×10^{-6} to 9.0×10^{-6} m/s. The variance is lowest in Vareborg and Renen and highest in Österleden and Southern trough and tunnel (figure 44). The

pumping tests in Renen and Southern trough and tunnel where performed during the first testing campaign (figure 8 and 9). Pumping tests at Österleden and Vareborg were carried out during the second testing campaign (figure 10 and 11).

Table 14. Displays the difference between the median hydraulic conductivity (median K) and K values obtained from pumping tests (K pumping tests). The ratio is the difference between the median K and K pumping tests. Southern trough and tunnel is called ST in the table.

Area	Median K (m/s)	K pumping test (m/s)	Ratio
Renen	9.0×10^{-6}	2×10^{-5}	2.2
ST	3.8×10^{-6}	1×10^{-4}	26.6
Österleden	2.5×10^{-6}	1.1×10^{-5}	4.3
Vareborg	3.6×10^{-6}	1.5×10^{-5}	4.2

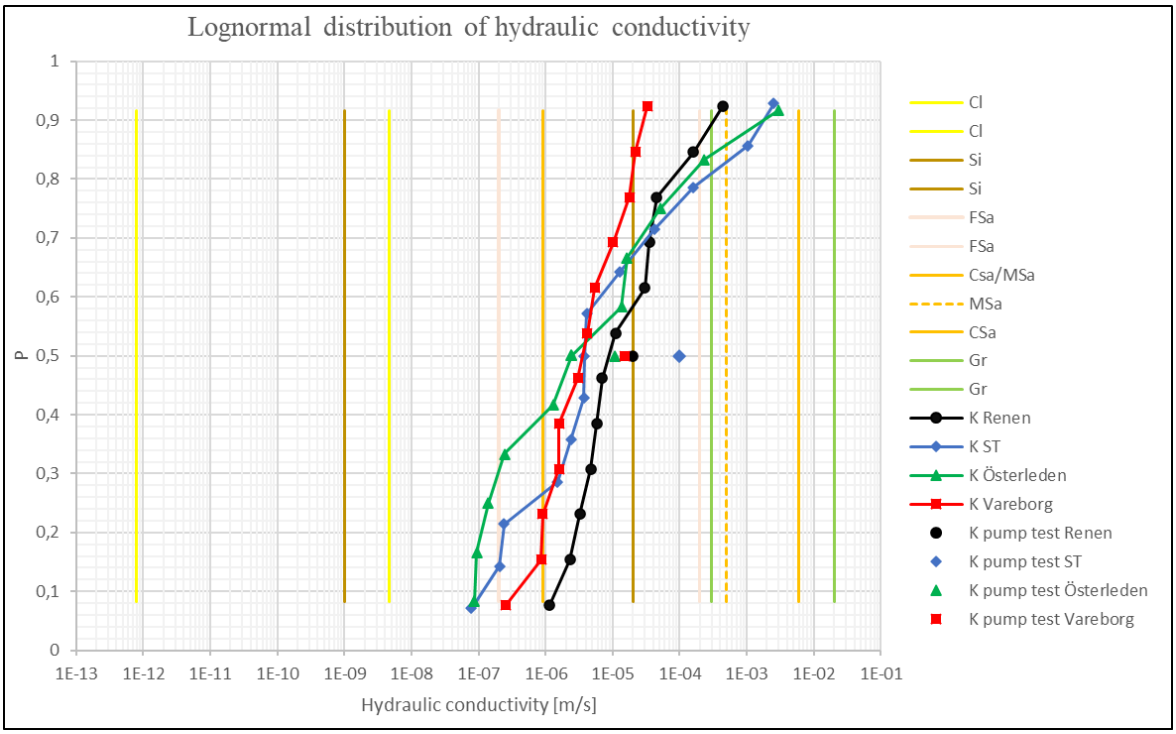

Figure 44. Display the lognormal distribution of hydraulic conductivity obtained from short duration hydraulic tests and obtained hydraulic conductivities from pumping tests for all investigation areas. Southern trough and tunnel is called ST in the figure.

The ratio between effective hydraulic conductivity from the pump test at Southern trough and tunnel and trough deviates most from the median hydraulic conductivity from short duration hydraulic conductivity (figure 44 and table 14). The pumped well is positioned in the good permeable area that can be seen in figure 36. If only the median from the hydraulic conductivity from the five wells within this area (14T714, 14T7041, U04G16, 17T706 and U04G38) the median hydraulic conductivity would be 1.6×10^{-4} m/s. This would agree relatively good with the effective hydraulic conductivity of 1×10^{-4} m/s (table 14). The reason for the extreme ratio

compared to the other investigation areas could be explained by the pump well position at Southern trough and tunnel and through.

At Österleden the ratio between the effective hydraulic conductivity and the median K from short duration hydraulic tests are the second highest (table 14). Still, the difference between the ratio for Vareborg and Österleden is 26.6 to 4.3. The variance is similar at Österleden and at Southern trough and tunnel (figure 44). Here the pump well is positioned within the till rather than glaciofluvial deposit (figure 42) which agrees with the median K. This is suggested to be the reason for having a dramatically lower ratio than in Southern trough and tunnel and through and still higher variance. There are different structures that are tested.

Vareborg has the second lowest ratio between the effective K and the median K (table 14) but the lowest variance (figure 44). The variability of hydraulic conductivity (figure 38) is varying more locally then in the other areas. This compared to Österleden (figure 42), Southern trough and tunnel (figure 36) and Renen (figure 34) where larger connective geological formation is found. The radius of influence was rather symmetrical during the pumping test from the second testing campaign (figure 38). Butler Jr and Healey (1998) proposed that small-scaled high-K conduits do not impact the parameter estimate evaluated from pumping test. This indicates difficulties to detect small-scaled variations with pumping tests. Therefore, without the usage of short duration hydraulic tests these local variations may not have been detected. The symmetrical radius of influence from the pumping test at Vareborg are not in agreement with suggested push-moraine deposits, with low connectivity and high heterogeneity. The radius of influence and the median hydraulic conductivity indicate connectivity but still a generally low hydraulic connectivity. At Renen, during the first testing campaign, highly fractured shallow bedrock was identified during installation wells 14T3051O. This well is within the granodioritic-granitic gneiss (figure 6). The same bedrock is found at Vareborg (figure 6). A possible explanation of the symmetrical appearance of the radius of influence at Vareborg could be connectivity and groundwater flow in fractures in the shallow bedrock rather than in the sediments.

The lowest ratio is found at Renen (table 14). The pumped well was concluded to be positioned in the under aquifer (figure 34). This means that the pumping test is not representative for the upper aquifer. Since the under aquifer (14T3090-92, U19G94 and U19G97) are a different aquifer system the median value for the upper aquifer should contain the other measure wells (table 4 and 1). A median value for the upper unconfined aquifer (U09G87, U09G83, 14T3073, 14T3100, 17T335, 14T3065 and U09G84) are 1.1×10^{-5} m/s. This is lower than the effective hydraulic conductivity in the under aquifer but higher than the median value for all short duration hydraulic tests. The median value for the lower aquifer (14T3090, 14T3091, 14T3092, U19G94 and U19G97) are 7.0×10^{-6} which is lower than for the upper aquifer. The ratio for the lower aquifer between median K and the effective hydraulic conductivity are larger compared to the ratio for the entire area. This is probably due to that the upper aquifer is related to postglacial depositional processes rather than glacial as described by Påsse (1998). The ratio in the lower aquifer could therefore be explained by the position of the pumped well in a more permeable area. Still, the relatively little change between the effective K in the under aquifer

compared to the median in the upper indicate that the hydraulic properties do not differ that much. However, the upper aquifer would respond differently during pumping or infiltration since the aquifer is not under pressure and the radius of influence would develop slowly due to precipitation (Fetter, 2001; Kruseman & De Ridder, 1994).

Generally, the median hydraulic conductivity obtained from short duration hydraulic tests are lower compared to hydraulic conductivity calculated from pumping tests. This appearance has also been found by Butler Jr and Healey (1998) which found that K estimated from pumping tests are generally considerable larger than the estimated K from a series of slug test within the same geological structure. Butler Jr and Healey (1998) reported that slug test is extremely sensitive to altered, near-well conditions. A vertical anisotropy within the screen section can lead to an underestimation of hydraulic conductivity with a factor of three. Pumping tests performed with observation wells will be unaffected by vertical anisotropy (or the Cooper-Jacob semi-log method is used) (Butler Jr & Healey, 1998). All earlier performed pumping tests during the first and second testing campaign used observation wells. Therefore, vertical anisotropy could be neglected as an influence factor in the effective hydraulic conductivity result. Still, Butler Jr and Healey (1998) point out that the most common reasons for differences between obtained values from slug tests and pumping-tests are related to well installation and well development. The wells where not developed prior the short duration hydraulic test. This leads to a shorter effective screen length and hydraulic conductivity may be underestimated (Butler Jr & Healey, 1998).

Further, pumping tests are contributed by flow from the entire aquifer thickness. When converting the transmissivity to hydraulic conductivity a good estimation of the aquifer thickness is required. This is pointed out by Butler Jr and Healey (1998). For the data in table 14 with lower K-value obtained from pumping test the aquifer thickness could have been underestimated. Renard et al. (2000) found that the algebraic techniques (such as median and mean) always show a large dispersion of the estimated value around reference values. The reason was that the spatial arrangement of the hydraulic conductivity. Therefore, heterogeneity within an area and dependence on the position of the pumped well and used wells for short duration hydraulic tests will also influence the ratio between obtained hydraulic conductivity from the two methods.

The results from the median K from short duration hydraulic tests compared to the effective hydraulic conductivity (figure 44 and table 14) implies that with a higher variance the methods tends to deviate more from each other in measured K. For a two-dimensional isotropic system with a lognormal distribution of K, the median K should describe the effective hydraulic conductivity obtained from pumping test (Gupta et al., 2006; Renard et al., 2000). Therefore, the difference in ratio between the investigation areas are suggested to be influenced by anisotropy and heterogeneity in the aquifers, where stronger anisotrophy and heterogeneity results in a higher ratio.

Also, with a lower variance the difference between the median K and the effective hydraulic conductivity tend to have a lower ratio (figure 44 and table 14). This implies that the aquifer characteristic is closer to a two-dimensional isotropic medium. Therefore, it is suggested that

short duration hydraulic tests are a good method for detecting heterogeneities and gives a good indication of the spatial variation of hydraulic conductivity (figure 34 to 43). This was also suggested by Mas-Pla et al. (1997) and Brauchler et al. (2012).

5.4 Infiltration and pumping

For a homogenous isotropic medium it was assumed that the effective hydraulic conductivity can be expressed by the median hydraulic conductivity. In section 5.3 it was suggested that a high difference between the effective hydraulic conductivity and the median K could be explained by the variability of hydraulic conductivity. In this section the effect of the spatial variability on the radius of influence from infiltration wells will be discussed.

The new railway (figure 45) and the related excavations will have an effect on groundwater levels. At Renen the train trac will be in a trough. At the Southern trough and tunnel the excavation starts in a tunnel and goes into a trough. At Österleden and Vareborg the train tracs will go at ground level but at both places a bridge will be constructed and excavations will be made for a road below. If needed (to avoid damage) the effect of the excavations can be reduced using infiltration wells. For an unconfined and isotropic and homogenous aquifer (equation 2) the radius of influence for the infiltration wells will depend upon the increase in hydraulic head (water column) at the infiltration point and the hydraulic conductivity. In table 15 estimated of the radius of influences are presented. The estimates represent an increase in hydraulic head with 1 and 10 meters in infiltration wells (or a drawdown, s_w, or pumping) for the lowest, median, and highest hydraulic conductivity value within each investigation area. For a confined aquifer the development of the radius of influence will depend upon the specific storage (S) as well (equation 3). Equation 2 will be used to demonstrate the development of the radius of influence dependent on hydraulic conductivity for both unconfined and confined aquifers.

Table 15. Displays theoretical radius of influences (R) for a drawdown (s_w) in the pumped well or an increase in hydraulic head in an infiltration well. The radius of influence was calculated using equation 2. Southern trough and tunnel is named ST in the table.

Renen	**K (m/s)**	**R for s_w=1 (m)**	**R for s_w=10 (m)**
high	4.4×10^{-4}	63	629
median	9.0×10^{-6}	9	90
low	1.1×10^{-6}	3	31
ST			
high	1.0×10^{-3}	95	949
median	3.9×10^{-6}	6	58
low	2.1×10^{-7}	1	14
Österleden			
High	3.0×10^{-3}	164	1643
median	2.5×10^{-6}	5	47
low	8.6×10^{-8}	0.9	9
Vareborg			
high	4.4×10^{-5}	20	199
median	4.3×10^{-6}	6	62
low	2.6×10^{-7}	2	15

At Renen the new railway will be located at approximately the same position as the old one but in a trough (figure 45). There are three boreholes with high hydraulic conductivity in the northern part of the area (unconfined aquifer) and two within the under confined aquifer (figure 45). Both areas with high hydraulic conductivity displays an oblong structure in the west-easterly direction and along the bedrock slope (figure 34). As can be seen in table 15 the radius of influence would grow 7 times larger for the highest hydraulic conductivity compared to the median. Hillefors (1979) suggested that drainage patterns under the glacier potential could be found from heights down into valleys. This agrees with the material found (sand and gravel) in the filter section of the pumped well (figure 34) during the first testing campaign. Also, this agrees with the radius of influence and short duration hydraulic tests with high hydraulic conductivity along the bedrock slope (figure 34). Further, the conceptual model presented in figure 12 agrees with the spatial variability of hydraulic conductivity and interpreted sediment in the filter section of the pumped well, with high hydraulic conductivity within bedrock depressions (well 14T3091 and 14T3090) (figure 34). The origin of these elliptical (oblong) sediment deposits are therefore suggested to be drainage channels. This implies that the radius of influence would grow larger in the east-wester direction within these formations (figure 45) and along the bedrock slope. In the north-southerly direction the connectivity is not as high due to lower hydraulic conductivity (figure 45) and the growth of the radius of influence will not be as wide (table 15).

Further, the variance at Renen (figure 44) is low and all measured hydraulic conductivities was moderate or high (figure 34). Also, the highest median hydraulic conductivity, compared to the other investigation areas, was estimated for Renen (figure 34 and table 14). The spacing needed

between infiltration points is therefore thought to be quite large compared to the other areas since every individual infiltration point is likely to affect a larger area (table 15).

In the (upper) unconfined aquifer recharge is occurring by direct infiltration of precipitation. This will slow down the growth of the radius of influence during infiltration and pumping. As a result, an unconfined aquifer may not result in a deficit in the input parameter in the hydrologic equation and infiltration may not be necessary (Fetter, 2001). For the confined (lower) aquifer, which do not get direct recharge from precipitation and is under pressure, the situation would be different. During pumping or infiltration, the radius of influence will grow until it reach a recharge boundary (Kruseman & De Ridder, 1994). Also, in an confined aquifer pumping could lead to compression of the aquifer which is generally irreversible (Bouwer, 2002). Therefore, the need for infiltration in a confined aquifer could be greater.

At the Southern trough and tunnel the aquifer is mainly expected to be confined. Hence, no direct recharge from precipitation is possible. The recharge to the aquifer is restricted to areas where the confining layer is absent. The radius of influence as an effect of an excavation or from pumping will continue to develop until it reaches the recharge or discharge area (Fetter, 2001). In the north and northeast part of the area the bedrock along the hillside is considered a boundary which will limit the radius of influence from further growth (figure 36 and 45). These areas could be recharge boundaries if water can infiltrate the till in the bedrock slope or water is added from shallow rock, fractures, or deformation zones.

The location of the new railway at the Southern trough and tunnel can be seen in figure 45. The area with high hydraulic conductivity, indicated from southwest to northeast, would cause the radius of influence to grow in the directions of the area with high hydraulic conductivity (figure 36). This area is likely to increase the connectivity of the aquifer in the southwest-northeast direction compared to the northwest-southeasterly direction (se radius of influence from transient pumping test in figure 36). In the conceptual model of the sediments (figure 12) glaciofluvial material was expected to be found in bedrock depression and deformation zones. The short duration hydraulic tests could confirm that (often) sediments within lower areas in the bedrock resulted in high hydraulic conductivity. This can be seen in figure 36. According to Påsse (1990) the glaciofluvial sediments found in Varberg could be widespread. This can also be seen in figure 36 by combining the radius of influence from the pumping test and the short duration hydraulic tests. Therefore, this area of high hydraulic conductivity is suggested to be a glaciofluvial deposit. A radius of influence of an infiltration well within the glaciofluvial formation could therefore affect a rather widespread area. This can be seen in table 15. An infiltration well within this location also means that the capacity that is possible to apply in the well would be large compared to the rest of the investigation area related to the Southern trough and tunnel. This due to that the infiltration capacity depends on soil properties (K) (Pedretti et al., 2012).

The trough is suggested to cross sediments with high, moderate, and low hydraulic conductivity (figure 45). The effect of the excavation and the response related to infiltration along the trough will react differently dependent on the hydraulic conductivity. To produce an increase in head along the trough where the hydraulic conductivity is low, infiltration wells must be more closely

spaced since the radius of influence is smaller (table 15). The increase of head that can be applied on an infiltration well would also be lower due to the lower infiltration capacity in fine grained sediments (Zhang et al., 2017). This implies that to maintain the mass balance within the system (Fetter, 2001) more infiltration points could be needed.

Where there is high hydraulic conductivity the radius of influence is larger and hence infiltration wells can be positioned with a larger distance from each other. Therefore, in figure 45, since the trough goes through both moderate, low, and high hydraulic conductivity areas (figure 36), the amount of infiltration points (needed if there is a risk for damage) is suggested to be more compared to if the entire area was homogenous and had a high hydraulic conductivity.

The discussion above does also apply to Österleden. On the east side of the trough the infiltration wells must be more closely spaced due to the much lower hydraulic conductivities than the west side (figure 45). Here, the high hydraulic conductivity area located within the deformation zone mapped by SGU (2020) (figure 42) agrees with Hillefors (1979) deglaciation model for the highlands in the west, with deposits of glaciofluvial material along deformation zones. The result from the short duration hydraulic tests (figure 42) suggests that this deglaciation model and the conceptual model in figure 12 would apply for Österleden. The outline of the glaciofluvial deposit was not found by the result in figure 42. Påsse (1998) found larger glaciofluvial deposits within the same deformation zone further inland. Therefore, if this is a continuous formation within the deformation zone the radius of influence could reach long distances (table 15). Hence, this formation is suggested to be further investigated, especially in the eastern direction, to be able to predict the radius of influence.

At Vareborg the moraines ridges suggest a flow pattern that is not continuous (figure 41). The sediments within these structures varies from clay to till and sand (Påsse, 1990). No preferred flow directions were found at Vareborg (figure 38). This indicate that the radius of influence could vary rather locally. Not as in the other areas where there are flows aligned with bedrock depressions. Therefore, the radius of influence is suggested to be the most symmetrical one compared to the other areas. This is supported by the radius of influence from the second testing campaign in figure 38. This indicate that at Vareborg the distribution and spacing of the infiltration points could be more even compared to the Southern trough and tunnel and Österleden. Therefor, as discussed in section 5.3, both the bedrock and the high local variability of hydraulic conductivity could produce a rather symmetrical radius of influence.

In this discussion based on equation 3 by Kirieleis-Sichardt (1930) aquifer storativity (storage coefficient) was neglected. This equation and resulting radius of influence (table 15) is assuming a two-dimensional isotropic and homogenous unconfined aquifer. It is suggested that the radius of influence from an infiltration well will be unsymmetrical due to heterogeneities within the aquifer as been discussed for all investigation areas. This in agreement with the growth of the radius of influence as an effect of pumping in heterogeneous aquifers explained by Pedretti et al. (2012) and Kruseman and De Ridder (1994). Though, in a confined aquifer the radius of influence is also affected by the storage coefficient (S) as can be seen in equation 4. This equation suggests that with a smaller storage coefficient (for constant T and t) the radius of influence will be wider (Cooper & Jacob, 1946).

The flow pattern in the aquifers in Varberg is generally disturbed by channel flows in structures with high hydraulic conductivity (glaciofluvial materials) that creates deviation from two-dimensional isotropic aquifers (Renard et al., 2000). This can be seen in Renen, Southern trough and tunnel and for Österleden (figure 45). The resulting radius of influence will, because of this, exhibit an elliptical rather than circular form. Where the pumped well was positioned in these channel flows (Southern tunnel and trough) the result was a large ratio between the median hydraulic conductivity from short duration hydraulic tests and the effective hydraulic conductivity (table 14 and figure 36) and a high variance (figure 44). Where the pumping well was representing the general properties of the aquifer rather than the channel (Österleden), the ratio was smaller (figure 42 and table 14). Still, the variance for the short duration hydraulic test was high (figure 44). However, the high K channels are important since the effect from an excavation, infiltration well or pumping will be greater. Further, within these channel flows, where glaciofluvial sediments are in direct contact with the bedrock and the bedrock are highly fractured (as found by the first testing campaign at Renen) water could be infiltrated into the bedrock.

Both Österleden and the Southern tunnel and trough are suggested to result in a radius of influence that grows along the channels. Where no channel flows were detected (Vareborg) the variance was lower (figure 44) and the ratio was smaller (table 14 and figure 38). Here, the suggestion is that the radius of influence will not have as a strong elliptical shape (as can be seen from the pumping test in figure 38). Still, if the development of the radius of influence during a pumping test reached a channel flow this is expected to not largely influence the effective hydraulic conductivity as pointed out by Butler Jr and Healey (1998). Therefore, short duration hydraulic tests are suggested to be a valuable method and complement to pumping tests to further determent the spatial variability of hydraulic conductivity and determination of infiltration locations.

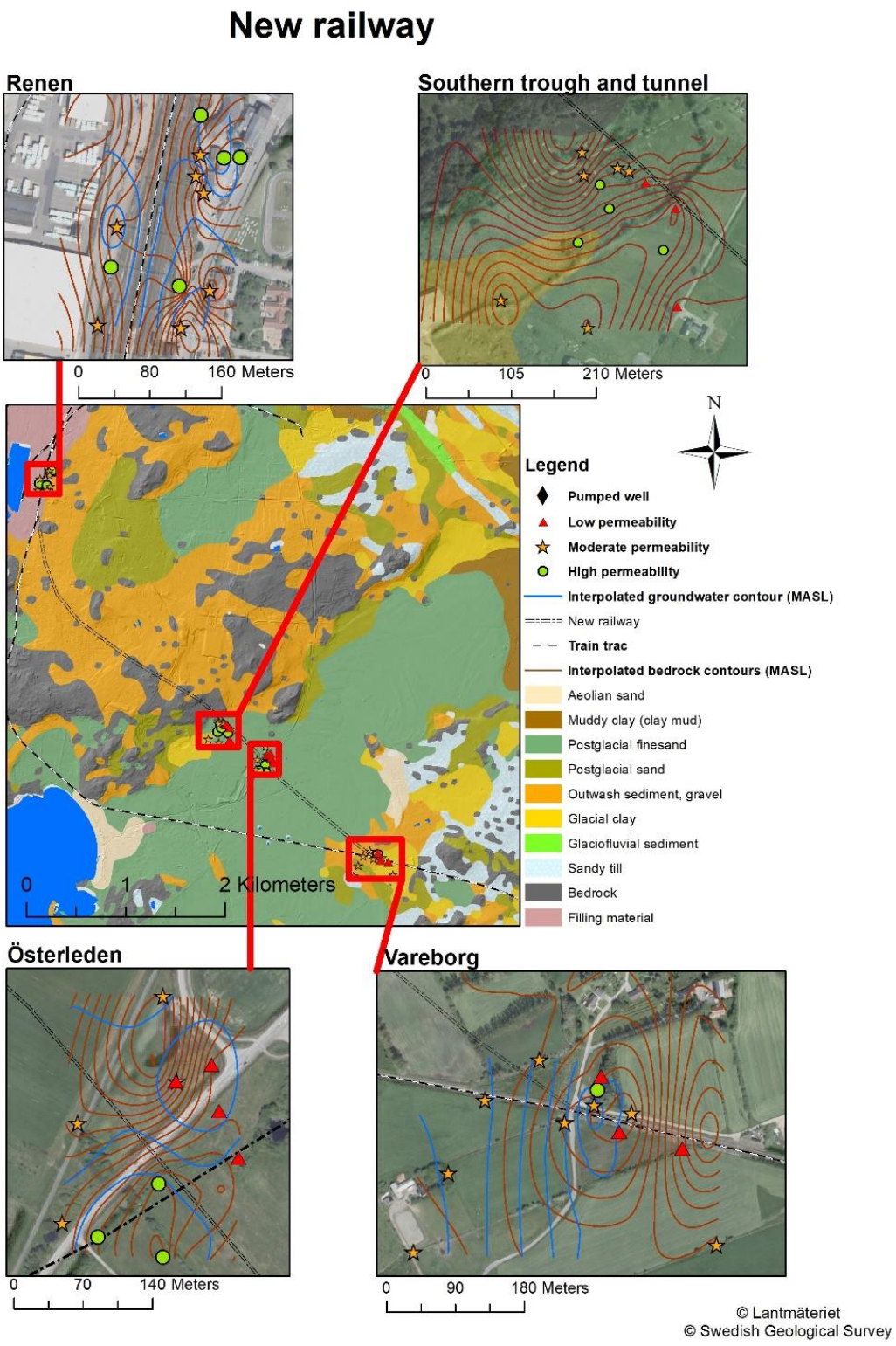

Figure 45. The new railway stretches through the investigation areas.

6. Conclusions

This thesis aimed to describe a conceptual model of the sedimentology for Swedish (or Nordic) conditions to facilitate the identification of main water-bearing units (e.g. upper and lower aquifers, two-dimensional and one-dimensional flow). The spatial variability in hydraulic conductivity was measured by short duration hydraulic tests to evaluate the conceptual model. The main assumption for the analysis was that the geometric mean (median) of the saturated hydraulic conductivity in a lognormal isotropic two-dimensional medium (aquifer) is the exact upscaled hydraulic conductivity (effective hydraulic conductivity) (Gupta et al., 2006; Renard et al., 2000). Based on this assumption the median hydraulic conductivity from short duration hydraulic tests was compared to the effective hydraulic conductivity obtained from transient (time dependent) pumping tests to explain aquifer heterogeneity and spatial variability (and anisotropy) in hydraulic conductivity.

1. The conceptual model of the sedimentology was found to be a valuable tool for the understanding of the relative values and the spatial distribution of hydraulic conductivity. Both for the case of agreement with the model (Renen, Österleden, Southern trough and tunnel) and for the situation of a deviation from the model (Vareborg). The latter was further developed from the conceptual model in figure 2 and 12, based on local processes and conditions for sedimentology and by the detection of geomorphological features.
2. Determination of aquifer heterogeneity and spatial variability by short duration hydraulic test were found to be a valuable complement to pumping tests by detecting small scale variations in hydraulic conductivity (Vareborg) and areas of higher hydraulic conductivity (Österleden).
3. Hydraulic conductivity parameter estimates from short duration hydraulic tests results in hydraulic conductivities in the range of the effective hydraulic conductivity estimation from pumping tests within the same aquifer. Differences between hydraulic conductivity from a pumping test and the median hydraulic conductivity obtained from short duration hydraulic tests can be explained by aquifer heterogeneity (variance) and the location of the pumped well representing a sub-area of the aquifer.
4. The flow pattern in the aquifers in Varberg generally seem to be disturbed by channel flows in structures or geological materials with high hydraulic conductivity (glaciofluvial) that create deviation from a two-dimensional isotropic aquifer (Renard et al., 2000). This was indicated for Renen, for Southern trough and tunnel and for Österleden (figure 45). The resulting radius of influence will, because of this, exhibit an elliptical rather than circular form.
5. A low variance and a high(er) median and effective hydraulic conductivity are suggested to lead to the need of fewer infiltration points (Renen). A higher variance is suggested (Österleden and the Southern tunnel and trough) to complicate the development of the radius of influence and could lead to the need of more infiltration points.

As a last remark, for mitigation measures (infiltration) to be needed a sensitive object need to be within a radius of influence (drawdown from pumping e.g. due to an excavation) and the decrease in hydraulic head need to be large enough to cause damage.

7. Acknowledgment

I would like to thank my supervisor Åsa Fransson for the support and the initial idea for this thesis. Her thorough comments and corrections were important for my learning during the project. Also, I want to thank Jakob Eng who was my practical advisor who taught me well about field work related issues. I want to thank Mark Johnson for reading my report and for giving me valuable comments.

Then I would like to thank Hannes Wiklund and Stefan Rhodin who helped me in field and at the office. Also, I would like to thank them for all the small chats which gave me energy during the project. Lastly, I want to thank my opponent Joakim Cooper Svensson for very thorough comments and language corrections.

8. References

Adrielsson, P., & Fredén, C. (1987). *Beskrivning till jordartskartan Marstrans SO/Göteborg SV*. Retrieved from Uppsala:

Andrén, T., Lindeberg, G., & Andrén, E. (2002). Evidence of the final drainage of the Baltic Ice Lake and the brackish phase of the Yoldia Sea in glacial varves from the Baltic Sea. *Boreas, 31*(3), 226-238. doi:10.1111/j.1502-3885.2002.tb01069.x

Anjar, J. (2012). *The Weichselian in southern Sweden and southwestern Baltic Sea: glacial stratigraphy, palaeoenvironments and deglaciation chronolog*. Retrieved from Lund:

Benn, D., & Evans, D. J. A. (2014). *Glaciers and Glaciation, 2nd edition*: Taylor and Francis.

Berglund, B. E., & Lagerlund, E. (1981). Eemian and Weichselian stratigraphy in South Sweden. *Boreas, 10*(4), 323-362. doi:10.1111/j.1502-3885.1981.tb00494.x

Bergman, S. (2018). *Geology of the Northern Norrbotten ore province, northern Sweden*. Retrieved from Uppsala:

Björck, S. (1995). A review of the history of the Baltic Sea, 13.0-8.0 ka BP. *Quaternary International, 27*(C), 19-40. doi:10.1016/1040-6182(94)00057-C

Bourdet, D. (2003). *Well Test Analysis: The use of Advanced Interpretation Models* (Vol. 3): Elsevier Science.

Bouvier, V., Johnson, M., & Påsse, T. (2015). Distribution, genesis and annual-origin of De Geer moraines in Sweden: insights revealed by LiDAR. *GFF, 137*, 1-15. doi:10.1080/11035897.2015.1089933

Bouvier, V., Johnson, M. D., & Påsse, T. (2015). Distribution, genesis and annual-origin of De Geer moraines in Sweden: insights revealed by LiDAR. *GFF, 137*(4), 319-333. doi:10.1080/11035897.2015.1089933

Bouwer, H. (2002). Artificial recharge of groundwater: Hydrogeology and engineering. *Hydrogeology Journal, 10*(1), 121-142. doi:10.1007/s10040-001-0182-4

Bouwer, H., & Rice, R. C. (1976). A slug test for determining hydraulic conductivity of unconfined aquifers with completely or partially penetrating wells. *Water Resources Research, 12*(3), 423-428. doi:10.1029/WR012i003p00423

Brauchler, R., Hu, R., Hu, L., & Ptak, T. (2012). Investigation of hydraulic parameters in unconsolidated sediments: A comparison of methods. *Grundwasser, 17*(2), 57-67. doi:10.1007/s00767-011-0185-6

Brauchler, R., Hu, R., Vogt, T., Al-Halbouni, D., Heinrichs, T., Ptak, T., & Sauter, M. (2010). Cross-well slug interference tests: An effective characterization method for resolving aquifer heterogeneity. *Journal of Hydrology, 384*(1-2), 33-45. doi:10.1016/j.jhydrol.2010.01.004

Brunner, P., Cook, P. G., & Simmons, C. T. (2009). Hydrogeologic controls on disconnection between surface water and groundwater. *Water Resources Research, 45*(1). doi:10.1029/2008WR006953

Butler Jr, J. J. (1998). *The Design, Performance and Analysis of Slug Tests*. Retrieved from New York:

Butler Jr, J. J., Bohling, G. C., Hyder, Z., & McElwee, C. D. (1994). The use of slug tests to describe vertical variations in hydraulic conductivity. *Journal of Hydrology, 156*(1-4), 137-162. doi:10.1016/0022-1694(94)90075-2

Butler Jr, J. J., Garnett, E. J., & Healey, J. M. (2003). Analysis of Slug Tests in Formations of High Hydraulic Conductivity. *Ground Water, 41*(5), 620-630. doi:10.1111/j.1745-6584.2003.tb02400.x

Butler Jr, J. J., & Healey, J. M. (1998). Relationship between pumping-test and slug-test parameters: Scale effect or artifact? *Ground Water, 36*(2), 305-313. Retrieved from https://www.scopus.com/inward/record.uri?eid=2-s2.0-0032031218&partnerID=40&md5=402d7569f8a1439c773fa5e15b1c8170

Chen, Q., Fan, G., Na, W., Liu, J., Cui, J., & Li, H. (2019). Past, present, and future of groundwater remediation research: A scientometric analysis. *International Journal of Environmental Research and Public Health, 16*(20). doi:10.3390/ijerph16203975

Cooper, H. H., Bredehoeft, J. D., & Papadopulos, S. S. (1967). Response of a finite-diameter well to an instantaneous change of water. *Water Resources Research, 3*, 263-269.

Cooper, H. H., & Jacob, C. E. (1946). A gereralized grapical method for evaluating formation constants and summarizing well field history. *Am. Geophys. Union Trans., 47*, 526-534.

Daniel, E. (1986). *Beskrivning till Jordartskartan Tomelilla SO/Simrishamn SV/Ystad NO/Örnahusen NV*. Retrieved from Uppsala:

Domenico, P. A. (1998). *Physical and chemical hydrogeology* (2. ed. ed.): New York : Wiley.

Duffield, G. M. (2007). Aqtesolv (Version 4.50 Professional). www.aqtesolv.com: HydroSOLVE, Inc.

Ebert, K., Hall, A. M., & Hättestrand, C. (2012). Pre-glacial landforms on a glaciated shield: The inselberg plains of northern Sweden. *Norsk Geologisk Tidsskrift, 92*(1). Retrieved from https://www.scopus.com/inward/record.uri?eid=2-s2.0-84876295534&partnerID=40&md5=4f6be31786a9ac8ee63e0bd12329ca33

Evans, D., & Benn, D. I. (2004). *Practical Guide to the Study of Glacial Sediments*. London, UNITED KINGDOM: Routledge.

Fabbri, P., Ortombina, M., & Piccinini, L. (2012). Estimation of Hydraulic Conductivity Using the Slug Test Method in a Shallow Aquifer in the Venetian Plain (NE, Italy). *AQUA mundi, 3*, 125-133. doi:10.4409/Am-045-12-0048

Fetter, C. W. (2001). *Applied hydrogeology* (4. ed. ed.): Upper Saddle River : Prentice Hall.

Fromm, E. (1976). *Beskrivning till Jordartskartan Linköping NO*. Retrieved from Stockholm:

Geology of Sweden. (2019). Retrieved from https://www.sgu.se/en/geology-of-sweden/

Gette-Bouvarot, M., Volatier, L., Lassabatere, L., Lemoine, D., Simon, L., Delolme, C., & Mermillod-Blondin, F. (2015). Ecological Engineering Approaches to Improve Hydraulic Properties of Infiltration Basins Designed for Groundwater Recharge. *Environmental Science and Technology, 49*(16), 9936-9944. doi:10.1021/acs.est.5b01642

Gibbard, P. L. (1992). Formal Stratigraphy in the pleistocene of Finland *Bull. Geol. Soc. Finland 64*, 125—134.

Göransson, M., Bergström, U., Shomali, H., Claeson, D., & Hellström, F. (2008). *Beskrivning till bergkvalitetskartan delar av Kungsbacka och Varbergs kommuner*. Retrieved from

Grånäs, K., & Ising, J. (2008). *Beskrivning till Jordartskartan 13F Falun NO*. Retrieved from

Gupta, A., Rudra, R., Parkin, G., & Parkin, R. (2006). Analysis of spatial variability of hydraulic conductivity at field scale. *Canadian Biosystems Engineering, 48*.

Hambrey, M. J., & Glasser, N. F. (2012). Discriminating glacier thermal and dynamic regimes in the sedimentary record. *Sedimentary Geology, 251-252*, 1-33. doi:https://doi.org/10.1016/j.sedgeo.2012.01.008

Hättestrand, C., & Stroeven, A. P. (2002). A relict landscape in the centre of Fennoscandian glaciation: Geomorphological evidence of minimal Quaternary glacial erosion. *Geomorphology, 44*(1-2), 127-143. doi:10.1016/S0169-555X(01)00149-0

Hebrand, M., & Mark, M. (1989). Esker formation and glacier dynamics in eastern Skane and adjacent areas, southern Sweden. *Boreas, 18*(1), 67-81. doi:10.1111/j.1502-3885.1989.tb00372.x

Hillefors, Å. (1979). Deglaciation models from the Swedish West Coast. *Boreas, 8*(2), 153-169. doi:10.1111/j.1502-3885.1979.tb00796.x

Hölting, B., & Coldewey, W. G. (2019). *Hydrogeology*. Berlin, Heidelberg: Berlin, Heidelberg: Springer Berlin Heidelberg.

Hvorslev, M. J. (1951). *Time lag and soil permeability in ground-water observations* (36). Retrieved from Vicksburg, Mississippi:

Hyder, Z., & Butler, J. J., Jr. (1995). Slug Tests in Unconfined Formations: An Assessment of the Bouwer and Rice Technique. *Groundwater, 33*(1), 16-22. doi:10.1111/j.1745-6584.1995.tb00258.x

Hyder, Z., Butler, J. J., Jr., McElwee, C. D., & Liu, W. (1994). Slug tests in partially penetrating wells. *Water Resources Research, 30*(11), 2945-2957. doi:10.1029/94WR01670

Johnson, M. D., & Ståhl, Y. (2010). Stratigraphy, sedimentology, age and palaeoenvironment of marine varved clay in the Middle Swedish end-moraine zone. *Boreas, 39*(2), 199-214. doi:10.1111/j.1502-3885.2009.00124.x

Johnson, M. D., Ståhl, Y., Larsson, O., & Seger, S. (2010). New exposures of Baltic Ice Lake drainage sediments, Götene, Sweden. *GFF, 132*(1), 1-12. doi:10.1080/11035891003597067

Johnson, M. D., Wedel, P. O., Benediktsson, Í., & Lenninger, A. (2019). Younger Dryas glaciomarine sedimentation, push-moraine formation and ice-margin behavior in the Middle Swedish end-moraine zone west of Billingen, central Sweden. *Quaternary Science Reviews, 224*. doi:10.1016/j.quascirev.2019.105913

Jones, L. (1993). A Comparison of Pumping and Slug Tests for Estimating the Hydraulic Conductivity of Unweathered Wisconsian Age Till in Iowa. *Groundwater, 31*(6), 896-904. doi:10.1111/j.1745-6584.1993.tb00862.x

Jones, S. J., & Jones, S. J. (2015). *Introducing Sedimentology*. Edinburgh: Edinburgh, London: Dunedin Academic Press.

Kitanidis, P. K. (1994). The concept of the Dilution Index. *Water Resources Research, 30*(7), 2011-2026. doi:10.1029/94WR00762

Kleman, J., Borgström, I., Robertsson, A., & Lilliesköld, M. (1992). Morphology and stratigraphy from several deglaciations in the Transtrand Mountains, western Sweden. *Journal of Quaternary Science, 7*(1), 1-17. doi:10.1002/jqs.3390070102

Kleman, J., Stroeven, A. P., & Lundqvist, J. (2008). Patterns of Quaternary ice sheet erosion and deposition in Fennoscandia and a theoretical framework for explanation. *Geomorphology, 97*(1-2), 73-90. doi:10.1016/j.geomorph.2007.02.049

Koussis, A. D., & Akylas, E. (2012). Slug Test in Confined Aquifers, the Over-Damped Case: Quasi-Steady Flow Analysis. *Ground Water, 50*(4), 608-613. doi:10.1111/j.1745-6584.2011.00855.x

Kruseman, G. P., & De Ridder, N. A. (1994). *Analysis and Evaluation of Pumping Test Data Second Edition*. Retrieved from Wageningen, The Netherlands:

Kulessa, B., Hubbard, B., Williamson, M., & Brown, G. H. (2005). Hydrogeological analysis of slug tests in glacier boreholes. *Journal of Glaciology, 51*(173), 269-280. doi:10.3189/172756505781829458

Lagerbäck, R., & Robertsson, A. M. (1988). Kettle holes - stratigraphical archives for Weichselian geology and palaeoenvironment in northernmost Sweden. *Boreas, 17*(4), 439-468. doi:10.1111/j.1502-3885.1988.tb00561.x

Lemdahl, G., Broström, A., Hedenäs, L., Arvidsson, K., Holmgren, S., Gaillard, M. J., & Möller, P. (2013). Eemian and Early Weichselian environments in southern Sweden: A multi-proxy study of till-covered organic deposits from the Småland peneplain. *Journal of Quaternary Science, 28*(7), 705-719. doi:10.1002/jqs.2664

Lindén, M., & Möller, P. (2005). Marginal formation of De Geer moraines and their implications to the dynamics of grounding-line recession. *Journal of Quaternary Science, 20*(2), 113-133. doi:10.1002/jqs.902

Lundquist, I., & Kero, L. (2008). *Beskrivning till berggrundskartan 5B Varberg NO*. Retrieved from

Lundqvist, J. (1969). *Beskrivning till jordartskartan över Jämtlands län*. Retrieved from Stockholm:

Lundqvist, J. (1997). Rogen moraine - An example of two-step formation of glacial landscapes. *Sedimentary Geology, 111*(1-4), 27-40. doi:10.1016/S0037-0738(97)00004-3

Lundqvist, J., Lundqvist, T., & Lindström, M. (2011). *Sveriges Geologi från urtid till nutid* (Vol. 3). Lund: Författarna och Studentlitteratur.

Lundqvist, J., & Wohlfarth, B. (2001). Timing and east-west correlation of south Swedish ice marginal lines during the Late Weichselian. *Quat. Sci. Rev.*(20), 1127-1148.

Magnusson, E. (2009). *Beskrivning till jordartskartan 5E Växsjö NO*. Retrieved from Uppsala:

Mangerud, J., Gyllencreutz, R., Lohne, Ø., & Svendsen, J. I. (2011). Chapter 22 - Glacial History of Norway. In J. Ehlers, P. L. Gibbard, & P. D. Hughes (Eds.), *Developments in Quaternary Sciences* (Vol. 15, pp. 279-298): Elsevier.

Martí, V., Jubany, I., Pérez, C., Rubio, X., De Pablo, J., & Giménez, J. (2014). Human Health Risk Assessment of a landfill based on volatile organic compounds emission, immission and soil gas concentration measurements. *Applied Geochemistry, 49*, 218-224. doi:https://doi.org/10.1016/j.apgeochem.2014.06.018

Mas-Pla, J., Yeh, T. C. J., Williams, T. M., & McCarthy, J. F. (1997). Analyses of slug tests and hydraulic conductivity variations in the near field of a two-well tracer experiment site. *Ground Water, 35*(3), 492-501. doi:10.1111/j.1745-6584.1997.tb00110.x

McElwee, C. D. (2001). Application of a nonlinear slug test model. *Ground Water, 39*(5), 737-744. doi:10.1111/j.1745-6584.2001.tb02364.x

McElwee, C. D. (2002). Improving the analysis of slug tests. *Journal of Hydrology, 269*(3-4), 122-133. doi:10.1016/S0022-1694(02)00214-7

McElwee, C. D., & Zenner, M. A. (1998). A nonlinear model for analysis of slug-test data. *Water Resources Research, 34*(1), 55-66. doi:10.1029/97WR02710

Moench, A. F. (1998). Erratum: Flow to a well of finite diameter in a homogeneous, anisotropic water table aquifer (Water Resources Research (1997) 33:6 (1397-1407)). *Water Resources Research, 34*(9), 2431-2432. doi:10.1029/98WR01858

Möller, P. (2006). Rogen moraine: an example of glacial reshaping of pre-existing landforms. *Quaternary Science Reviews, 25*(3), 362-389. doi:https://doi.org/10.1016/j.quascirev.2005.01.011

Möller, P. (2010). Melt-out till and ribbed moraine formation, a case study from south Sweden. *Sedimentary Geology, 232*(3-4), 161-180. doi:10.1016/j.sedgeo.2009.11.003

Möller, P., Anjar, J., & Murray, A. S. (2013). An OSL-dated sediment sequence at Idre, west-central Sweden, indicates ice-free conditions in MIS 3. *Boreas, 42*(1), 25-42. doi:10.1111/j.1502-3885.2012.00284.x

Möller, P., & Murray, A. S. (2015). Drumlinised glaciofluvial and glaciolacustrine sediments on the Småland peneplain, South Sweden – new information on the growth and decay history of the Fennoscandian Ice Sheets during MIS 3. *Quaternary Science Reviews, 122*, 1-29. doi:https://doi.org/10.1016/j.quascirev.2015.04.025

Nielsen, D., & Biggar, J. E. K. (1973). Spatial variability of field-measured soil-water properties. *Hilgardia, 42*(7), 44. doi:10.3733/hilg.v42n07p215

Paradis, D., Lefebvre, R., Gloaguen, E., & Giroux, B. (2016). Comparison of slug and pumping tests for hydraulic tomography experiments: a practical perspective. *Environmental Earth Sciences, 75*(16). doi:10.1007/s12665-016-5935-4

Påsse, T. (1990). *Beskrivning till jordartskartan Varberg NO*. Retrieved from Uppsala:

Påsse, T. (1998). Early Weichselian interstadial deposits within the drumlins at Skrea and Vinberg, southwestern Sweden. *GFF, 120*(4), 349-356. doi:10.1080/11035899801204349

Påsse, T., & Daniels, J. (2015). *Past shore-level and sea-level displacements*. Retrieved from Uppsala:

Pedretti, D., Barahona-Palomo, M., Bolster, D., Sanchez-Vila, X., & Fernàndez-Garcia, D. (2012). A quick and inexpensive method to quantify spatially variable infiltration capacity for artificial recharge ponds using photographic images. *Journal of Hydrology, 430-431*, 118-126. doi:10.1016/j.jhydrol.2012.02.008

Plink-Björklund, P., & Ronnert, L. (1999). *Depositional Processes and internal architecture of Late Weichselian ice-margin submarine fan and delta settings, Swedish west coast*. Retrieved from Gothenburg:

Renard, P., Le Loc'h, G., Ledoux, E., De Marsily, G., & Mackay, R. (2000). A fast algorithm for the estimation of the equivalent hydraulic conductivity of heterogeneous media. *Water Resources Research, 36*(12), 3567-3580. doi:10.1029/2000WR900203

Ringberg, B. (1988). Late Weichselian geology of southernmost Sweden. *Boreas, 17*(2), 243-263. doi:10.1111/j.1502-3885.1988.tb00554.x

Ringberg, B. (1989). Upper Late Weichselian lithostratigraphy in western Skåne, southernmost Sweden. *GFF, 111*(4), 319-337. doi:10.1080/11035898909453130

Ringberg, B. (1991). *Beskrivning till Jordartskartan Kristianstad SO*. Retrieved from Uppsala:

Rudmark, L. (2000). *Beskrivning till jordartskartan Uppsala NO*. Retrieved from Uppsala:

Şen, Z. (2015). Chapter 2 - Basic Porous Medium Concepts. In Z. Şen (Ed.), *Practical and Applied Hydrogeology* (pp. 43-97). Oxford: Elsevier.

SGU (Cartographer). (2019). Jordarter 1:25000-1:100000

SGU. (2020). SGU Kartvisare. Retrieved 2020-06-04, from Swedish Geological Surveys

SMHI. (2017). Årsavdunstning medelvärde 1961-1990. from SMHI

SMHI. (2020). Sveriges Klimat. Retrieved 20200423, from www.smhi.se/kunskapsbanken/klimat/sveriges-klimat/sveriges-klimat-1.6867

Stroeven, A. P., Hättestrand, C., Kleman, J., Heyman, J., Fabel, D., Fredin, O., . . . Jansson, K. N. (2016). Deglaciation of Fennoscandia. *Quaternary Science Reviews, 147*, 91-121. doi:10.1016/j.quascirev.2015.09.016

Svensson, C., & Sällfors, G. (1985). *Berakning av dimensionerande grundvattentryck* Retrieved from Göteborg:

Thompson, A., & Taylor, B. N. (2008). *Guide for the Use of the International System of Units (SI)*. Retrieved from Gaithersburg, MD 20899

Tuli, A., Kosugi, K., & Hopmans, J. W. (2001). Simultaneous scaling of soil water retention and unsaturated hydraulic conductivity functions assuming lognormal pore-size distribution. *Advances in Water Resources, 24*(6), 677-688. doi:10.1016/S0309-1708(00)00070-1

Tyréns, A. B. (2016). *Tillstånd för vattenverksamhet och arbeten i anslutning till Natura 2000-område Varbergstunneln, Västkustbanan, Varberg-Hamra*. Retrieved from Gothenburg:

Dom; Ansökan om tillstånd för vattenverksamhet och arbeten i anslutning till Natura 2000-område: Varbergstunneln, Västkustbanan, Varberg - Hamra, (2018).

Wada, Y., Van Beek, L. P. H., Van Kempen, C. M., Reckman, J. W. T. M., Vasak, S., & Bierkens, M. F. P. (2010). Global depletion of groundwater resources. *Geophysical Research Letters, 37*(20). doi:10.1029/2010GL044571

Wen, X. H. (1994). Estimation of statistical parameters for censored lognormal hydraulic conductivity measurements. *Mathematical Geology, 26*(6), 717-731. doi:10.1007/BF02086868

Werner, A. D., Bakker, M., Post, V. E. A., Vandenbohede, A., Lu, C., Ataie-Ashtiani, B., . . . Barry, D. A. (2013). Seawater intrusion processes, investigation and management: Recent advances and future challenges. *Advances in Water Resources, 51*, 3-26. doi:10.1016/j.advwatres.2012.03.004

Wiklund, H. B., Lindqvist, E., Fransson, Å., Eng, J., Berg, A., & Karlatou, A. C. (2019). *PM Hydrauliska Tester i Jord FAS 1 och 2 Varbergstunneln, Västkustbanan, Varberg-Hamra* Retrieved from Gothenburg:

Zarlenga, A., Janković, I., Fiori, A., & Dagan, G. (2018). Effective Hydraulic Conductivity of Three-Dimensional Heterogeneous Formations of Lognormal Permeability Distribution: The Impact of Connectivity. *Water Resources Research, 54*(3), 2480-2486. doi:10.1002/2017WR022141

Zech, A., Müller, S., Mai, J., Heße, F., & Attinger, S. (2016). Extending Theis' solution: Using transient pumping tests to estimate parameters of aquifer heterogeneity. *Water Resources Research, 52*(8), 6156-6170. doi:10.1002/2015WR018509

Zemansky, G. M., & McElwee, C. D. (2005). High-resolution slug testing. *Ground Water*, *43*(2), 222-230. doi:10.1111/j.1745-6584.2005.0008.x

Zhang, Y. Q., Wang, J. H., Chen, J. J., & Li, M. G. (2017). Numerical study on the responses of groundwater and strata to pumping and recharge in a deep confined aquifer. *Journal of Hydrology*, *548*, 342-352. doi:10.1016/j.jhydrol.2017.03.018